Investigation of the Interfacial Friction and Adhesion of Thin PDMS Network Lubricant Films

by Lucas James Landherr

INVESTIGATION OF THE INTERFACIAL FRICTION AND ADHESION OF THIN PDMS NETWORK LUBRICANT FILMS

A Dissertation

Presented to the Faculty of the Graduate School

of Cornell University

in Partial Fulfillment of the Requirements for the Degree of

Doctor of Philosophy

by

Lucas James Landherr

August 2010

INVESTIGATION OF THE INTERFACIAL FRICTION AND ADHESION OF THIN PDMS NETWORK LUBRICANTS FILMS

Lucas James Landherr, Ph.D.

Cornell University, 2010

The lubrication properties of several variations on a polydimethylsiloxane (PDMS) network – self-assembled monolayer (SAM) hybrid lubricant and the effect that structural and chemical modifications can have on the friction, adhesion, and wear are investigated. The primary lubricant structure studied in this thesis consisted of a model cross-linked PDMS network tethered to an anchoring SAM layer. Modifications of this structure including ultrathin hyperbranched films, micron-thick films with pendent chains, networks swollen with free chains, and a deconstructed polymer brush are also studied. These hybrids created high degrees of internal tethering with a flexible surface layer exhibiting low interfacial shear and low surface energy.

The friction and adhesion properties of these lubricants were determined from a series of experiments conducted with atomic force microscopy, nanoindentation, and bulk rheology and tribology. The PDMS-SAM lubricants demonstrated dramatically low friction coefficients, as low as $\mu = 0.0024$, which is the lowest friction coefficient recorded for a dry polymer film. These low friction properties are a result of a negligible contribution of adhesion to the friction force.

Structural modifications to the network allowed for the effect of the physical properties on the friction and lubrication to be determined. Incorporating pendent chains and free chains into the network layer increased the surface viscous dissipation. While the elastic moduli and the network stiffness decreased, the structural modifications also served to increase the surface shear and viscosity, resulting in

larger friction coefficients. Wear measurements conducted on the networks swollen with free chains indicated that increasing the lubricant viscous dissipation also dramatically reduced the wear resistance of the film.

Polymer brushes were developed at several surface coverages and with different polymer chemistries to determine the physical and chemical effects on friction and lubrication. High surface coverages creating stretched elastic chains yielded a significant reduction in the friction coefficient, relative to more deformed, mushroom conformations. PDMS brushes exhibited significantly lower friction than brushes made from polymers with higher surface energies, despite the chemical effects being minimized as a result of a minimal adhesion contribution to the friction force at the ultrathin lubricant lengthscale.

BIOGRAPHICAL SKETCH

Lucas James T. Landherr was born in southeastern Connecticut on February 4, 1983. He graduated as valedictorian from St. Bernard's High School in Uncasville, CT, in 2001. He attended Lafayette College in Easton, PA, and received a B.S. in Chemical Engineering in 2005, graduating Summa Cum Laude with honors. Upon completion of the requirements for a Ph.D. in Chemical Engineering at Cornell University, Lucas will begin a post-doctoral research investigation at the National Institute of Standards and Technology in Gaithersburg, MD.

for Maret and my parents

(Anyone who puts up with me deserves this as much as I do.)

ACKNOWLEDGMENTS

Thank you to Dr. Lynden Archer and Dr. Claude Cohen for their insight, recommendations and intellectual challenges that made me a better chemical engineer.

Thank you to Dr. Christopher Ober for serving on my thesis committee and helping at various points along the way.

Thank you to Dr. Qing Zhang for training me during my first year at Cornell.

Thank you to Henry Lau for repeatedly serving as a sounding board over five years and helping to refine my academic teaching skills as a teaching advisor partner for two years. Thank you to all other members of the Archer and Cohen research groups who have contributed with their suggestions and criticisms.

Thank you to Fluids students who showed me graduate school was the right decision.

Thank you to National Science Foundation and Department of Energy for their funding support, and to the research facilities providing the equipment needed for the many experiments described within.

Finally, and most importantly, thank you to my family for their support. Without the guidance, encouragement and humor of many people over many years, I would never have gotten to this point. Thank you to my wife, Maret, for providing a much-needed anchor to a world outside research. Thank you to my parents, my sisters, grandparents, pets, the rest of my extended family and a number of close friends for helping me become someone who could take on this challenge and succeed.

TABLE OF CONTENTS

LIST OF FIGURES

LIST OF TABLES

CHAPTER 1

INTRODUCTION: FRICTION, ADHESION, AND LUBRICATION SYSTEMS

1.1. INTRODUCTION

Recent advancements in the capability and application range of small devices, such as microelectromechanical systems (MEMS) or self-administered syringes for the elderly, have increased the need for improved high-performance lubricants that will function on the lengthscale of these devices.[1-3] The current demand for better lubrication systems has developed as a result of the surface effects dominating the material characteristics on small lengthscales in comparison to volume effects. Thus, friction, adhesion, and wear are much more significant factors. Many properties of high-performance lubricants remain crucial with the increased role of surface effects. For example, the lubricant must still be deposited as a thin film at the nanoscale in order to maintain the substrate structure, the film must be strongly tethered to the substrate to increase the wear resistance, and a low interfacial shear stress and minimal contact area are necessary to reduce friction.[4-7] This lengthscale eliminates standard industrial lubricants as applicable solutions, as the static friction forces and lubrication particle sizes can interrupt the operation of the devices.[7-9]

1.2. FRICTION AND ADHESION

Because surface effects have increased importance at the nano- and micro-scale, it is important to understand the source of microscopic friction. A modified form of Admonton's Law recognizes that there are two contributions to the friction force (F_f): a load (N) component, and an adhesion component determined by the critical shear stress (τ_o), which is a strong factor of the surface chemistry, and the actual contact area (A) between two interfaces:

$$F_f = \tau_o A + \mu (N + N_c) \quad (1)$$

Here N_c is the critical load, a finite value expressing the normal force required to separate the two materials at the interface.[10] The load component by itself provides the simplified friction force equation where N is directly proportional to F_f with the coefficient of friction (COF), μ, as the proportional constant. For this simplification to be applicable, the adhesive contribution (τ_o*A) to friction must be negligible.

Several studies have attempted to evaluate the nature of friction for various interfaces. Greenwood and Tabor described a continuum model based on a sliding rigid body causing deformation of a softer, viscoelastic material.[11] They recognized that indentation into a softer body resulted in elastic work, and lateral sliding caused further deformation developing in front of the indenter. Greenwood and Tabor found that the loss of energy in the deformation recovery process for an elastomer was a main contributor to friction increases at soft interfaces. Schallamach used an Eyring model to explain sliding friction, where individual polymer chains create short-lived bonds as a result of molecular attraction during lateral movement across a surface.[12,13] The chain ends form an attachment across the interface, elongate and increase in tension as sliding continues, then detach and relax before forming a new attachment and continuing the process. A cartoon of this classical depiction[14] of these so-called "working" chains is depicted in Figure 1.1. This shearing of attachments created by adhesion is considered to be an example of a molecular model of the contribution of adhesion to sliding friction. While the example provided focuses on individual polymer chains, this model of molecular adhesion also holds for individual molecular adhesive attachments to other surfaces. Because both the continuum and molecular models provide accurate interpretations of the friction force, the interplay between the effects described by the two different models defines the surface interaction and determines the size of the overall friction.

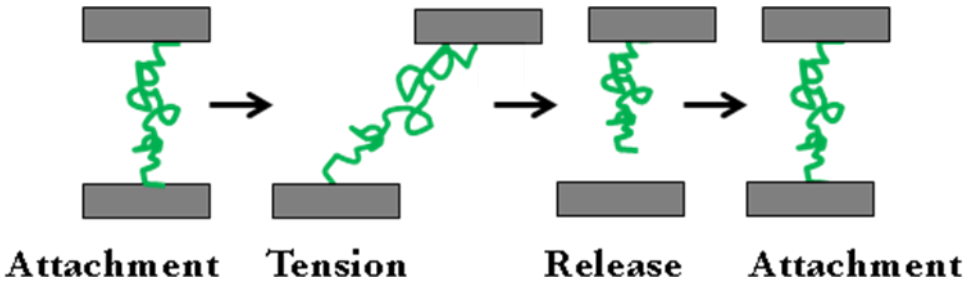

Figure 1.1. Classical depiction of a working polymer chain moving laterally, where the chain is attached to the top horizontal surface and is interacting with the bottom surface. The chain becomes briefly adhered to the bottom surface as a result of attractive forces and adhesion, stretches, releases and relaxes to overcome tension, then attaches to the surface again. The cyclic attachment and release creates a slip-stick movement.

The friction force has also been shown to have some dependence on sliding velocity. Chernyak and Leonov developed the molecular model of adhesion and sliding friction further to recognize that the tension in each polymer chain increases with the sliding velocity.[15] They showed that the number of working chains that can attach to the opposing surface at the interface, or have some tension distributed within them, is dependent on the number of polymer chains in contact at the interface. Because the lifetime of the adhesive contact depends on the velocity, the number of working chains will decrease as the sliding velocity increases. The number of working chains per unit area, N_w, can be determined from the relationship:

$$N_w = N_o \frac{<t>_b}{<t>_b + \tau} \quad (2)$$

where N_o is the total number chains, $<t>_b$ is the timescale of the short-lived adhesion between the polymer chains and the surface, and τ is the relaxation time of the free, non-attached polymer chains. From this model, Chernyak and Leonov showed that the size of the adhesion contribution to friction can be changed by slowing or increasing the lateral speed of the opposing surface at the interface. Ludema and Tabor recognized that a maximum in the stress and the friction force occurs at a critical velocity for the sliding friction at an elastomer interface.[16] As the sliding velocity increases, the friction increases with the size of the surface shear. However, the tension throughout the elastomer will rise, temporarily stiffening the network and increasing the elasticity in the immediate vicinity of the contact area. This assumes single asperity contact, or contact area with no roughness. Because the elasticity temporarily increases, both the contact area and the friction force will decrease.

The dependence of friction on the sliding velocity is especially important when defining the material thickness participating in the interfacial friction or when a lubrication layer is introduced at the interface. Either molecular adhesion or the bulk

deformation will be the dominating mechanism of interfacial friction depending on the scale of the thickness and the sliding velocity. The interplay between these two mechanisms can be predicted by the three specific lubrication regimes that exist for an elastic solid.[17,18] Figure 1.2 depicts an example Stribeck curve illustrating the three lubrication regimes, where the coefficient of friction (COF) is plotted against the Stribeck number ($\eta * v / P$). Here η is the lubricant viscosity, v is the sliding velocity, and P is the exerted pressure at the interface. At the lowest sliding speeds, a molecular thin boundary lubrication layer exists. The film thickness at the sliding interface in this regime is at most a few monolayers, and is comparable to, or less than, the interfacial surface roughness. Viscosity effects are negligible in comparison with the direct interaction between the lubrication material and the opposing solid surface. In this range of velocities, the molecular adhesive forces are the primary source of friction. As the sliding speeds increase, lubrication progresses through a transition regime until becoming completely elastohydrodynamic. The coefficient of friction is significantly lower and the lubricant viscosity has a greater role in this regime. High viscosity at the interface results in a large energy dissipation during shearing of the fluid, thus increasing the friction force.[19] However, when the sliding velocity is large enough for elastohydrodynamic lubrication to occur, the higher viscosity will prevent the spreading of liquid-like or freely mobile lubricant particles. This can prevent a thinning of the lubrication films for liquid systems, which would induce a transition back to the boundary lubrication regime. In solid or elastomer films, the high localized pressures will cause the lubricant to deform elastically and maintain a continuous film in order to prevent wear and penetration.[20] Friction thus primarily occurs as a result of deformation and recovery of the film in the elastohydrodynamic regime. Liquid-based lubricants can potentially progress through all three regimes if

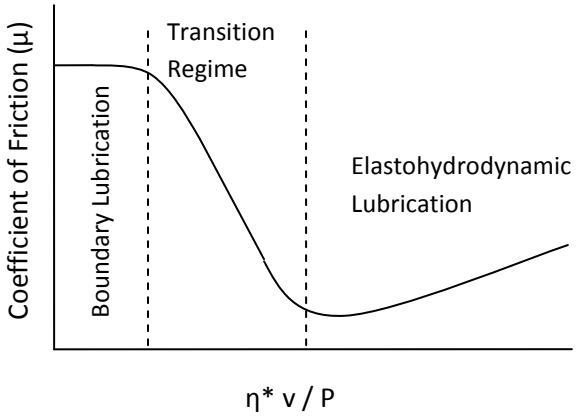

Figure 1.2. Example of a typical Stribeck curve, denoting three distinct lubrication regimes. The curve is not necessarily to scale, as the transition regime can be much shorter with a larger slope. On the x-axis, η is the lubricant viscosity, v is the sliding velocity, and P is the pressure existing as a result of friction and/or torque.

the sliding speed changes, as the lubricant thickness can readily increase with sliding velocity, thus minimizing molecular adhesive friction effects in favor of bulk deformation. Solid or surface-adhered lubricants do not necessarily have the flexibility to change the thickness, and are more likely to remain constrained to one regime over a wide range of sliding velocities. It is likely that a solid-like lubricant will begin to wear away before progressing to a different friction regime, typically from elastohydrodynamic to boundary lubrication for thicker films.[21]

More recently, the dependence of the friction force on sliding velocity has been associated with changes in the effective areal density of the polymer chains in an elastomer. In a study conducted by Vorvolakos and Chaudhury using the rate-dependent molecular debonding model developed by Chernyak and Leonov, the researchers analyzed the effect of chain areal density.[12] When elastomers are created from precursor telechelic polymer chains of increasing molar mass in an end-linking synthesis, the cross-link density of a network will decrease. Thus, the number of chain ends present in some interfacial area for single asperity contact decreases as well, where 'chain ends' refers to the free and cross-linked telechelic ends of the precursor chains within the network. Conversely, decreasing the molar mass of the precursor chains will shorten the distance between cross-links, increasing the cross-link density and number of chain ends within a specific volume. The number of chain ends is also directly related to changes in the immediate elastic moduli that develop as a result of an applied stress and the network tension. In consideration of this relationship, the shear stress is a normalized evaluation of the sliding friction force. As single-asperity contact with an AFM allows the stress, σ, to be calculated from:

$$\sigma = F_f / A \qquad (3)$$

the shear stress provides a measurement that is independent of the contact area.[22] Thus, converting to stress provides a better evaluation of sliding velocity experiments.

The effect of the areal density of chain ends can still be calculated and determined by comparing networks with different crosslink densities,

The interplay between the roles of adhesion and load for friction presents the opportunity for one mechanism to dominate the friction force, depending on the physical and chemical properties of the materials at the interface. This interplay was investigated in a series of studies conducted by Zhang and Archer focusing on the effect of structure and medium on the interfacial friction and adhesion.[23] They showed that self-assembled monolayer (SAM) blends consisting of both short and long alkylsilane chains have significantly lower friction than monolayers of a single length. Using an Eyring-type analysis, they concluded the lower friction for the two-tiered structure develops from high surface disorder and mobility in the canopy layer. The densely packed shorter chains prevent penetration to the substrate and provide a means of internal tethering for the surface layer. Zhang and Archer were able to dramatically reduce the COF by changing the medium from air to ethanol, thus reducing the interfacial shear stress and eliminating the adhesion contribution to friction. They concluded from these results that working with low shear stress materials would create an optimal environment for low friction results.

It is important to note that eliminating the adhesion contribution to friction does not mean that adhesive forces at the interface are non-existent. Depending on the surface materials present at the interface, movement normal to the interface can still result in large pull-off adhesive forces. The assumption is instead made based on low interfacial shear stresses that these adhesive forces do not contribute to the friction developed from lateral movement. This is an important distinction to make so incorrect conclusions are not made assuming the non-existence of adhesion, in particular when high viscosity lubricants with high adhesive forces are used.

1.3. LUBRICATION SYSTEMS

Many studies have already been conducted on a wide range of lubricant types. Self-assembled monolayers can produce low COFs but have poor resistance to wear, making them unviable for long-term use.[24-28] Several strong polymer gels have been shown to achieve low friction in the presence of a solvent used to either swell the network or create a viscous film or coating across the lubricant surface.[29,30] Polyelectrolyte brushes have also been reported to exhibit extremely low friction coefficients in the presence of a solvent.[31] While some of these solvent-based systems also show a significant resistance to wear, introducing a solvent can limit the potential applications of such a lubricant. Many small mechanical devices are unable to work in the presence of a solvent as a result of large stiction forces, while medical devices, e.g. self-administered syringes for the elderly, may require a dry lubricant in order to prevent accidental exposure to a fluid solvent.[7-9]

A two-tier hybrid lubricant is proposed consisting of a polydimethylsiloxane (PDMS) polymer network tethered to a SAM coating which acts as a well-ordered surface-adhered anchoring layer.[32] PDMS is an ideal lubricating material because of its low surface energy, high molecular flexibility, and relative ease in its synthesis process. Utilizing a polymer network as the surface layer will decrease the wear typically seen for SAMs, while also allowing for low shear stresses that will reduce the adhesion contribution to friction without introducing a solvent.[30] The SAM layer serves as a dense sublayer creating internal tethering for the flexible PDMS network surface.

The network – SAM hybrid lubricants can be created at two very different thicknesses. A micron thick network film is fully cross-linked with a uniform surface and thickness on the microscale (~5 to 30 μm). The networks are synthesized in an end-linking hydrosilylation reaction with telechelic PDMS chains and a tetrafunctional

cross-linking agent on a functionalized SAM-coated substrate. The extractable material from these networks, i.e. material that does not cross-link, is less than one percent. A cartoon of this system is depicted in Figure 1.3.1. An ultrathin PDMS network (~10 nm) can be made by diluting the precursor polymer solution in toluene to 20 percent polymer by volume, resulting in a poorly cross-linked hyperbranched surface film as depicted in Figure 1.3.2.

One of the characteristics of polymer network lubricants determined from previous studies is that the COF decreases as the molar mass of the precursor polymer chains increases. This result is counterintuitive as the higher precursor molecular weights have lower elastic moduli as a result of a lower cross-link density, and this has been attributed to a number of sources. Galliano et al. studied interfacial friction properties of PDMS networks cross-linked in the presence of a platinum catalyst.[33] They attributed the molar mass effect to increased elastic contact for low molar mass systems and thus increase the diffusion of stress to the network. This conclusion focuses on the continuum mechanism for friction. Vorvolakos and Chaudhury also recognized this relationship between the precursor molar mass and the friction and attributed it to the molecular mechanism for friction.[12] They recognized that the number of load-bearing or working chains decreases with the molar mass and theorized that the areal density of chain ends instead plays a significant role. They thus concluded that bulk dissipation cannot be the entire source of the interfacial friction force.

In order to further investigate the role of the physical structure on the interfacial properties, the network structure of the ultrathin films can be partially reproduced in the micron thick networks. The hyperbranched surface for the ultrathin films is expected to be similar to networks synthesized with high concentrations of pendent chains. While defects will create a small amount of pendent chains even

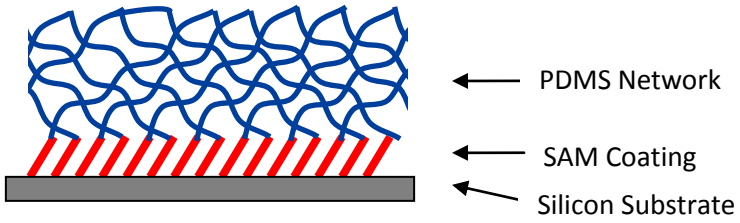

Figure 1.3.1. Illustration of an optimal system. The PDMS network is fully cross-linked and uniform; the SAM coating is not exposed to surface.

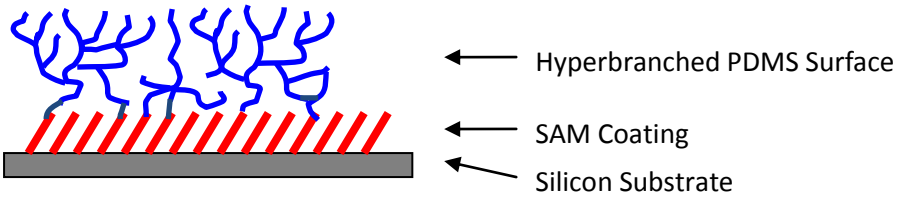

Figure 1.3.2. Illustration of an ultrathin system structure. PDMS is hyperbranched with some level of cross-linking present.

within model networks, a more controlled method of synthesizing the modified networks can be conducted by adding monofunctional PDMS chains to the precursor telechelic chain solution. Two tiers within the PDMS network as illustrated in Figure 1.3.3 will likely be created with high concentrations of these pendent chains at the surface of the network. The dangling chain ends at the surface can create a sparse polymer brush overcoat with high surface mobility above the elastic network. Increasing the degree of hyperbranching by synthesizing networks with greater concentrations of pendent chains also decreases the elastic modulus of the network and increases the interfacial contact area.

The lubricant structure can also be modified by creating networks swollen with free chains, as depicted in Figure 1.3.4. The networks can be synthesized as swollen films by introducing non-functionalized PDMS chains that do not participate in the cross-linking reactions. The PDMS network will then cure in a swollen state. The free chains serve to decrease the elastic modulus of the lubrication system while holding the interface constant. Synthesizing swollen networks enables a further investigation of the role of the physical structure in determining the friction properties, as well as the importance of viscoelasticity at the interface and within the lubricant system during friction and wear.

Studying this series of lubricant systems and network structures will not allow for complete conclusions in regards to the source of the frictional, adhesive and wear properties. Focusing solely on PDMS polymer systems may conceal any chemical contributions as results of the physical structure. The only differing element between each of the four network lubricants already described is the structure and resulting physical properties; the PDMS chemistry is held constant for all studies. In order to investigate the role of the surface chemistry, films synthesized from other polymers can also be investigated. A series of polymer brushes, as illustrated in Figure 1.3.5,

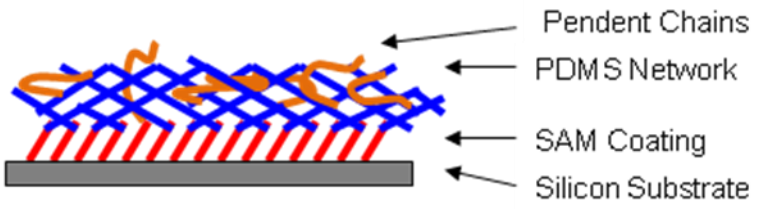

Figure 1.3.3. Illustration of a micro-thick system structure with pendent chain modifications. PDMS is not fully cross-linked and has some hyperbranching.

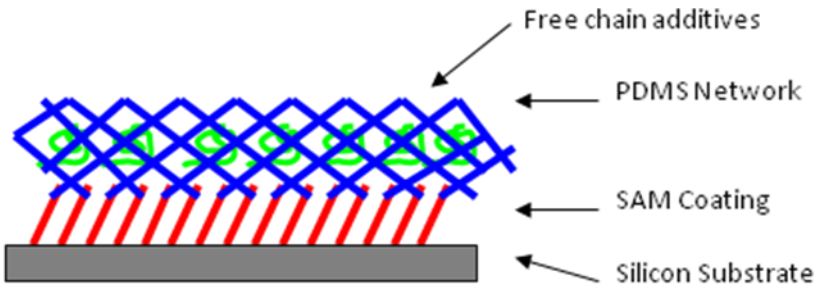

Figure 1.3.4. Illustration of a micro-thick system swollen with free chains. The PDMS network is fully cross-linked.

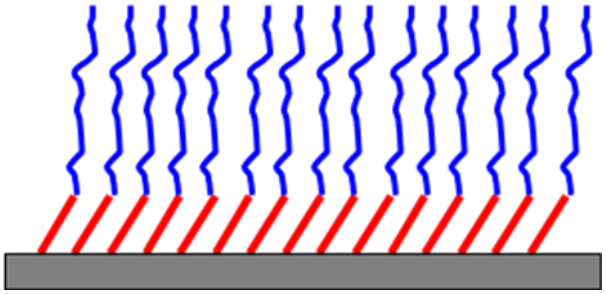

Figure 1.3.5. Illustration of polymer brushes in a stretched brush state anchored to a SAM-coated substrate. Surface coverage is high, and the distance between tethered ends of the polymer chains is low.

can be synthesized as the best approach to studying the chemical effects. In effect, the physical effects will be limited by deconstructing the PDMS-SAM lubricant to the most basic two-tiered structure. Tethered polymer brushes can be formed at different surface coverages and with different chain lengths. Friction and adhesion characterization studies on these surfaces will help to determine the contribution of the structural characteristics on the friction properties. Synthesizing brushes from other polymer with higher surface tensions and interfacial shear stresses, like polystyrene and polypropylene glycol/polyethylene glycol, then allow for an evaluation of the effects of surface chemistry. These analyses can help determine the interplay between friction and adhesion for several polymer lubricants.

REFERENCES

(1) Rymuza, Z. *Microsystem Technologies* **1999**, *5*, 173-180.

(2) Bhushan, B. *Proc. Instn. Mech. Engrs Part J* **2001**, *215*, 77-102.

(3) Cagin, T.; Che, J.; Gardos, M. N.; Fijany, A.; Goddard, W. A., III. *Nanotechnology* **1999**, *10*, 278-284.

(4) Bowden, F.P.; Tabor, D. *Friction and Lubrication.* Methuen & Co. Ltd.: London, 1967.

(5) Wang, W.; Wang, Y.; Bao, H.; Xiong, B.; Bao, M. *Sensors and Actuators* **2002**, *97-98*, 486-491.

(6) Maboudian, R.; Ashurst, W. R.; Carraro, C. *Sensors and Actuators* **2000**, *82*, 219-223.

(7) Sundararajan, S.; Bhushan, B. *J. Vac. Sci. Technol. A.* **2001**, *19(4)*, 1777-1785.

(8) K. Strawhecker, D.B. Asay, J. McKinney and S.H. Kim. *Tribology Letters* **2005**, *19*, 17-21.

(9) Bhushan, B. *Microelectronic Eng*. **2007**, *84*, 387-412.

(10) Zhang, Q.; Archer, L.A. *Langmuir* **2007**, *23*, 7562-7570.

(11) Greenwood, J.A.; Tabor, D. *Proc. Phys Soc*. **1957**, *71* (6), 989.

(12) Vorvolakos, K.; Chaudhury, M.K. *Langmuir* **2003**, *19*, 6778-6787.

(13) Schallamach, A. *Wear* **1963**, *6*, 375-382.

(14) Persson, B.N.J.; Volokitin, A.I. *Eur. Phys. J. E* **2006**, *21*, 69-80.

(15) Chernyak, Y.B.; Leonov, A.I. *Wear* **1986**, *108*, 105.

(16) Ludema, K.C.; Tabor, D. *Wear* **1966**, *9*, 329.

(17) Maru, M. M.; Tanaka, D.K. *J. of the Braz. Soc. of Mech. Sci. & Eng.* **2007,** *29*, 55-62.

(18) Lu, X.; Khonsari, M.M.; Gelinck, E.R.M. *J. of Tribology* **2006**, *128*, 789-794.

(19) Persson, B.N.J. *Sliding Friction: Physical Principles and Applications*. Springer, Berlin: **1998**.

(20) Mate, C. M. *Tribology on the Small Scale: A Bottom Up Approach to Friction, Lubrication and Wear*. Oxford University Press, New York: **2008**.

(21) Frene, J.; Cicone, T. Lemaitre Handbook of Materials: Behavior Models: Friction in Lubricated Contacts. Academic Press, **2001**, 760-767.

(22) Hurtado, J.A.; Kim, K-S. *Proc. R. Soc. Lond. A* **1999**, *455*, 3363.

(23) Zhang, Q.; Archer, L. A. *Langmuir* **2005**, *21*, 5405-5413.

(24) Bhushan, B.; Liu, H.; Hsu, S. M. *ASME J. Tribol* **2004**, *126*, 583-590.

(25) Bhushan, B.; Israelachvili, J. N.; Landman, U. *Nature* **1995**, *374*, 607-616.

(26) Xiao, X.; Hu, J.; Charych, D. H.; Salmeron, M. *Langmuir* **1996**, *12*, 235-237.

(27) Tsukruk, V.V.; Bliznyuk, V.N. *Langmuir* **1998**, *14*, 446-455.

(28) Yang, X.; Perry, S. S. *Langmuir* **2003**, *19*, 6135-6139.

(29) Ahn, H-S; Julthongpiput, D.; Kim, D-I; Tsukruk, V.V. *Wear* **2003**, *255*, 801-807.

(30) Julthongpiput, D.; Ahn, H-S; Kim, D-I; and Tsukruk, V.V. *Tribology Letters* **2002**, *13*, 35-40.

(31) Raviv, U.; Glasson, S.; Kampf, N.; Gohy, J. F.; Jerome, R.; Klein, J.. *Nature* **2003**, *425*, 163-165.

(32) Landherr, L.J.T.; Zhang, Q.; Cohen, C.; Archer, L.A. *J. Poly. Sci. B.*, **2008**, *46*, 1773-1787.

(33) Galliano, A.; Bistac, S.; and Schultz, J. *J. Adhesion* **2003**, *79*, 973-991.

CHAPTER 2

INTERFACIAL FRICTION OF THIN PDMS NETWORK FILMS*

2.1. ABSTRACT

This study focuses on developing dry, surface-tethered polymeric lubricant coatings capable of significantly decreasing friction and wear of nano- and micrometer scale machines. Vinyl-terminated polydimethylsiloxane chains are spin-coated with a crosslinking agent and platinum catalyst onto silicon wafers functionalized with a self-assembling monolayer containing reactive vinyl groups. Lateral force microscopy (LFM) measurements employing a bead probe are used to quantify the coefficient of friction (COF) and adhesion characteristics of the PDMS-SAM surface tethered networks. The combined polymer network and SAM layer manifest extremely low friction coefficients, $\mu \approx 4 \times 10^{-3}$, which is nearly one order of magnitude lower than the friction coefficient of the silicon substrate. The lowest friction forces are measured using silicon substrates covered with nanometer thick, peroxide cross-linked PDMS networks; though poorly cross-linked, these networks display COFs as much as ten-times lower than a solitary SAM coating layer. Micrometer thick end-linked optimal networks also manifest attractive interfacial friction properties, with COFs approximately three times larger than the thinner, imperfect networks. These observations are discussed in terms of the structure of the polymer networks and the role of adhesion forces on interfacial friction.

* This chapter is partially reproduced with permission and appeared in *J. Polym. Sci.: Part B: Polymer Physics* **2008**, *46*, 1773-1787.

2.2. INTRODUCTION

Advances in fabrication methods for assembling small devices, such as Microelectromechanical systems (MEMS) with micron scale feature sizes,[1-3] is fueling demand for new, high-performance boundary lubricants that can operate on the nanoscale. This demand is well-known to originate from the importance of surface forces such as friction and adhesion on these length-scales. The ideal lubricant for these applications must satisfy multiple, sometimes conflicting demands.[4-7] It must be applied as a thin film to preserve the spatial features of the substrate. It should present both a small contact area and low interfacial shear stress to minimize friction. It should be mechanically durable and strongly tethered to the substrate to minimize ware. Standard industrial lubricants and greases have been formulated and optimized over centuries to meet many of these requirements, but cannot be used because both the static friction forces and sizes of the fundamental lubrication units are large enough to disrupt operation of the devices.[7-9] In a seminal study, Sundararajan and Bhushan utilized Lateral Force Microscopy (LFM) to directly measure static friction forces in polysilicon micromotors lubricated with bound and unbound perfluoropolyether (ZDOL) lubricants. The authors reported that even when ultra thin films of the free, mobile lubricant are used, static friction forces as much as three times higher than those for the unlubricated devices are observed. On the other hand, micromotors lubricated using bound films of ZDOL manifested reduced static friction forces and stiction characteristics that are less sensitive to humidity.[7] These findings suggest that solid-like, hydrophobic, surface-bonded lubricant films can provide an effective means for minimizing stiction forces in small devices.

Self-assembling monolayers (SAMs) have received a great deal of interest as lubricants for small devices, not only for their good boundary lubrication and durability, but also for their relative ease of deposition.[1,10-14] Hexadecane-thiol SAMs

have been reported to reduce the coefficient of friction (COF) of bare silicon by as much as 90 percent.[10] This compares very well with results from diamond-like carbon coatings, which reduced the COF by only 45 percent. The authors attributed the improved friction reduction in the SAM layer to the lower adhesion forces in the SAMS. Xiao et al. investigated the effect of alkyl chain length on the COF of SAMS tethered to mica. These authors report that short SAMs (less than 8 C atoms) provided almost no lubrication, and in many cases increased friction forces on the substrate.[12] Longer SAMs (e.g. 18 C), on the other hand manifest friction force reductions as much one order of magnitude lower than the unlubricated substrate. These observations are generally understood in terms of the greater disorder (patchy structure) of SAMS based on lower molecular weight chains. Work by Liu and Evans for example demonstrate that as the hydrocarbon monolayers became shorter, and more rigid, shear forces produced during sliding result in faster deterioration of the films, which increases the friction force.[15] This effect has been explored in detail in a series of studies by Zhang and Archer, which use AFM and lateral force microscopy (LFM) to simultaneously probe the effect of SAM structure and packing density of interfacial friction and adhesion. Consistent with earlier studies, these authors report that longer alkane chains (C >10) lead to SAMS with lower COFs than shorter ones.[16-18] Significantly, they also observed that two-tiered SAMS created from symmetric blends of long and short alkylsilanes generally manifest friction coefficients lower than the single component SAMS. Zhang and Archer showed that LFM measurements performed in an ethanol medium eliminated the adhesion contribution to the friction force, resulting in dramatically lower friction in the two-component SAMs than in the single-component materials. Analysis of the friction data using a Eyring-type analytical model that accounts for the monolayer viscoelasticity indicate that the superior friction properties of the two-component SAMS are a consequence of

greater disorder and higher molecular mobility in the outermost or canopy layer of the mixed monolayer.[18]

Ultrathin polymer layers have been studied by several groups to determine the effect of chain mobility and molecular flexibility on interfacial friction properties.[19-21] Mobility refers to the ability of the polymer chains to adjust laterally to interfacial contact, while the chain flexibility describes the relative stiffness of the polymer chains, regardless of direction. Raviv et al., for example, characterized the interfacial friction coefficient of opposing mica sheets functionalized with sulphonated polyelectrolyte brushes in water using the surface forces apparatus (SFA).[19] Some of the lowest published COFs to date, $\mu = 0.0006$, were deduced from these studies. The authors attribute the low COF to high resistance to polymer chain interpenetration, which localizes sliding to a thin interfacial region at most one-three Kuhn segments thick. Ohsedo et al. studied the surface friction forces of poly(sodium 4-styrenesulfonate) brushes on a poly(2-hydroxethyl methacrylate) gel.[20] The authors found the COF was highly dependent on the chain length and mobility; long chains produced low COFs at low sliding velocities, but manifested reduced ability to lower the interfacial friction force at higher sliding velocities. Ohsedo et al. explained these results by arguing that longer chains were more likely to compress at higher sliding velocities and thus reduce the polymer chain mobility at the surface. An earlier study by Brown indeed found polymer mobility to be a major factor in setting the interfacial stress and friction force at polymer surfaces.[21] Specifically, Brown investigated interfacial friction forces between a polydimethylsiloxane (PDMS) network sliding against ultrathin PDMS films comprised of chains end-tethered to a polystyrene surface, and determined that while shorter, stiffer chains could penetrate the network and increase the interfacial friction force, longer chains with higher mobility showed more liquid-like interfacial qualities, lowering the interfacial shear stress.[21]

Several studies have compared the effectiveness of polymer films, surface tethered gels, and SAMS as wear resistant coatings. The low wear resistance of dry polymer films is generally believed to pose a serious obstacle to applications of these materials as lubricants, particularly at high sliding speeds.[22] Julthongpiput et al. reported that a dry polymer layer manifests only slightly better wear resistance than a bare silicon substrate.[23] On the other hand, these authors showed that wear resistance of a SAM layer is significantly better than the dry polymer coating, but that the wear resistance of polymer networks swollen with solvent (gels) is even better under both low and high normal loads. The authors also found that the coefficient of friction of the gels is generally lower than that of the SAMS, which are in turn typically lower than those measured using dry polymer coatings. Based on the findings from these earlier studies, it can be concluded that nano- and micro-scale lubricant coatings should consist of a two layer structure: a densely-packed sublayer, highly ordered to prevent penetration and surface contact; and a more disorganized layer, tethered to the sublayer, possessing high mobility and low shear resistance.

Herein we report synthesis and interfacial friction properties of two-tiered tethered lubricant coatings comprised of optimal PDMS-network films tethered to a dense SAM undercoating. PDMS is attractive as a lubricant coating for multiple reasons, including its low surface energy, exceptional molecular flexibility, low glass transition temperature, and ease with which it can be synthesized. Previously, Galliano et al. studied interfacial friction properties of PDMS networks cross-linked by a platinum catalyst.[24] These authors found that the frictional stress between the networks and glass particles decreased as the PDMS precursor molecular weight increased. However, the authors also showed the adhesion to the network was larger at higher molecular weights. These results can be explained in terms of a higher elastic contact for the lower molecular weight networks, which would increase the

stress transmission to the network. Recently, Zhang and Archer reported LFM studies of PDMS networks containing free chains. These authors reported that the COF for these swollen networks was lower than that of a dry network made from the same precursor chains, and that the COFs increased for the swollen networks with the swelling agent chain length. The authors attributed the COF changes to the swelling chain viscosity and concentration.[25]

2.3. EXPERIMENTAL SECTION.

2.3.1. Preparation of SAMs. Dichloromethane (CH_2Cl_2), methanol (CH_3Cl), hexadecane ($C_{16}H_{34}$), and chloroform ($CHCl_3$) were purchased from Aldrich Chemicals. 10-undecenyl trichlorosilane was purchased from Gelest, Inc. Three-inch (100) silicon wafers from University Wafer were cut into 2 cm by 2 cm pieces using a diamond tipped stylus. The wafer pieces were then prepared by cleaning with Kimwipes, rinsing in chloroform ultrasonically, and treating for 30 minutes in piranha solution of 12 mL hydrosulfuric acid (H_2SO_4) and 10 mL 30% hydrogen peroxide (H_2O_2) above 130 ^oC. The cleaned wafer pieces were then repeatedly rinsed in DI water and blown dry with nitrogen gas.

Solutions of hexadecane and chloroform were prepared with a 4:1 volume ratio in separate flasks for a total volume of 40 mL. These solutions, along with the cleaned wafers, were placed in a glovebox with a dry nitrogen atmosphere. Approximately five of the cut wafer pieces were placed in each flask, after which 24 µL of the 10-undecenyl trichlorosilane was added. The wafers were allowed to sit in the glovebox overnight to allow the SAM layers to form. Outside the glovebox, the silicon pieces were rinsed successively in dichloromethane, chloroform, and methanol baths for approximately five minutes each to remove any excess material. The monolayer-coated wafers were then dried under a nitrogen stream and stored.

2.3.2. Preparation of PDMS Networks. Vinyl-capped PDMS precursor molecules with molar mass ranging from 800 to 28000 g/mol, a crosslinking agent tetrakis(dimethylsiloxy)silane and platinum-divinyl tetramethyl-disiloxane were purchased from Gelest. Toluene was purchased from Aldrich. The crosslinking agent and PDMS were first mixed in vials at optimal ratios described previously.[26] If a thin network film is desired, toluene was added to the PDMS and crosslinker solution. In a separate vial, 100 µL of the platinum catalyst was diluted in 10mL of toluene. Immediately after mixing the correct amount of catalyst solution with the PDMS and crosslinker, the solution was poured onto the SAM-coated silicon wafer substrates. The cut wafers were spincoated at 3000 rpm for 60 seconds using a SCS P6708 spincoater. To ensure complete annealing of the PDMS chains and to remove any excess toluene, the silicon pieces were placed in a vacuum oven at 35 ^{o}C. After 24 hours, the vacuum line was shut off, and pressure was returned to atmospheric, but the temperature was maintained at 35 ^{o}C for three days. The final silicon pieces, after an initial thickness measurement, were twice rinsed in dichloromethane for five minutes each time to remove unbonded material. Excess solvent was removed by reheating the wafer pieces for one hour at 75 ^{o}C, and the thickness of the surface coatings remeasured.

2.3.3. Characterizing the Thickness of the PDMS Networks. The thickness of thin PDMS network coatings, developed from dilute solutions of the precursor polymer, was determined using a Rudolph Research Auto-EL Ellipsometer. At least three measurements were taken at multiple locations on the silicon substrate to compute the average thickness and to determine the film uniformity. For thicker PDMS networks produced from concentrated solutions and neat melts of the precursor polymer, the thickness was determined using a F20 Film Metrics Spectrophotometer. A constant refractive index of 1.4 was used for PDMS.[25] Approximately five measurements were

taken at multiple positions on the substrate to characterize the average thickness and uniformity of network films formed.

2.3.4. Preparation of Monofunctional PDMS chains. Cyclohexane (C_6H_{12}), n-butyl lithium (C_4H_9Li) and dried DMSO ($(CH_3)_2SO$) were purchased from Aldrich. Monofunctional PDMS chains were synthesized from purified hexamethylcyclotrisiloxane (D_3) dissolved at 33 ^oC in a solution of distilled cyclohexane at a ratio of 5mL D_3 : 4mL cyclohexane. The solution was placed in a glovebox with a nitrogen atmosphere, with n-butyl-lithium added as an initiator. The stoichiometric ratio of initiator to solution was selected to reproduce conditions reported by Batra et al.[27] After ten minutes, DMSO was added at a ratio of 1.2 mL DMSO : 30 mL D_3. Mixing continued for four hours at 33 ^oC until polymerization was completed.

2.3.5. AFM Analysis. Friction and indentation measurements were conducted using a DI3000 Atomic Force Microscope (AFM). Two different cantilevers were purchased from Novascan; both sets had reported spring constants of 4.5 N/m with beaded tips of 5 μm radius. Polyethylene-bead tips were used for most of the analysis reported in this paper because they provide good repeatability between experimental runs and do not contaminate easily. To evaluate the influence of the tip chemistry on friction force results, a smaller number of measurements were performed using 5 μm silica bead probes coated with a 10-undecenyl trichlorosilane SAM layer. The same SAM deposition procedure used for the wafers was used for surface functionalization of the beads.

Surface friction force data were obtained by scanning the AFM cantilever probe in the forward and reverse directions against the substrate in contact mode. Disabling other scan lines allowed a friction loop to be characterized, wherein the average difference between values from opposing scan directions provides a value for

the friction force. Data were collected at scan lengths of 5.0 μm and a fixed scan rate of 1.0 Hz. Applied load was varied by changing the operating height of the cantilever. Five different loads were used for each friction measurement, and friction values were tabulated after reaching a steady-state friction force value for each new load. The final friction-load plots were constructed from an average of data measured at several different points on each surface. The AFM provides normal and lateral force values (N and F) in terms of voltage (V), which can be converted to the proper units through the relations

$$N = \alpha V_n = K_n S_n V_n \quad (1)$$

$$F = \beta V_l = K_l S_l V_l \quad (2)$$

The normal sensitivity S_n was determined from the force-distance curves and used to calculate the lateral sensitivity S_l as described by Liu and Evans.[15] The dimensions of the cantilever were used to determine the lateral force constant K_l. The normal force constant K_n was determined using the added-force method described by Cleveland et al.[28] This method was important in determining the force constant of the SAM-coated silica bead cantilevers, as well as for checking the reported values for the polyethylene bead tips. In using this method, glass particles ranging in diameter from 10 to 50 μm were attached to the cantilever tip by pressing down on the tip while in contact with the glass particles. The resonant frequency of the cantilever with added weight was then recorded. The masses of the glass particles used were calculated from the bulk density of glass and from the diameter of the particle as compared to the AFM cantilever. The normal force constant of the SAM-coated cantilever was found to be 1.42 N/m, while the value for the polyethylene bead cantilever was determined to be 4.47 N/m, close to the reported value of 4.5 N/m.

Friction-load plots provide a straightforward elementary value for the COF from the average slope of each trendline. A deeper evaluation of the data sets also

considers the effect of adhesion. The necessary cantilever force required to overcome the adhesion between the AFM cantilever and lubricant surface is described by the intercept of Amonton's Law, where the lateral friction force (F) is equal to the product of the coefficient of friction and both the load (N) and a residual force (F_a),[29]

$$F = \mu * (N + F_a) \quad (3)$$

Thus, the intercept of a plot of F/μ versus N yields the residual force, F_a. F_a can also be estimated as the product of the contact area between cantilever probe and substrate and the adhesion controlled critical interface shear stress, τ_o. An extended form of Amonton's Law can be used to break down the residual force into "molecular" and adhesion-related components:

$$F = \tau_o * A + \mu * (N + N_c) \quad (4)$$

where N_c is the critical load.[25] This extended equation becomes particularly important when the friction-load relationship is nonlinear. However, because τ_o is proportional to the interfacial energy between the cantilever and the surface, the more basic form of the residual force is useful when the interfacial energy is low enough to yield a linear relationship.

Additional insight into the adhesion properties of the substrate can be obtained from force-distance curves obtained using the AFM. Specifically, the force required to separate the cantilever from the lubricant surface, also known as the pull-off force, can be determined from the depth of the deflection well on the AFM curve (denoted as *h* in Figure 2.1), while the distance traveled by the cantilever before separation occurs is collected from the width of the deflection well (*w* in Figure 2.1).[29] The product of *h* and *w* therefore provides an estimate of the work of adhesion at the measurement conditions.[25]

2.3.6. Characterizing the Elastic Modulus of PDMS network films. AFM force-distance curves can be used to characterize the elastic properties of a polymer film

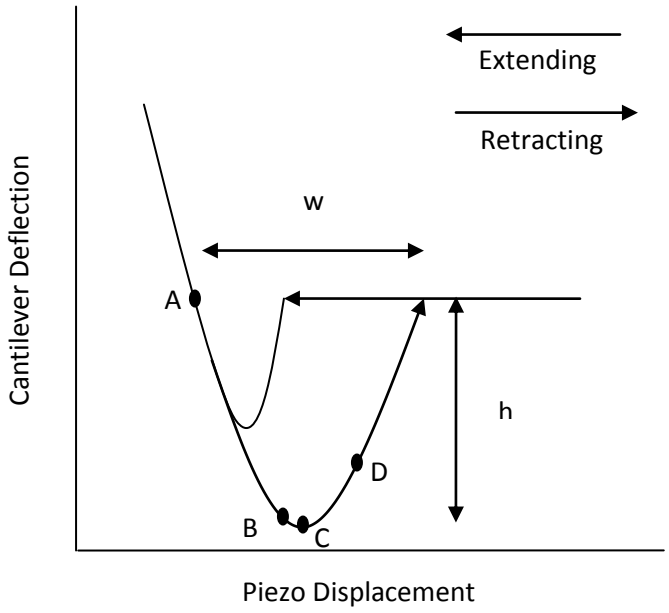

Figure 2.1. Schematic for an AFM force-distance curve, with important nanoindentation points depicted.

tethered to a rigid substrate. Force-distance curves are obtained from the movement and interaction of the AFM cantilever as it travels vertically, extending towards and retracting away from the surface. In a typical experiment, data collection begins as the piezo, the motor-controlled base for the cantilever, begins its approach to the surface. Eventually, adhesive forces between the cantilever and the sample will overcome the stiffness of the cantilever, and pull the cantilever tip down to the surface. The piezo continues its approach at a steady rate; once it has descended to the point where the cantilever is no longer deflected, the force on the cantilever returns to zero. Subsequent to this point, the piezo will continue to descend as the cantilever deflects upwards (Fig 2.1). The force-deflection relationship that develops during this step provides data on the sensitivity of the cantilever, as previously described. Once a maximum deflection setpoint is reached, the piezo will automatically begin to ascend to prevent physical damage to the cantilever. Adhesive forces can hold the cantilever to the surface beyond the zero-deflection setpoint, and can even lead to a stretching of a polymer film tethered to the surface. This stretching continues until the bond between the AFM probe and surface coating fails, releasing the probe and causing the cantilever deflection to return to zero.

Several published works have shown how the level of adhesive forces and actual contact area between cantilever tip and surface can modify indentation and influence physical properties deduced from them.[30-34] These studies indicate that four points (see Figure 2.1) on the cantilever retraction curve provide important information that can be used to determine the elastic modulus of the surface coating. Point (A) corresponds to the location where the deflection on the cantilever is zero; this signals a baseline that allows for normalization between force-distance data sets. Point (B) is the maximum indentation into the surface developing from interactions between the cantilever tip and the adhesive forces on the surface. The third datapoint

(C) corresponds to the maximum adhesive force exerted on the cantilever by the surface, and the fourth point (D) signals the breaking point at which the cantilever tip is released. Depending on how the cantilever interacts with the surface, all four datapoints are not necessary to determine the elastic modulus. From at least two, the modulus of the surface material can be determined; from all four points the interfacial energy and adhesive forces can also be calculated.

2.3.7. Characterizing PDMS networks using solvent swelling measurements. Additional information about elastic properties and molecular structure of PDMS networks can be obtained from swelling studies. To carry out these studies we use PDMS oligomer chains with molar mass of 800 g/mol purchased from Gelest as a swelling agent. The high molar mass of the PDMS swelling agent ensures low volatility, which is advantageous for room temperature analyses of the swollen film thickness. To quantify the equilibrium swelling ratio of surface-tethered networks, small amounts of oligomer were added to the networks in a series of intervals, and the film thickness characterized after allowing several hours for the oligomer to fully diffuse into the film. The procedure was repeated until the thickness of the swollen network film displayed a sudden increase. This increase was interpreted to correspond to the condition where excess of the oligomer simply accumulates on the surface of the network films, indicating that equilibrium swelling had been achieved.

The swelling ratio obtained in this manner can be compared with values expected from theory, allowing the cross-link density and elastic modulus of the tethered films to be computed. Two analytical expressions are used in this study to analyze data from the swelling measurements. The first analysis is based on the one-dimensional swelling equation proposed by Toomey et al.,[35]

$$\alpha_{1D}{}^{3} - \frac{2}{f\alpha_{1D}} = \frac{0.5-\chi}{V_1 N_{cd}} \qquad (5)$$

where χ is the Flory-Huggins interaction parameter, N_{cd} is the crosslink density, V_1 is the solvent molar volume, f is the network functionality, and α is the swelling ratio. The second expression was proposed by Zhang and Archer,

$$\alpha_{1D}{}^4 - \alpha_{1D}{}^2 - \frac{\xi}{2}\left(1 - 2\chi N_s\right)\alpha_{1D} - \frac{\xi}{3} = 0 \qquad (6)$$

where α is the swelling ratio, ξ is the ratio of molar mass between cross-links to swelling agent molar mass, and N_s is the mole fraction of swollen chains in the crosslinked network.[25] Toomey's equation is based on the assumptions of a small-molecule solvent as the swelling agent and that large swelling occurs, while Zhang and Archer's equation describes swelling by an oligomer. Considering short PDMS chains are to be used, it might seem that Eq. (6) is more relevant. However, because of the thinness of some of the network films studied, it is experimentally quite challenging to accumulate sufficiently accurate swelling data before reaching the *overcoated* end point described above. To circumvent this challenge, the oligomer was diluted in toluene, and this mixture used as the swelling agent. The toluene was then evaporated before measurements were taken.

2.4. RESULTS AND DISCUSSION.

2.4.1. Ultrathin Film PDMS Network Lubricants. Figure 2.2 summarizes friction force, *F*, data versus normal force, *N*, for various lubricant coatings on silicon. These measurements were obtained using LFM performed with polyethylene bead probes. For all materials studied, the figure shows that *F* versus *N* plots are straight lines with slope equal to the coefficient of friction (μ) of the coating. Table 2.1 compares COF data for three materials, a SAM layer, a cross-linked PDMS thin film physically attached to silicon, and an ultrathin PDMS-SAM system covalently tethered to silicon; both sets of PDMS results in the table are for a fixed precursor molar mass of 9400 g/mol ($\bar{R}_g = 2.7nm.$). The PDMS-SAM layer system evidently displays the lowest

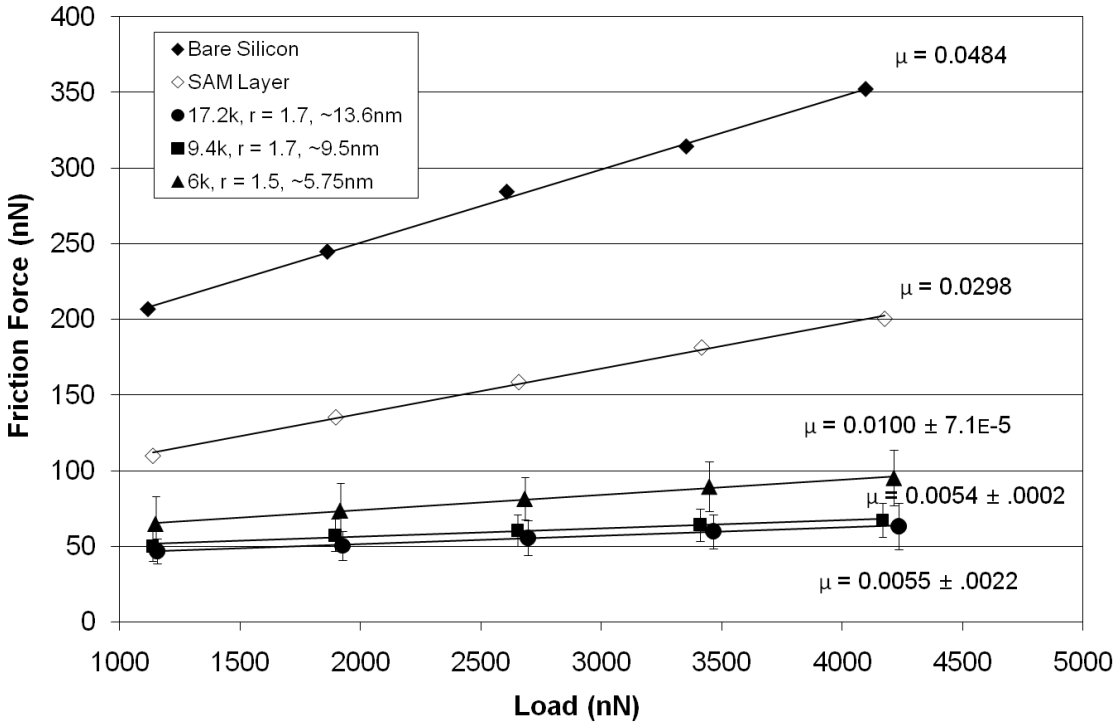

Figure 2.2. Friction force versus Normal Load for various ultrathin PDMS-SAM lubricant systems obtained by cross-linking different molar mass precursor chains.

Table 2.1. Friction coefficients for three lubricant systems obtained from LFM using PE bead probes. Here *d* is the thickness of the lubricant coating and all PDMS chains used have M_w = 9400 g/mol.

Lubrication System	**COF (μ)**
SAM (*d* ~ 1.2 nm)	0.03
PDMS on Silicon (*d* ~ 50 nm)	0.011
PDMS on SAM (*d* ~10 nm)	0.005

COF, approximately one order of magnitude lower than that measured using a bare silicon substrate (see Fig. 2.2). It is also apparent that lubricant coatings that are covalently tethered to a SAM layer provide close to a 50% reduction in COF, relative to physisorbed versions of the coatings. These results are consistent with those reported by Julthongpiput et al., where surface-attached polymer networks were also found to manifest the lowest COF.[23] Taken together, the consistency between the two sets of observations and the significant improvement in COF observed for the PDMS-SAM tethered lubricant system underscore the promise of these materials as lubricants. Additionally, the exceptional thinness of the polymer network coatings implies that these lubricant systems are compatible with small devices such as MEMS.

The effect of the PDMS precursor molar mass on interfacial friction of ultrathin PDMS-SAM lubricant systems was investigated by systematically varying the precursor PDMS polymer molar masses over the range 6000, 9400, and 17200 g/mol. This means that the mean radius of gyration of the PDMS network strands studied varies from 2.1 nm. to 3.6 nm. Thus, in every case, the network strand thickness is at least one half the film thickness. To produce optimal networks (ie. maximum cross-linking of the precursor chains) curing was performed using a ratio of crosslinker reaction site to PDMS vinyl functional end ratios of r = 1.5 and r = 1.7 found for bulk PDMS systems.[36] The critical molar mass M_e for PDMS strands to entangle is 12.3 x 10^3 g/mol, which means that for the highest polymer molar mass studied, some level of reinforcement (small) of the chemical cross-links by physical entanglements is possible. Friction force versus normal load data for PDMS networks with varying precursor polymer molar mass is presented in Figure 2.2. It is apparent from the plot that while all of the PDMS-SAM films manifest low friction coefficients, networks prepared using the higher molar mass precursors display the lowest COFs.

Inherent advantages of PDMS as a lubricant coating have already been described. They certainly play a role in the generally lower COFs of the PDMS-based coatings. However, these attributes alone cannot explain the superior performance of the PDMS-SAM tethered lubricant system, compared with coatings produced by physical adsorption of cross-linked PDMS to the substrate. Insight into this difference can be obtained by considering the coating resistance to dichloromethane (a good solvent for PDMS). Specifically, both the physically adsorbed and PDMS-SAM tethered networks manifest measurable changes in thickness upon treatment with dichloromethane. Whereas the thickness of PDMS-SAM coatings decrease by ca. 30 percent when treated with dichloromethane, the physically adsorbed systems loses almost 80 percent of its mass in the rinse. The latter observation is readily explained in terms of the absence of strong covalent bonds to anchor these networks to the silicon surface. The former implies that a significant fraction of the precursor PDMS chains are not linked to the rest of the network or the SAM underlayer.

To produce the ultrathin PDMS-SAM network coatings used in the study, the precursor polymer must be highly diluted in toluene; we were unable to consistently produce ultrathin films below 20 volume percent PDMS in toluene. The overlap volume fraction for PDMS in toluene ranges from 8.1 percent for 6000 g/mol to 4.8 percent for 17200 g/mol. Because the polymer concentration is several times above the overlap limit, the chains should be clustered enough for at least some cross-linking to develop. However, the degree of molecular interpenetration is substantially lower than in a melt of the precursor chains, which limits the degree of cross-linking that can be achieved. We therefore tentatively explain the thickness loss in terms of a large soluble fraction of polymer structures unattached to the SAM layer.

This explanation implies that the PDMS network layer should contain a large concentration of defects, including pendent chains and loops. It also implies that the

overall network structure is quite different from than proposed (Figure 2.3.1). Specifically, while the relatively low level of weight loss indicates that some level of cross-linking certainly exists near the SAM-PDMS interface, we suspect that the remainder of the coating is closer in appearance (as in Fig. 2.3.2) to a brush of hyperbranched chains than to a well cross-linked network. In this scenario, the underlying SAM layer would still serves as a densely packed, high-modulus support layer, while the branched coating acts as a high-mobility fluid overcoat that remains anchored to the substrate. Such a two-tiered coating has already been argued to produce superior boundary lubrication performance in SAMs[16], and could account for the low COFs we observe.

The poor cross-linking nonetheless brings into question the efficiency of the hydrosilylation reactions between the vinyl endcapped SAMs and PDMS chains and the Si-H bonds on the crosslinking agent. To prove that dilution in toluene is the source of this reduction in cross-linking efficiency, we developed other PDMS-SAM systems using benzoyl peroxide as a free radical catalyst. As with the previous systems, precursor polymer chains were diluted in toluene and spin-coated onto the substrate produce networks films a few polymer radii thick. This method has been used before to produce PDMS networks on SAM layers, and has been shown to result in similar bonding between polymer chains as achieved in hydrosilylation reactions.[36] The thickness of ultra thin film PDMS networks produced in this manner were found to decrease by 30 to 50 percent when rinsed with dichloromethane, confirming that incomplete cross-linking occurs in these systems. Figure 2.4 plots the friction force versus normal load obtained from LFM experiments employing polyethylene bead probes for a range of precursor polymer molar masses. Again the *F* versus *N* plots are found to be straight lines over the entire range of *N* studied. The friction coefficients deduced from these plots are also seen to be quite consistent with the ones reported in

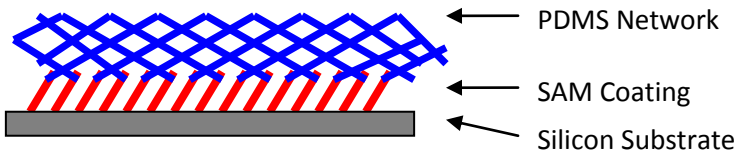

Figure 2.3.1. Illustration of an optimal system. The PDMS network is full crosslinked and uniform; the SAM coating is not exposed to surface.

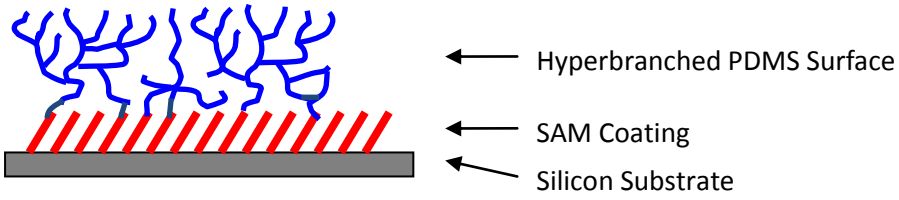

Figure 2.3.2. Illustration of an ultrathin system structure. PDMS is hyperbranched with some level of crosslinking present.

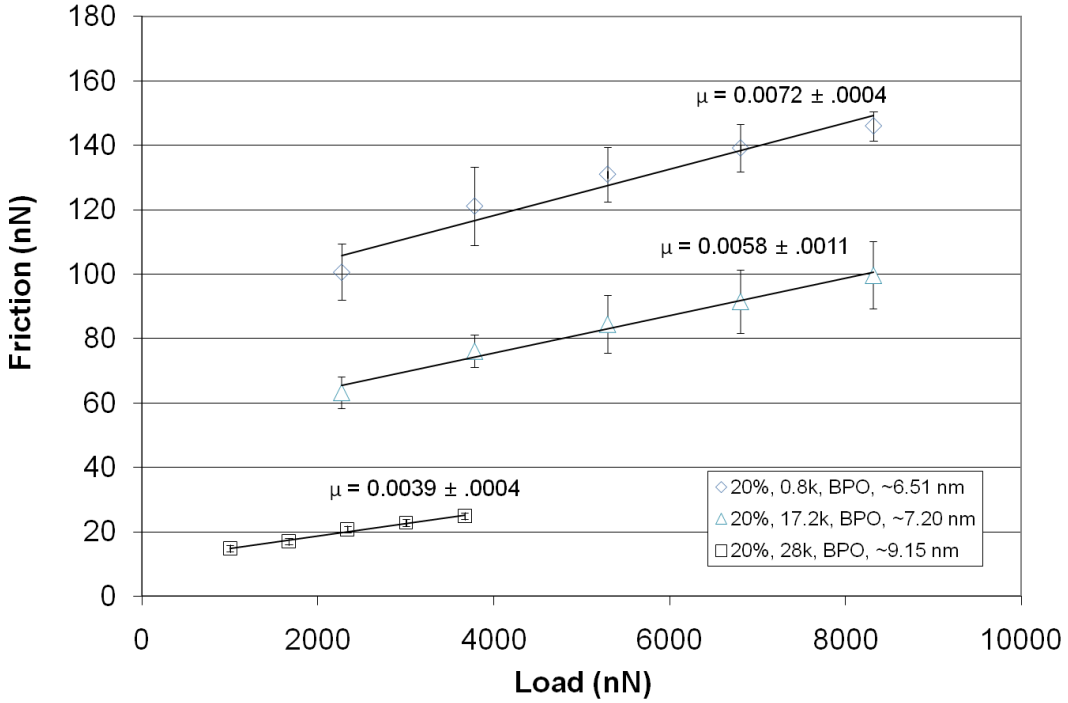

Figure 2.4. Friction coefficients of ultrathin PDMS networks from different precursor chain molar masses cured with free radical catalyst.

Figure 2.2; where the trend towards lower COF as the precursor polymer molar mass increases is also quite clearly observed.

While an analysis of the amount of polymer lost in a dichloromethane rinse provides some information about the structure and stability of the PDMS-SAM systems, more detailed analysis is needed to reach firm conclusions about the coating structure. Swelling experiments, for example, can be used in conjunction with theory to provide a wealth of insight into the structure and mechanical properties of cross-linked polymer systems. To characterize the swelling properties of thin film PDMS coatings, the multistep procedure described earlier was used. Swelling ratios obtained from these measurements are reported in Table 2.2. The table also includes theoretical predictions for the swelling ratios expected if the cross-linking procedure yields the perfect network structure depicted in Figure 2.3.1. The theoretical predictions are based on small-molecule (Toomey) and oligomer (Zhang and Archer) swelling agents. With the exception of the networks prepared using the 17.2k PDMS chains, the experimentally determined swelling ratios are substantially higher than the predicted ones. Based on the measured swelling ratios it is possible to use EQ 6 to estimate the molar mass, M_c, of the equivalent PDMS network strands that would produce this level of swelling. M_c for the networks produced by cross-linking the 6000 g/mol PDMS chains is, for example, calculated to be 0.7×10^6 g/mol, which is close to 100 times larger than the targeted cross-link molar mass. The corresponding calculations for the 9400 g/mol PDMS network yield $M_c = 0.16 \times 10^6$ g/mol, for the 28000 g/mol network, M_c = 381000g/mol. These large differences between targeted and actual PDMS cross-link size, is consistent with the picture of poorly cross-linked coatings of irregularly branched/hyperbranched chains proposed in Fig. 2.3.1. The relatively low swelling ratio seen in networks comprised of the 17.2k PDMS chains is inconsistent

Table 2.2. Comparison of experimentally determined swelling ratio with swelling ratios predicted from the Toomey et al. equation (EQ 5) and the Zhang and Archer (Z-A) equation (EQ 6).

Predicted Swelling Ratios			**Measured Swelling Ratio**
MW	**α (Toomey)**	**α (Z-A)**	**α**
6k	1.68	1.91	4.30
9.4k	1.92	2.14	2.96
17.2k	2.30	2.52	2.02
28k	2.68	2.90	3.55

with this conclusion, however, and point to a different explanation of the low COFs manifested by these coatings.

The intercept of an F versus N plot provides information about the residual force F_a and adhesion characteristics of the coatings. AFM force-distance curves provide additional information about the adhesion properties of these coatings. Table 2.3 summarizes F_a and the depth h and width w of the force-distance minima (Fig. 2.1) for all of the materials studied. The product of h and w can be used to obtain a very rough estimate of the work of adhesion. It is striking that even surface coatings that manifest well-controlled low friction coefficients, display exceptionally large (as high as 32 percent) variations in residual force. While this behavior can in principle originate from surface contamination, it is consistently observed in experiments performed under controlled clean-room conditions. We believe it originates from the patchy morphology of the thin coatings. Additionally, the data reveals no correlation between the COF and F_a, or between the COF and the work of adhesion, for networks cross-linked using the hydrosilylation scheme. With the exception of the 9.4k networks, the BPO cross-linked systems show a trend towards lower F_a as the precursor molar mass increases. This trend is, however, opposite of what is seen from the work of adhesion data. The apparent contradiction is at least partially a result of the increase in the coating thickness as the precursor molar mass increases. It is also consistent with an increase in elasticity of the networks (increase distance to pull-off) as the precursor polymer molar mass increases.

2.4.2. Thin Film PDMS Network Lubricants. Thicker lubricant coatings (d ≈ 2-10 μm) comprised of networks with better defined structure can be developed when the polymer and crosslinker are not diluted with toluene.[36] An advantage of these systems is that by systematically varying the amount of monofunctional precursor chains in the networks, it is possible to introduce defects (e.g. dangling or pendent chains) [37] in a

Table 2.3. COF, residual force, and AFM force-distance curve depth and width data for both the hydrosilylation and BPO crosslinked ultrathin lubricant systems.

	MW	μ	F_a (nN)	h (nN)	w (nm)	h x w (nN-nm * 10^3)
Ultrathin	6000	0.0100 ± 7.1E-5	5342 ± 1707	1586 ± 137	375 ± 176	595 ± 284
	9400	0.0054 ± .0002	8411 ± 1346	1666 ± 31	550 ± 70	916 ± 118
	17200	0.0055 ± .0022	7747 ± 2131	1863 ± 33	450 ± 282	838 ± 526
BPO	800	0.0072 ± .0004	12426 ± 2521	1055 ± 38	310 ± 14	327 ± 19
	6000	0.0078 ± .0019	10155 ± 421	1193 ± 4	315 ± 7	376 ± 8
	9400	0.0058 ± .0006	12853 ± 3506	1193 ± 14	330 ± 10	394 ± 13
	17200	0.0058 ± .0011	9037 ± 1251	1398 ± 51	350 ± 9	489 ± 22
	28000	0.0039 ± .0004	2818 ± 854	1374 ± 3	480 ± 42	660 ± 58

controlled manner to evaluate their role on interfacial properties of the coatings. PDMS-SAM networks synthesized from polymer melt precursors displayed dramatically lower volume of material lost (polymer loss < 1%); providing strong support that the networks are optimally cross-linked and close to the model system envisaged in Fig. 2.3.1.

To characterize the effect of polymer precursor molar mass on surface properties of the networks, micron-sized cross-linked PDMS coatings were synthesized on silicon using precursor molar masses of 9400, 17200 and 28000 g/mol. Cross-linking was performed using the hydrosilylation chemistry described earlier. The friction force versus normal load results determined from LFM measurements employing polyethylene bead probes are summarized in Figure 2.5. As observed previously for the ultra thin coatings, *F* versus *N* is a straight line for all materials studied. The friction coefficients deduced from the slope of the plots reveal several important features. First, the COF decreases as the precursor polymer molar mass is increased. This trend is similar to that observed previously for the ultrathin BPO cross-linked networks, but is more pronounced. In an optimally cross-linked polymer network, the molar mass of the precursor chains is close to the average molar mass between cross-links. Thus, a decreasing COF with increasing precursor molar mass is equivalent to a decreasing COF with decreasing elastic modulus of the PDMS-SAM coating.

Second the magnitude of COFs is comparable to those observed for the ultrathin coating systems. The greatest decrease in friction for the ultrathin coatings (the 9.4k and 17.2k materials) is about 88 percent, compared to the COF for bare silicon. For the 28k micron-sized coating system, the COF reduction from bare silicon is approximately 78 percent, roughly equivalent to the reduction for the 6k ultrathin lubricant system. This means that the while the complex topology of PDMS molecules

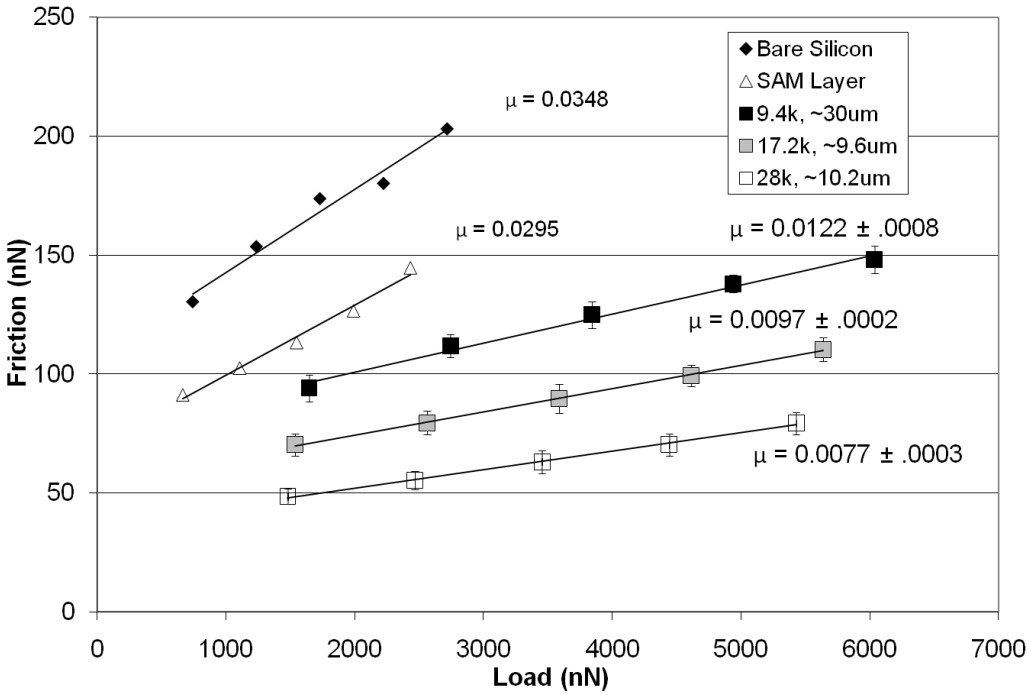

Figure 2.5. Molar mass comparison between micro-film network PDMS-SAM lubricant systems.

in the former systems might have an effect on the friction coefficient, the effect is not large. It also means that the thickness of PDMS-SAM coatings does not substantially impact the COF.

2.4.3. Effect of the surface chemistry of the bead probe. All of the results described so far have been obtained using a polyethylene bead probe. As discussed earlier, PE bead probes are advantageous in LFM studies because they minimize material transfer to the probe, do not contaminate easily, and yield exceptional repeatability in friction measurements. They nonetheless suffer from drawbacks associated with the roughness of the beads and uncertainty about the role the low surface energy of polyethylene plays in the friction measurements. To evaluate the effects of these factors on the COF of PDMS-SAM coatings, LFM studies were performed using silica bead probes functionalized with a SAM. The densely packed nature of the SAM is advantageous for reducing surface contamination of the bead probe. Thermogravimetric analysis (TGA) of the developed SAM beads indicates a monolayer thickness of almost 300 nm; as ellipsometry shows SAMs on the planar silicon surfaces to be consistently 1.2 nm thick, the TGA results suggest uniform multilayering of the SAMs. A comparison of the data can be seen in Table 2.4.

The change in COFs results from the difference in van der Waals and adhesive forces between the networks and each cantilever tip. We can see the size of the decrease in COF with increasing molar mass of precursor chains is comparable between cantilevers, with each data set dependent on the magnitude of the measurements.

The adhesion and residual forces for the thin film systems are collected in Table 2.5. We first measured the adhesion for bare silicon and SAM coatings at different testing environment relative humidities. The humidity can significantly increase the surface contamination of ultrathin or bare systems. Thus, we conducted

Table 2.4. AFM cantilever comparison between the COF measured on the micro-film systems as well as the reduction from the bare silicon COF measured with that cantilever.

MW	Thickness	COF (PE)	COF (SAM)
9400	~ 30 um	0.012	0.039
17200	~ 9.6 um	0.01	0.034
28000	~10.2 um	0.008	0.029

Table 2.5. COF, residual force, and AFM force-distance curve depth and width data for the micro-film systems, including bare silicon and SAM coating at two different relative humidities.

System		**μ**	**F_a (nN)**	**h (nN)**	**w (nm)**	**h x w (nN-nm * 10^3)**
Silicon	(65% RH)	0.049	3184	1676	660	1106
	(35% RH)	0.035	3101	1321	280	370
SAM	(65% RH)	0.03	2613	1709	550	940
	(35% RH)	0.03	2372	1330	430	572
9.4k Microfilm		0.012 ± .0008	6389 ± 181	1358 ± 136	330 ± 4	448 ± 45
17.2k Microfilm		0.01 ± .0002	5434 ± 312	1258 ± 106	480 ± 35	604 ± 76
28k Microfilm		0.008 ± .0003	4541 ± 300	1149 ± 19	320 ± 14	368 ± 17

all friction and adhesion measurements on the PDMS networks at the controlled humidity level of 35 percent. The variations in the residual forces are significantly smaller (at most six percent) than the measurements for the ultrathin films, which is indicative of the improved surface uniformity of the micro-film networks. The residual forces can be seen to decrease with increased molar mass for the PDMS networks. This is striking because the network elasticity is also increasing, and indicates a significant drop in the shear strength smaller despite larger contact areas. All the adhesion forces are much higher than we would expect for PDMS systems in comparing the results to other reported data determined with different probe materials.[38] Several AFM studies of the adhesion hysteresis with PDMS systems have found the polymer viscoelasticity to be the dominant factor.[39] To quantify this contribution to adhesion, more information is needed concerning stress relaxation in the network at the cantilever tip – polymer interface. However, by Eq. (4), we recognize that any adhesion based contribution to friction should be discernable in Figure 2.5. Because of the decided linearity of all data in the F vs. N plot, the adhesion term cannot play a significant role. Thus the COFs can be of the same magnitude for both the ultrathin and micro-film networks as the effects of contact area, thickness and shear stress are minimal.

AFM nanoindentation characterization studies can be conducted on these thin PDMS films. A sufficient thickness is needed to prevent the silicon substrate from providing the majority of the modulus characteristics. The micro-film network systems have enough cross-linked material to allow for maximum indentation. An algorithm to complete the calculation of the Young's modulus from the AFM force-distance curves was provided by Dr. David Lin of NIH. We would expect the elastic modulus would range from 0.5 MPa to 2 MPa, depending on the PDMS molar mass.[40] However, the nanoindentation results show moduli values two orders of magnitude

higher using the polyethylene cantilevers and one order higher with the SAM bead cantilever (Table 2.6).

We can attribute the moduli values to two different factors. First the polyethylene tip cantilever is stiffer than the SAM cantilever. Once zero-force is achieved between the AFM piezo and the network surface, further movement by the piezo into the network is resisted and results in a sharp increase in the force on the cantilever. The slope of the curve increases with cantilever stiffness and becomes more difficult to analyze. Thus, the more flexible SAM cantilever is desired and will provide more accurate moduli values. Second, the adhesive forces also play a major role in the indentation experiment. Without some attraction between the cantilever tip and the surface, the data points used in the modulus calculation would be almost indiscernible from the force-distance curves. However, a flexible surface and high adhesion force can create a deep indentation curve and as a result a sharp final curve. The viscoelastic addition to the adhesion forces only further deepens the indentation curve, thus causing an overestimation in the elastic moduli results.

To corroborate these elastic moduli values we conduct one-dimensional swelling experiments on the micro-film PDMS networks, with results in Table 2.7. For all micro-film systems, the equilibrium swelling ratios are 33 to 50 percent lower than the theoretical equilibrium values. The calculated elastic moduli are thus higher than expected, ranging from 5.15 MPa for the 17200 g/mol precursor network to 7.74 for the 28000 g/mol network. Both the swelling and AFM nanoindentation determine the elastic modulus to be five to eight times larger than theoretical and reported values for equivalent precursor PDMS chains.

There are several explanations for the high elastic moduli values obtained. First the crosslink densities that correspond to the calculated moduli indicate significantly shorter distances between cross-links than the precursor PDMS chains.

Table 2.6. AFM nanoindentation results on micro-film network systems using different AFM cantilevers.

		Polyethylene Bead		**SAM Bead**	
MW	Thickness	COF	E (MPa)	COF	E (MPa)
9400	~ 30 um	0.012	89.1	0.04	11.1
17200	~ 9.6 um	0.01	63.8	0.03	6.2
28000	~10.2 um	0.008	18.3	0.03	13.6

Table 2.7. Predicted swelling ratios from the Toomey et al. equation and the Zhang and Archer equation, the experimental swelling ratios and calculated elastic moduli for the micro-film systems.

Predicted Swelling Ratios			**Micro-Film Networks**	
MW	Toomey α	Z+A α	Exp. α	E (MPa)
9.4k	1.92	2.14	1.27	6.07
17.2k	2.30	2.52	1.24	5.15
28k	2.68	2.90	1.32	7.74

These distances could be the result of modification to the precursor chains prior to cross-linking or a high amount of entanglements. Precursor PDMS chain modification is unlikely because the hydrosilylation cross-linking reaction is well-controlled. While some of the precursor chains are larger than the M_e of 12.3 x 10^3 g/mol for PDMS, it is unlikely for entanglements to develop to the extent required by the calculated M_c. Second the spincoating process restricts the mobility of the PDMS chains and may change the network structure. High crystallinity has been previously found for ultrathin spincast polymer networks, for example.[41] However, there do not appear to be similar reported findings for micrometer thick networks, and PDMS has a very low melting temperature of -60 ^oC. Third, the constrained network with near one-dimensional thickness may limit the diffusion of swelling agents. This would be particularly true if the surface was stiffer than the rest of the polymer and thus not indicative of the entire network. While there may be some specific chain orientation developing from the spincoating, we do not believe the network structure deviates significantly throughout the polymer. Finally a viscoelastic component causes the adhesion forces to be overpredicted. We suspect that several of these effects contribute to the high moduli values calculated from the nanoindentation experiments.

2.4.3. Role of Pendent Chains. Earlier we concluded that nanometer thick PDMS networks are poorly crosslinked and contained defects in the form of pendent chains, branches and loops. However, these systems generally manifest lower COFs than the optimal micrometer thick network films. A perhaps obvious question is whether one could systematically lower the COF of an optimal network through controlled introduction of defects. Pendent chains can be formed by adding a low concentration of monofunctional PDMS to the difunctional polymer network precursor. The effect of pendent chains in PDMS networks has previously been studied by Galliano et al.[37] The authors found that networks with larger numbers of pendent chains have lower

friction stresses. The authors concluded that the dangling ends create a surface layer with low shear stress and poor cohesion. Thus by incorporating a controlled concentration of pendent chains in the micro-film systems, a lower COF should be obtainable.

The effect of pendent chains on the COF was determined by adding 9500 g/mol PDMS monofunctional chains with a PDI of 1.30 to 9400 g/mol telechelic PDMS chains in solution. Figure 2.6 shows the LFM friction results obtained as a function of monofunctional PDMS fraction, and Table 2.8 shows the adhesion and residual force data. As expected, the pendent chains generally reduce the surface friction coefficient. The linearity of the *F* vs. *N* lines again indicates the insignificance of adhesion on the friction force.

Networks containing 5 volume percent monofunctional chains in solution were seen to have a 21 percent COF reduction from the 9400 g/mol network with no pendent chains added. However, beyond a certain concentration of monofunctional chains, the friction coefficient is observed to increase. At 10 percent monofunctional chains the COF reduction is only 15 percent lower, and by 20 percent monofunctional chains, the COF of the networks is increased by about 48 percent. We conclude that addition of pendent chains beyond an optimal concentration destabilizes the network in a manner that is qualitatively different from what must be present in the nanometer network films. This suggests that other types of defects are perhaps required to produce the low levels of friction evident for the thinnest PDMS films. Further research is clearly required to understand and exploit these defects for reducing the COF of PDMS surface coatings.

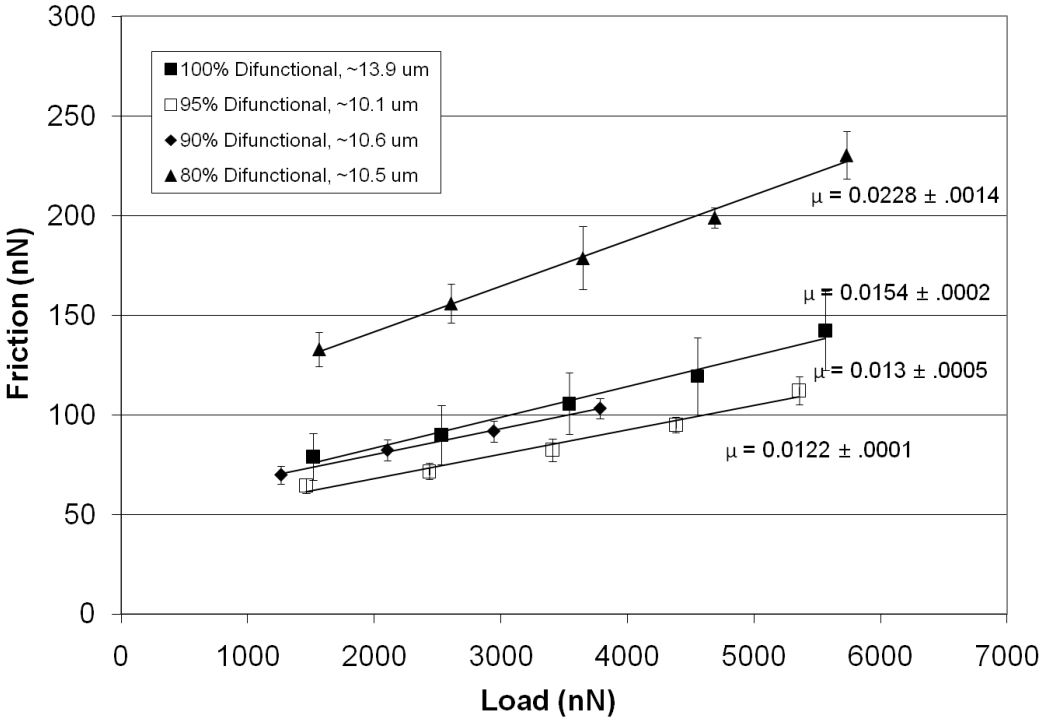

Figure 2.6. Friction vs. load data for micrometer thick networks synthesized with varying percentages of monofunctional PDMS chains, leading to different amounts of pendent chains in the networks.

Table 2.8. COF, residual force, and AFM force-distance curve depth and width data for the micro-films with added pendent chains.

System	μ	F_a (nN)	h (nN)	w (nm)	h x w (nN-nm * 10^3)
0% Pendent Chains Added	0.0154 ± .0002	3414 ± 538	1568 ± 187	350 ± 13	549 ± 68
5% Pendent Chains Added	0.0122 ± .0001	3569 ± 173	1435 ± 30	395± 7	567 ± 16
10% Pendent Chains Added	0.013 ± .0005	4262 ± 152	1261 ± 83	400 ± 15	504 ± 38
20% Pendent Chains Added	0.0228 ± .0014	4198 ± 160	1641 ± 121	445 ± 21	730 ± 64

2.5. CONCLUSIONS.

Interfacial friction and adhesion properties of a tethered, dry PDMS network – SAM monolayer lubricant coating have been investigated. Vinyl-terminated difunctional PDMS chains were spincoated with a cross-linking agent and platinum catalyst onto silicon wafers covered with a self-assembling monolayer. Friction and adhesion analysis were performed using LFM measurements based on polyethylene and SAM-coated bead probe cantilevers. Ultrathin network films (thickness ~ 10 nm) manifest COFs as low as 0.004. Increasing the molar mass of the network chains leads to higher surface flexibility and lower COFs. The COF of the most defective network films is about an order of magnitude lower than that of bare silicon or of silicon functionalized with a tethered SAM lubricant layer. Swelling measurements using oligomer PDMS chains was used to analyze the quality of the networks. The measured swelling ratios are generally significantly higher than expected from predicted estimates based on the molar mass of the precursor chains. This finding is consistent with a high level of extracted material from dichloromethane treatment of the networks and indicates that the ultrathin films are poorly cross-linked and have structures akin to hyperbranched polymer systems.

Micrometer-sized PDMS network films were created using difunctional PDMS melt precursor chains. These films are generally more uniform, produce considerably lower levels of extractables with dichloromethane treatment, and manifest swelling and indentation properties consistent with expectations of well-formed, optimally cross-linked polymer networks. They also generally display moderately higher surface friction coefficients than the nanometer thick films. Increasing the precursor molar mass reduces the COF to as low as 0.0077. The F vs. N curves indicate that the friction force has no significant dependence on the network adhesion strength. We conclude that the weak adhesion characteristics make it possible to produce effective

tethered lubricant coatings based on PDMS, even under circumstances where increased contact areas should favor higher friction coefficients.

Previous studies suggest that the optimal coating configuration for reducing interfacial friction should yield high surface mobility with a densely-packed surface-adhered base. Pendent chains are introduced into the optimal network films to increase the surface mobility. At low monofunctional PDMS concentrations the measured COF is indeed lower. Increasing the number of pendent chains beyond a small critical value, however, leads to much higher surface friction.

2.6. ACKNOWLEDGMENTS.

We are grateful to the National Science Foundation Tribology Program (Grant CMS0510239), and to the Department of Energy Basic Energy Sciences Program (Grant DE-FG02-07ER46455). The LFM sliding friction measurements were performed using facilities of the Cornell Center for Materials Research (CCMR), a Materials Research Science and Engineering Center of the National Science Foundation (DMR-0079992).

REFERENCES

(1) Rymuza, Z. *Microsystem Technologies* **1999**, *5*, 173-180.

(2) Bhushan, B. *Proc. Instn. Mech. Engrs Part J* **2001**, *215*, 77-102.

(3) Cagin, T.; Che, J.; Gardos, M. N.; Fijany, A.; Goddard, W. A., III. *Nanotechnology* **1999**, *10*, 278-284.

(4) Bowden, F.P.; Tabor, D. *Friction and Lubrication.* Methuen & Co. Ltd.: London, 1967.

(5) Wang, W.; Wang, Y.; Bao, H.; Xiong, B.; Bao, M. *Sensors and Actuators* **2002**, *97-98*, 486-491.

(6) Maboudian, R.; Ashurst, W. R.; Carraro, C. *Sensors and Actuators* **2000**, *82*, 219-223.

(7) Sundararajan, S.; Bhushan, B. *J. Vac. Sci. Technol. A.* **2001**, *19(4)*, 1777-1785.

(8) K. Strawhecker, D.B. Asay, J. McKinney and S.H. Kim. *Tribology Letters* **2005**, *19*, 17-21.

(9) Bhushan, B. *Microelectronic Eng*. **2007**, *84*, 387-412.

(10) Bhushan, B.; Liu, H.; Hsu, S. M. *ASME J. Tribol* **2004**, *126*, 583-590.

(11) Bhushan, B.; Israelachvili, J. N.; Landman, U. *Nature* **1995**, *374*, 607-616.

(12) Xiao, X.; Hu, J.; Charych, D. H.; Salmeron, M. *Langmuir* **1996**, *12*, 235-237.

(13) Tsukruk, V.V.; Bliznyuk, V.N. *Langmuir* **1998**, *14*, 446-455.

(14) Yang, X.; Perry, S. S. *Langmuir* **2003**, *19*, 6135-6139.

(15) Liu, Y.; Evans, D. F. *Langmuir* **1996**, *12*, 1235-1244.

(16) Zhang, Q.; Archer, L.A. *J. Phys. Chem. B.* **2003**, *107*, 13123-13132.

(17) Zhang, Q.; Archer, L. A. *Langmuir* **2006**, *22*, 717-722.

(18) Zhang, Q.; Archer, L. A. *Langmuir* **2005**, *21*, 5405-5413.

(19) Raviv, U.; Glasson, S.; Kampf, N.; Gohy, J. F.; Jerome, R.; Klein, J.. *Nature* **2003**, *425*, 163-165.

(20) Ohsedo, Y.; Takashina, R.; Gong, J.P.; Osada, Y. *Langmuir* **2004**, *20*, 6549-6555.

(21) Brown, H.R. *Science* **1994**, *263*, 1411-1413.

(22) Ahn, H-S; Julthongpiput, D.; Kim, D-I; Tsukruk, V.V. *Wear* **2003**, *255*, 801-807.

(23) Julthongpiput, D.; Ahn, H-S; Kim, D-I; and Tsukruk, V.V. *Tribology Letters* **2002**, *13*, 35-40.

(24) Galliano, A.; Bistac, S.; and Shcultz, J. *J. Adhesion* **2003**, *79*, 973-991.

(25) Zhang, Q.; Archer, L.A. *Langmuir* **2007**, *23*, 7562-7570.

(26) Tordjeman, P.; Mutin, P. H.; Tixier, T. *Rheol Acta* **2004**, *43*, 550-558.

(27) Batra, A.; Cohen, C.; Archer, L. *Macromolecules* **2005**, *38*, 7174-7180.

(28) Cleveland, J.P.; Manne, S.; Bocek, D.; Hansma, P.K. *Rev. Sci. Instrum.* **1993**, *64*, 403-405.

(29) Beake, B.D.; Legget, G.J. *Phys. Chem. Chem. Phys.* **1999**, *1*, 3345-3350.

(30) Dimitriadis, E.K.; Horkay, F.; Maresca, J.; Kachar, B.; Chadwick, R.S. *Biophysical Journal* **2002**, *82*, 2798-2810.

(31) Lin, D.C.; Dimitriadis, E.K.; Horkay, F. *Recent Res. Devel. Biophys.* **2006**, *5*, 333-370.

(32) Lin, D.C.; Dimitriadis, E.K.; Horkay, F. *J. Biomech. Eng.* **2007**, *129*, 430-440.

(33) Jaasma, M.J.; Jackson, W.M.; Keaveny, T.M. *Annals of Biomed. Eng.* **2006**, *34*, 748-758.

(34) Guo, S.; Akhremitchev, B.B. *Biomacromolecules* **2006**, *7*, 1630-1636.

(35) Toomey, R.; Freidank, D.; Ruhe, J. *Macromolecules* **2004**, *37*, 882-887.

(36) Patel, S.K.; Malone, S.; Cohen, C.; Gillmor, J.R.; Colby, R.H. *Macromolecules* **1992**, *25*, 5241-5251.

(37) Galliano, A.; Bistac, S.; Schultz, J. *J. Col. Int. Sci.* **2003**, *265*, 372-379.

(38) Vaenkatesan, V.; Li, Z.; Vellinga, W-P; de Jeu, W.H. *Polymer* **2006**, *47*, 8317-8325.

(39) Sun, Y. and Walker, G.C. *Langmuir* **2005**, *21*, 8694-8702.

(40) Bistac, S.; Galliano, A. *Tribology Letters* **2005**, *18*, 21-25.

(41) Frank, C.W.; Rao, V.; Despotopoulou, M.M.; Pease, R.F.W.; Hinsberg, W.D.; Miller, R.D.; Rabolt, J.F. *Science* **1996**, *273*, 912-915.

CHAPTER 3

THE EFFECT OF PENDENT CHAINS ON THE INTERFACIAL AND BULK PROPERTIES OF THIN PDMS NETWORKS

3.1. ABSTRACT.

The interfacial and rheological properties of polydimethylsiloxane (PDMS) networks with different extent of inelastic pendent chains are examined. Thin networks (~10 microns thick) were synthesized over a self-assembled monolayer supported on a silicon wafer. Different concentrations of pendent chains were used to cover the range from a near model elastic network to a thick hyperbranched polymer structure. Network characterization was conducted with both an atomic force microscope and a rheometer to measure the interfacial friction, shear stress and viscosity as well as the rheological properties. All networks demonstrated low interfacial friction; PDMS networks with the lowest pendent chain content demonstrated a friction coefficient almost 88 percent lower than that of bare silicon. At low sliding velocities, these networks also produce lower friction. Higher sliding velocities prevent chain relaxation and cause the more viscous-like brush systems to exhibit lower friction despite higher shear stresses and viscosity.

3.2. BACKGROUND.

Developments in small lengthscale device applications, such as microelectromechanical systems (MEMS) or micro-syringe systems used in medicine, have motivated research into advanced lubricants that will function on the lengthscale of these devices.[1-3] In order to address these needs, a wide range of lubricant systems have been studied, including untethered oils,[4-6] self-assembled monolayers,[7-11] polymer films,[12] and tethered gels.[13,14] From these studies, it has been determined that

the ideal lubricant must be deposited as a thin film in order to maintain the substrate structure, the film must be strongly tethered to the substrate to increase the wear resistance, and a low interfacial shear stress and minimal contact area are necessary to reduce friction.[4,15-17]

Motivation for our work specifically stems from a series of studies conducted by Zhang and Archer investigating the effect of structure and medium on the interfacial friction and adhesion properties of SAM films.[18] These authors showed that SAM blends consisting of both short and long alkylsilanes have significantly lower friction than monolayers of uniform molecular length. An Eyring-type analysis indicated the lower friction for the two-tiered structure develops from high surface disorder and mobility in the canopy layer, with a densely packed underlayer to prevent penetration to the substrate. By changing the medium from air to ethanol, Zhang and Archer reported dramatically lower COFs can be achieved in these systems by reducing the interfacial shear stress, thus decreasing and limiting the adhesion contribution to friction. They concluded from these results that working with low shear stress materials would create an optimal environment for low friction results.

In consideration of these ideal lubricant characteristics, we have proposed a two-tier system, consisting of a self-assembled monolayer acting as a well-ordered surface-adhered base layer coated with a polydimethylsiloxane (PDMS) polymer network to form a softer surface layer.[19] PDMS is an ideal lubricating material because of its low surface energy, high molecular flexibility, and relative ease in its synthesis process. Utilizing a polymer network as the surface layer will decrease the wear typically seen for SAMs, while also allowing for low shear stresses that will reduce the adhesion contribution to friction, importantly without introducing a solvent.[14] The SAM layer serves as a dense sublayer of anchoring sites for the flexible PDMS network surface layer.

As described in our previous paper,[19] PDMS network – SAM hybrids of nano- and micro-scale thicknesses provide a range of interesting results. First, the COFs are extremely low for the lubricant systems at both thickness levels. The ultrathin networks have COFs as low as 0.004, a reduction in friction from the COF of bare silicon by almost one order of magnitude. This is approximately the lowest COF ever recorded for dry lubrication systems. The micro-thick films also manifest COFs as low as 0.0077 despite the film thickness being three orders of magnitude larger than the ultrathin systems. The essential difference between these two films was the structure of the network. The micro-thick network is fully cross-linked with a uniform surface and thickness on the microscale (~5 to 30 μm). The extractable material (soluble fraction) from these networks is less than one percent. The structure of such a system is schematically represented in Figure 3.1.1. The ultrathin PDMS networks (~10 nm) were made by diluting the precursor polymer solution in toluene to 20 percent polymer by volume before spincoating over the template, resulting in a poorly cross-linked hyperbranched surface coating, as schematically illustrated in Figure 3.1.2.

In order to investigate further the role of the network structure on the interfacial properties and to reproduce the network structure of the ultrathin films in the micron thick networks, monofunctional PDMS chains were added to the telechelic chains at different concentrations in the synthesis of the networks. Because monofunctional chains attach to the network at only one end, different concentrations of pendent chains can be synthesized within a network. Given the low surface energy of PDMS, the surface of the network is likely to have high concentrations of these chains, creating a two-tiered system within the PDMS network as Figure 3.1.3 illustrates. While many pendent chain ends will fill spaces within the network created

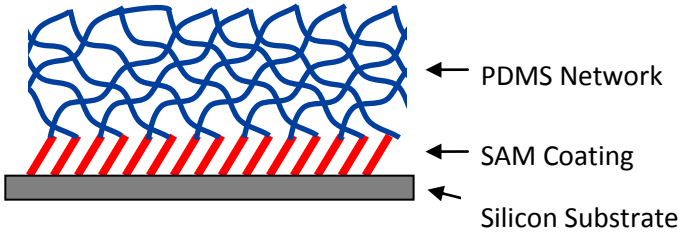

Figure 3.1.1. Illustration of an optimal system. The PDMS network is nearly fully cross-linked and uniform; the SAM coating is not exposed to surface.

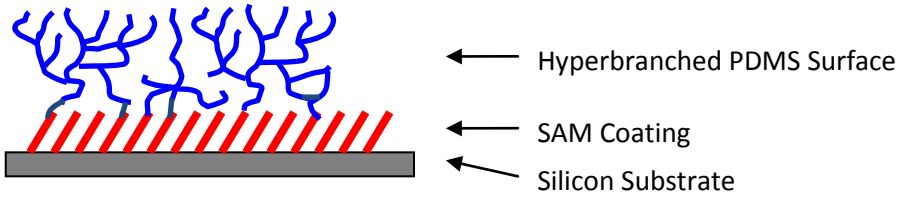

Figure 3.1.2. Illustration of an ultrathin system structure. PDMS is hyperbranched with some level of cross-linking present.

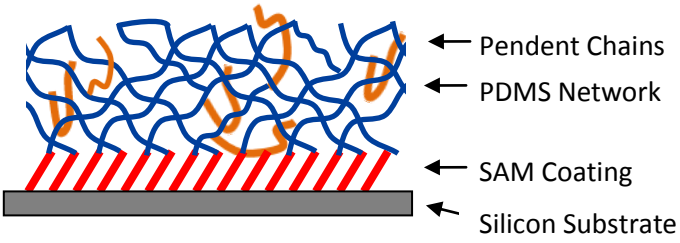

Figure 3.1.3. Illustration of a micro-thick system structure with pendent chain modifications. PDMS is not fully cross-linked and has some hyperbranching.

by decreased network functionality during synthesis, the dangling chain ends present at the surface post-synthesis can create a sparse polymer brush overcoat with high surface mobility above an elastic network. Incremental increases in the hyperbranching of the network by systematically creating more pendent chains in the network also decrease the elastic modulus of the network and increase the interfacial contact area.

3.3. EXPERIMENTAL.

3.3.1. Preparation of SAMs. Hexadecane ($C_{16}H_{34}$), chloroform ($CHCl_3$), dichloromethane (CH_2Cl_2), and methanol (CH_3Cl) were purchased from Aldrich Chemicals. 10-undecenyl trichlorosilane was purchased from Gelest, Inc. Three-inch (100) silicon wafers from University Wafer were cut using a diamond tipped stylus into 1 inch by 1 inch pieces. The wafer pieces were prepared by cleaning with Kimwipes, rinsing ultrasonically in chloroform, and treating for at least 30 minutes in a piranha solution of 12 mL hydrosulfuric acid (H_2SO_4) and 10 mL 30% hydrogen peroxide (H_2O_2) above 130 ^oC. The cleaned wafer pieces were subsequently rinsed in DI water a minimum of eight times and blown dry with nitrogen gas.

Media bottles were placed in a glovebox with a dry nitrogen atmosphere along with the prepared wafers. Solutions of hexadecane and chloroform were then prepared with a 4:1 volume ratio in the media bottles for a total volume of 40 mL. Approximately five of the cut wafer pieces were placed and arranged in each flask to maximize exposed surface, after which 24 µL of the 10-undecenyl trichlorosilane was added. The wafers were allowed to sit in solution in the glovebox overnight to allow for the formation of the SAM layers. Outside the glovebox, the silicon pieces were rinsed successively in dichloromethane, chloroform, and methanol baths for approximately five minutes in each to remove any residual solvent and unattached

trichlorosilane. The monolayer-coated wafers were then dried under a nitrogen stream and stored.

3.3.2. Synthesis of Difunctional PDMS. Vinyl-terminated difunctional PDMS chains were anionically synthesized from the monomer D_3 (hexamethylcyclotrisiloxane) purchased from Gelest. Purified D_3 was dried for 24 hours with calcium hydride and toluene. The monomer and toluene solution was filtered into a round bottom flask. A small amount of HPLC water dependent on the projected molar mass of the PDMS chains desired was added to the flask. The solution was allowed to mix and was heated to 65 ^{o}C. Benzyltrimethyl ammonium catalyst dissolved in dimethyl sulfoxide was added to the solution based on previously determined ratios. After thoroughly mixing for 24 hours to facilitate complete monomer reaction, pyridine, an acid scavenger, and vinyldimethylchlorosilane were added in excess to functionalize the PDMS chain ends. The polymer solution was then washed with deionized water in a separatory funnel before precipitation and decanting with an excess of methanol. The molar mass of the PDMS chains was measured using a Waters 510 GPC to be 27000 g/mol.

3.3.3. Synthesis of Monofunctional PDMS. Purified hexamethylcyclotrisiloxane (D_3) was dissolved in benzene to a 20 weight percent solution and dried with calcium hydride. The monomer solution was filtered into a round bottom flask and placed in a glovebox filled with nitrogen. In the glovebox, sec-butyl lithium was added at previous determined ratios to the monomer solution, which was then heated to 30 ^{o}C. After 2 hours, THF was added to the flask to reduce the D_3 concentration to 10 weight percent. Vinyldimethylchlorosilane was added in excess to the flask after completion of the polymerization. The final monofunctional PDMS chains were washed and decanted in a similar procedure as described for the difunctional PDMS chains. The

PDMS chain molar mass and polydispersity index was determined using a Waters 510 GPC.

3.3.4. Preparation of Cross-linked PDMS Networks. Networks were synthesized according to a procedure developed by Patel et al.[20] The cross-linking agent tetrakis(dimethylsiloxy)silane and Karstedt's catalyst platinum-divinyl tetramethyl-disiloxane were purchased from Gelest. Toluene was purchased from Aldrich. The cross-linking agent and PDMS were mixed in vials at optimal ratios described previously.[21] 100 µL of the platinum catalyst was diluted in 10 mL of toluene in a separate vial. Immediately after adding the correct amount of catalyst solution to the PDMS and cross-linker and vigorously mixing, the solution was poured onto the SAM-coated silicon wafer substrates. Just enough precursor polymer solution was poured to cover the entire surface of the wafer. The solution and cut wafers were spincoated at 3000 rpm for 60 seconds using a SCS P6708 spincoater. The silicon pieces were placed in a vacuum oven at 35 ^{o}C to cure the sample and to remove any toluene solvent remaining from the catalyst solution. After heating the samples under vacuum for 24 hours, the vacuum line was shut off and the pressure returned to ambient atmosphere. The annealing process continued for three more days at 35 ^{o}C to ensure cross-linking reactions had come to completion. The final silicon pieces, after an initial thickness measurement, were twice rinsed in dichloromethane for five minutes each time to remove excess unbonded material. Excess dichloromethane was removed by reheating the wafer pieces for one hour at 75 ^{o}C, and the thickness of the surface coatings was remeasured.

Pendent chains were introduced in controlled amounts by adding the monofunctional PDMS chains to the difunctional PDMS network solution prior to cross-linking. Small concentrations of pendent chains (~10 percent) are likely to occur even in networks developed from low PDI telechelic chains; achieving perfect

functionality from a tetra-functional cross-linker is not possible as a result of steric hindrance.[22] It is normal to assume functionality around 3.3 - 3.4 instead of the optimal 4.0.[20] In order to determine the influence of pendent chains on the friction and wear, higher concentrations need to be added to prevent the results from residing within the range of naturally forming network irregularities.

Monofunctional chains were added to the difunctional precursor solution to create 20, 40, and 50 weight percent concentrations. The monofunctional chains had a precursor molar mass of approximately 61000 g/mol with a PDI of 1.21. The difunctional chains had a much shorter precursor molar mass of approximately 27000 g/mol with a PDI of 1.31. The difference in the chain length ensures any differences seen between network samples are a result of the monofunctional pendent chains and not pendent chains that may develop as cross-linking defects.

3.3.5. Characterizing the Thickness of the PDMS Cross-linked Films. The thickness of the PDMS film was determined using a F20 Film Metrics Spectrophotometer. A constant refractive index of 1.4 was used for the PDMS layer.[23] Approximately five measurements were taken at multiple positions on the substrate to characterize the average thickness and uniformity of films formed.

The analysis was based on a one-layer film on a silicon substrate. Analysis of the SAM layer coating using a Rudolph Research Auto-EL Ellipsometer has shown the SAMs to consistently have an average thickness of 1.2 nanometers. This thickness was ignored in comparison to the cross-linked PDMS film thickness, which are generally three orders of magnitude larger.

3.3.6. AFM Analysis. Friction and indentation measurements were conducted using a DI3000 Atomic Force Microscope (AFM). Cantilevers were purchased from Veeco and Novascan for surface imaging, friction, and indentation analysis. Surface imaging tests were conducted using Veeco silicon nitride pyramid tip cantilevers with a spring

constant of 0.58 N/m. These cantilevers were used specifically in tapping mode measurements during the nanoidentation experiments. The Novascan cantilevers included polyethylene and silica bead tips of 5 μm radius; the spring constant of the polyethylene bead-probe cantilevers was 4.5 N/m, while silica bead-probe cantilevers were purchased at both 4.5 N/m and 0.58 N/m. Polyethylene-bead tips were used for most of the friction analysis reported in this article because they provided highly reproducible data between experimental runs and did not contaminate easily. The silica-bead tips were used for nanoindentation and to corroborate the salient features of results found by the polyethylene bead tips.

Surface friction force data were obtained by scanning the AFM cantilever probe in the forward and reverse directions against the sample in contact mode. By disabling other scan lines to create a friction loop, the friction force could be determined from the average difference between values from opposing scan directions. The substrate was held in place by both vacuum suction and double-sided tape. Data were collected at scan lengths of 5.0 μm and fixed scan rates ranging from 0.1 to 122 Hz. The applied load was varied by changing the cantilever operating height. Each set of friction measurements was conducted at five applied loads, and friction values were recorded after reaching a steady-state friction force value for each new load. The final friction-load plots were constructed from an average of multiple (typically three) measurements at several different points on each surface. The AFM provides normal and lateral force values (N and F) in terms of voltage, V, which can be converted through the relations

$$N = \mathrm{K_n} S_\mathrm{n} V_\mathrm{n} \quad (1)$$

$$F = \mathrm{K_l}\, S_\mathrm{l}\, V_\mathrm{l} \quad (2)$$

The normal sensitivity S_n was determined from force-distance curves for each sample and used to calculate the lateral sensitivity S_l as described by Liu and Evans.[24] The

dimensions of the cantilever were used to determine the lateral force constant K_l. The normal force constant K_n was determined using the added-force method described by Cleveland et al.[25] This method was used to check the reported values for all cantilevers. Glass particles ranging in diameter from 10 to 50 μm were attached to the cantilever tip by coming into contact with the glass particles and pressing down on the tip. The resonant frequency of the cantilever was then recorded with the added weight. The mass of each attached glass particle was calculated from the diameter of the particle, which was measured with respect to the width of the AFM cantilever, and from the bulk density of glass. The normal force constant was determined to be 4.47N/m for the reported 4.5 N/m polyethylene bead cantilever, 4.48 N/m for the reported 4.5 N/m silica bead cantilever, and 0.60 N/m for the 0.58 N/m silica bead cantilever.

3.4. RESULTS.

3.4.1. Effect of Pendent Chains on Friction. Friction force vs. load curves for the pendent chain systems at a low scan rate are presented in Figure 3.2. From these results it is apparent that friction increases linearly with load, and that the presence of pendent chains only increase the COF. It is important to remember that by adding pendent chains to the networks, branching develops during cross-linking and the final network produced becomes more like a thick hyperbranched polymer structure when large concentrations of pendent chains are added. Thus, as the amount of monofunctional precursors are increased, the networks may progress through a series of structures from model elastic networks, consisting mostly of difunctional elastic chains, to elastic systems with an appreciable viscous component, and finally a hyperbranched structure that develops from a large amount of pendent chains. This

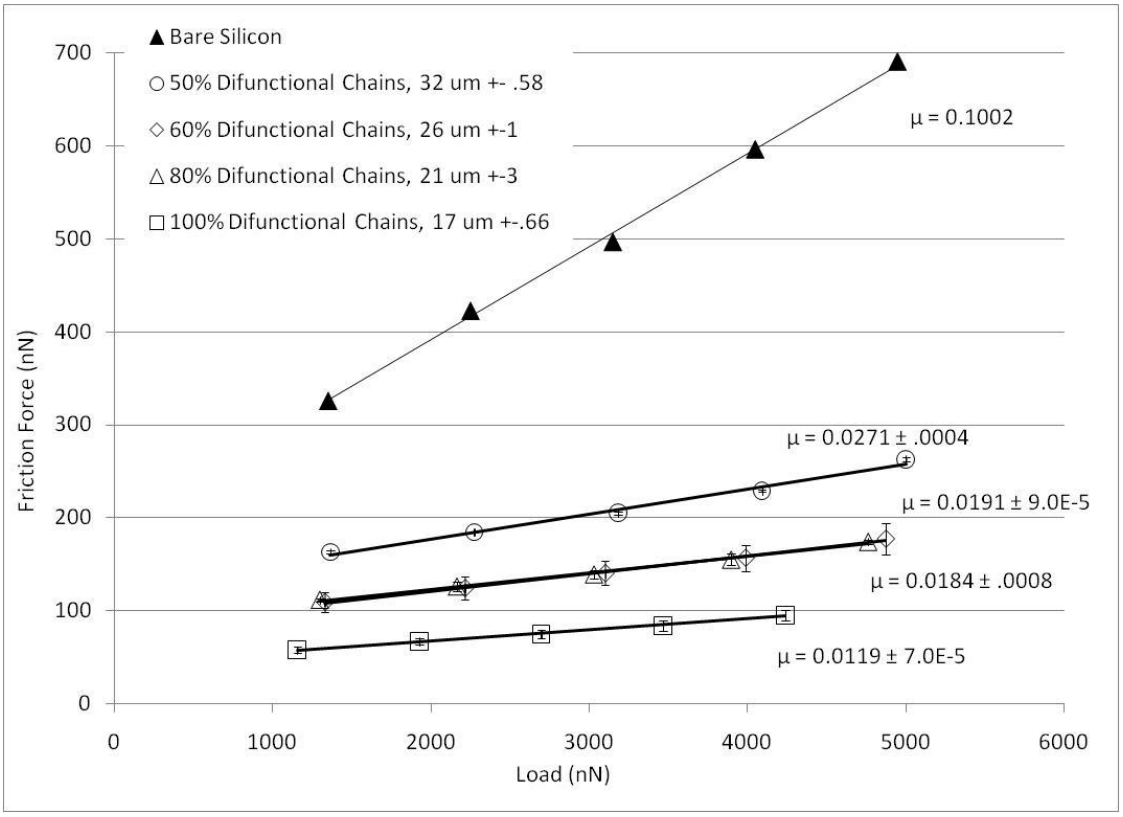

Figure 3.2. Friction force vs. load curves for the pendent chain networks at a scan rate of 1 Hz that corresponds to a sliding velocity of 10 μm/s.

progression of increasing network viscoelasticity may explain the different values of the COF caused by different network surface structures.

A major result to consider is the decided linearity in the F_f vs. N data, either when comparing different networks or evaluating one system at different sliding velocities. A modified form of Admonton's friction law recognizes that there are two contributions to the friction force (F_f): a load (N) component, and an adhesion component consisting of the product of the critical shear stress (τ_o), indicative of the surface chemistry, and the contact area (A) at the interface.

$$F_f = \tau_o * A + \mu * (N + N_c) \quad (3)$$

Here N_c is the critical load, the finite force required to separate the surfaces vertically.[23] Johnson, Kendall, and Roberts (henceforth referred to as JKR) proposed a theory showing the relationship between the contact area and load is non-linear.[26] Thus a linear F_f vs. N relationship implies that the second term in Eq. (3) dominates and the adhesion contribution to the friction is negligible. We can thus conclude that with the PE bead the friction process on our PDMS networks is dominated by the deformation of the network as a result of elastic work than by adhesion effects caused by molecular attachment and detachment of individual chains. The friction force can be better considered as an evaluation of the network's ability to deform and recover as result of interfacial sliding in the range of loads investigated.

In order to fully evaluate the effect of the pendent chains, the friction is measured over a series of sliding speeds, ranging from 10 to 122 μm/s. The sliding speed is determined as the product of the scan distance traveled laterally by the cantilever, and the scan rate. The friction force vs. sliding velocity data for the pendent chain systems are presented in Figure 3.3. Two distinct friction regions are apparent from these results. At low sliding velocities, the more elastic networks with fewer pendent chains exhibit the lowest friction forces, while the most poorly cross-

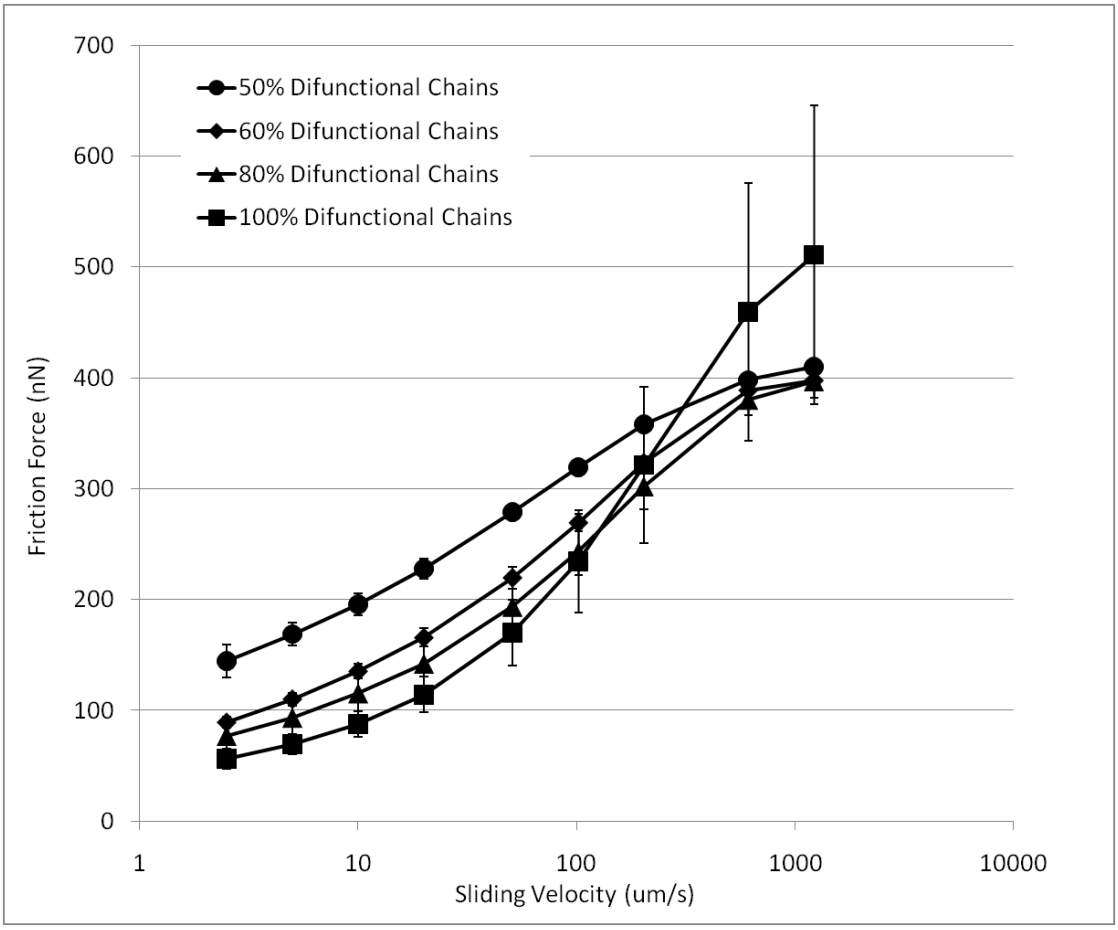

Figure 3.3. Friction force vs. sliding velocity curves for PDMS network systems made of varying amounts of 27000 precursor molar mass difunctional chains and 61000 precursor molar mass monofunctional chains. The load is constant at 4000 nN.

linked system has friction forces almost three times larger. At high sliding velocities, the friction forces begin to crossover, and the mostly difunctional system exhibits higher friction forces than any of the other more viscous systems. This would suggest the greater surface disorder apparent in the higher concentrations of pendent chain systems is a detriment at low sliding speeds, but is beneficial at higher velocities. At low sliding velocities, the pendent PDMS chains may remain in a relaxed conformation, thus introducing a viscous-like layer along the surface that would increase the interfacial friction. This viscous-like layer would become more prevalent as the concentration of pendent chains in the system increases. At high sliding speeds, the elastic network would become highly constrained as a result of tension in the system. Elastic chains would resist deformation because of the increased tension distributed throughout the entire network structure as a result of the increased sliding speeds, while pendent chains along the surface would be able to align in the sliding direction of the cantilever. The distinct structural effects on friction are better represented in Figure 3.4, where the COFs of the different networks as measured at different sliding velocities are compared. The more elastic networks can be seen to have lower COFs at low scan rates, but much higher COFs at high velocities. The variation in COF is likely attributable to the different relaxation mechanisms for the different structures.

The transition in friction as the sliding velocity increases can be better understood is similar to the conformation of thin polymer brushes under applied stresses. Leger et al. conducted a series of adhesion measurements on PDMS chains grafted to silica.[27] The researchers determined that while the grafted chains are flexible and mobile, at lower applied stresses the brushes remain in a relaxed, entangled state that increases the shear at the surface. Leger et al. also found that at

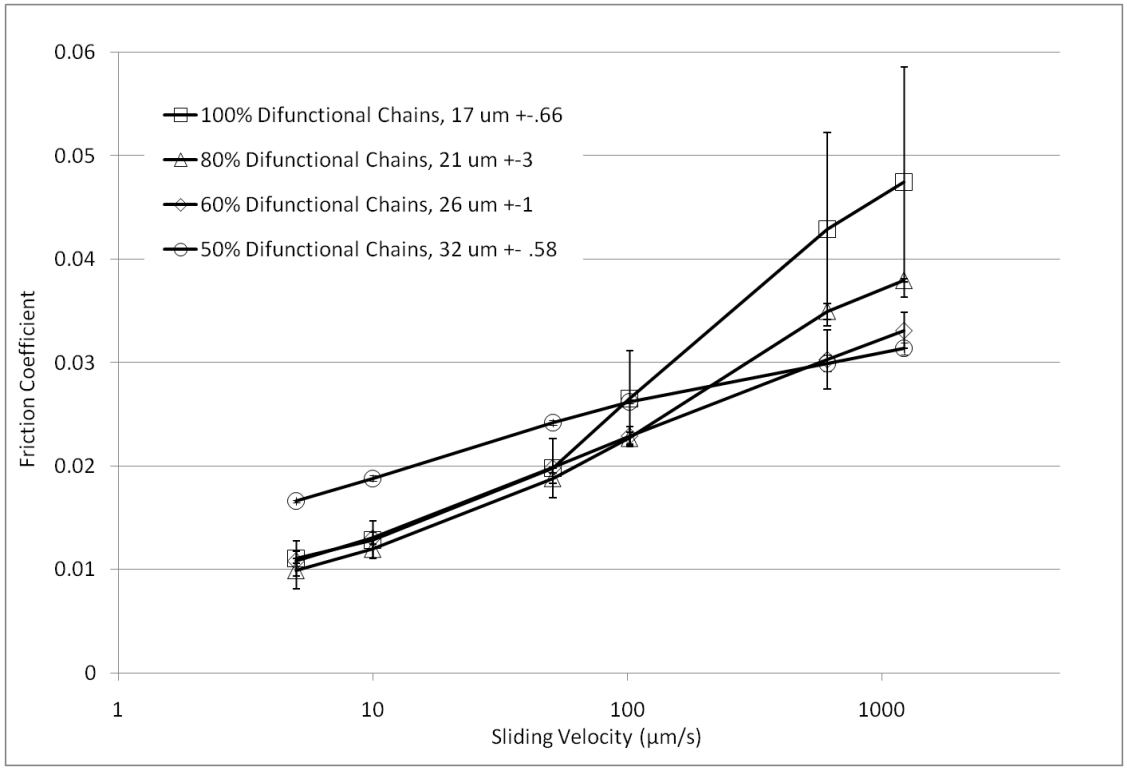

Figure 3.4. Friction coefficient vs. frequency curves for PDMS network systems made of varying amounts of 27000 precursor molar mass difunctional chains and 61000 precursor molar mass monofunctional chains.

high applied stresses, the grafted chains can elongate in the direction of the lateral stress to decrease entanglements and the viscous-like layer at the interface. While the PDMS brush layers that Leger et al. studied were almost three orders of magnitude thinner than the pendent chain networks involved in our study, the principle of chain relaxation and elongation changing the surface mobility and friction is still applicable for our complex systems. However, especially in consideration of the thick hyperbranched structures, friction does not provide a complete evaluation of the effect of the pendent chains. Shear stress, elasticity and other surface properties help to better elucidate the structural effects.

3.4.2. Surface Characterization. The AFM in force mode analysis was used to determine the elastic modulus, E, of the samples produced. In force mode, the cantilever moves vertically with respect to the sample, and the deflection of the cantilever resulting from surface attraction and adhesion forces is recorded. As the piezo retracts from the surface, the cantilever will be adhered to the surface beyond the piezo distance where the cantilever came into contact while approaching the sample surface. The depth of the force curve developed from the cantilever vs. piezo distance in retraction in comparison to extension provides the pull-off adhesive force between the surfaces. The indentation of the cantilever into the PDMS surface is calculated from the difference of the piezo location and cantilever deflection in relation to the cantilever zero force point before attractive forces introduce the effect of adhesion.

The actual contact area, A, between the cantilever tip and the surface can be determined using the JKR theory[26] of surface contact:

$$A = \pi(R/K)^{2/3}\{N + 3\pi R\gamma + [6\pi R\gamma N + (3\pi R\gamma)^2]^{1/2}\}^{2/3} \quad (4)$$

where R is the tip radius, γ is the reduced surface tension:

$$\gamma = \gamma_1 + \gamma_2 - \gamma_{12} \quad (5)$$

and K is the reduced elastic modulus:

$$K = \frac{4}{3}[(1-\nu_1{}^2)/E_1 + (1-\nu_2{}^2)/E_2]^{-1} \quad (6)$$

Here E_1 and E_2 are the elastic moduli of the two materials in contact and ν_1 and ν_2 are the corresponding Poisson ratios. For the network – AFM cantilever interfaces, these two materials represent the PDMS surface and the polyethylene (PE) bead. The elastic modulus value for the PE bead can be obtained from known bulk values, meaning that the elastic modulus of the PDMS network remains unknown. The reduced surface tension is also directly related to the pull-off force, F_a, by

$$F_a = -3\pi R\gamma/2 \quad (7)$$

The negative sign in Eq. (7) assumes that the normal load force is applied in a positive direction, and the force required to overcome adhesive forces would be applied in an opposite and therefore negative direction. Combining Eqs. (4) and (7), we see the only remaining unknown constants are the elastic modulus of the sample and the interfacial contact area. We can use a modified Hertzian analysis[28] to estimate the elastic modulus of the PDMS surface (referred to as E in the Hertzian analysis equations) that accounts for the film thickness, h, of the sample and expresses the applied force F as:

$$F = \frac{16E}{9}R^{1/2}\delta^{3/2}[1+1.133\chi+1.283\chi^2+0.769\chi^3+0.0975\chi^4] \quad (8)$$

where

$$\chi = \sqrt{R\delta}/h \quad (9)$$

and δ is the indentation at the interface, determined from the difference between the normalized piezo distance and the normalized cantilever deflection. A plot of E vs. δ using Eq. 8 results in a plateau region for the value of E for the PDMS network that represents an average elastic modulus for the entire network. This value can later be compared to macroscopic modulus measurements to determine the accuracy of the

calculation. The PDMS modulus value can then be used with reported values for the modulus of PE to determine K and the contact area.

The Hertzian calculation works best for measuring systems with high elastic moduli at low adhesion forces, or for systems with high adhesion forces at low elastic moduli. High elastic moduli in the presence of high adhesion forces leads to smaller and less well-defined plateaus on the E vs. δ curve. The difficulty in measuring these systems can be by minimized by conducting the experiments with a more flexible cantilever, which increases the range of the force on the cantilever between initial attraction to the surface and the maximum indentation. A typical E vs. δ curve for several PDMS networks measured is shown in Figure 3.5. Table 3.1 reports values for E and A for the materials used in this study.

The contact area determined from these relationships can then be used to normalize the friction force and determine the surface shear stress, σ.

$$\sigma = F_f / A \qquad (10)$$

By normalizing the friction in terms of shear stress, cross-linked films of different elasticity can be more readily compared over a range of sliding speeds. Scan rate can be treated as a shear rate, $\dot{\gamma}$, thus allowing for the surface viscosity, η, to be calculated by

$$\eta = \sigma / \dot{\gamma} \qquad (11)$$

These relationships allow for surface rheological characterization to be extracted from surface microscopy measurements, and provide an expanded analysis of the surface characteristics.

Friction force results converted to shear stress using Eq. (10) are depicted in Figure 3.6. As the more elastic systems do not conform to cantilever tip in the presence of load, the increased cross-link density means the deformed area is higher as

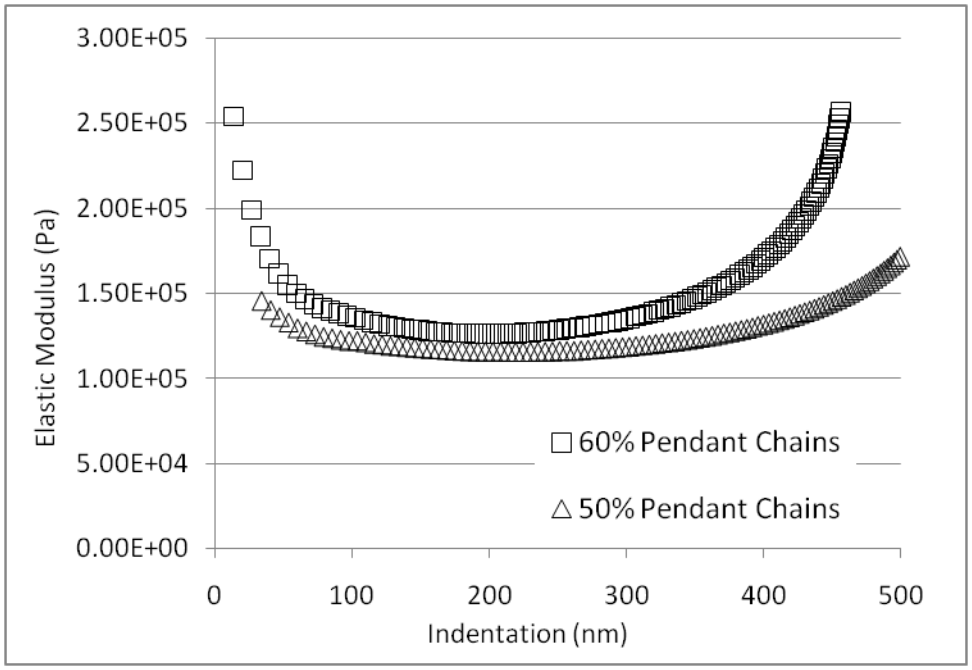

Figure 3.5. Elastic modulus vs. indentation curves developed from AFM force-distance data for a 27000 g/mol precursor molar mass difunctional network with 61000 g/mol pendent chains.

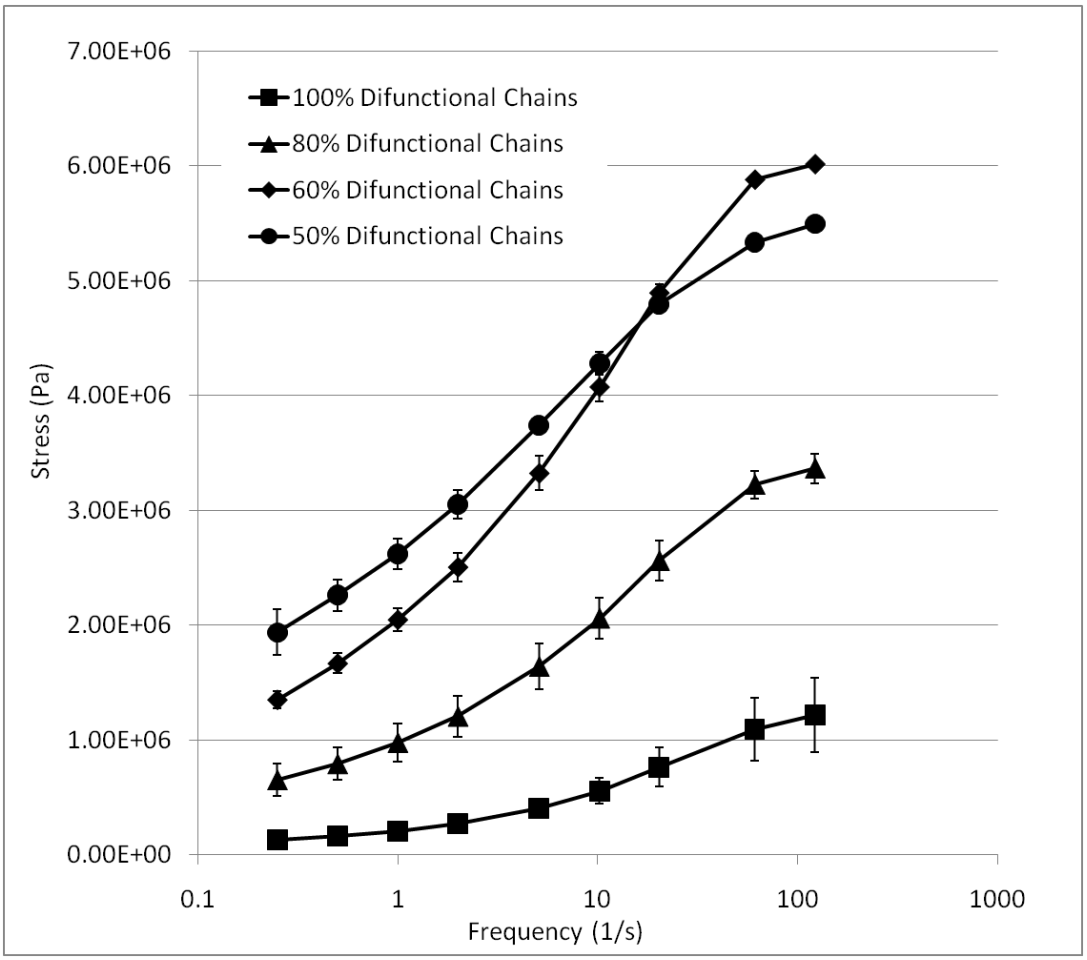

Figure 3.6. Shear stress vs. frequency curves for PDMS network systems made of varying amounts of 27000 precursor molar mass difunctional chains and 61000 precursor molar mass monofunctional chains. The load is constant at 4000 nN.

reported in Table 3.1. Increases in the concentration of pendent chains and network hyperbranching cause the contact area to decrease, as the surface deformation is much more localized than in an elastic network (see Figure 3.7). Thus stress is highly localized and much higher for the system with more pendent chains. As a result the more model network exhibits significantly lower surface stresses. The stark proximity in the overlay of the friction force curves (Figure 3.3) and the wide separation of the stress curves (Figure 3.6) clearly represents the effect of the pendent chains and the increase in viscous dissipation that they create. Their effect on the surface structure is further seen in the apparent viscosity of the lubrication systems, calculated using Eq. (11) and reported in Figure 3.8. The viscosity increases as the elasticity of the networks decreases, as is expected as a result of the increased number of pendent chains at the surface.

Another distinct trend between the different lubrication systems are the extrapolated values for the intercepts of the F_f vs. N curves in Figure 3.2. Based on the decided linearity of all the curves, the modified Admonton's equation reduces to the product of the critical load, N_c, and the COF when N is zero. This product has sometimes been called the 'residual force' and has been suggested to roughly correlate to the measured adhesive pull-off force,[29-31] even though the former is measured in shear while the latter is measured in the normal (pull-off direction). As reported in Figure 3.2, the intercept increases with the network concentration of pendent chains. The molecular model of friction and adhesion suggests that adhesion will increase with the number of polymer chain ends that can form a temporary adhesive contact at the interface. As the number of pendent chains is increased, the adhesion should increase as well. Thus the F_f vs. N intercepts demonstrate the presence of adhesion within the system, despite the negligible contribution of adhesion to the friction. The

Table 3.1. Comparison of AFM surface microscopy and bulk rheology experiments for the pendent chain networks.

	AFM					Rheometer	
	F_a (nN)	**Area (μm^2)**	**E (MPa)**	**σ exp.**	**η exp.**	**E (MPa)**	**η' exp.**
100%	208	0.419	0.495	0.380	-0.62	0.522	-0.77
80%	47.7	0.118	0.137	0.282	-0.72	0.510	-0.77
60%	22.9	0.066	0.152	0.255	-0.75	0.405	-0.78
50%	26.9	0.074	0.121	0.176	-0.82	0.120	-0.78

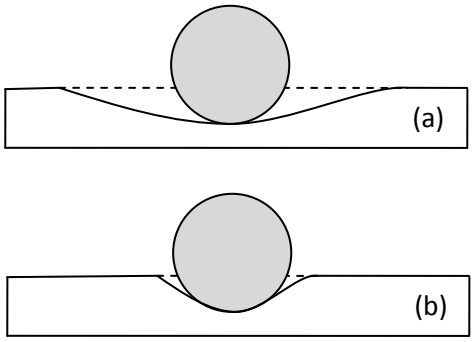

Figure 3.7. An illustration of the impact of cantilever bead on the surface geometry for network samples with both (a) high and (b) low elastic moduli. The diameter of deformed area is highly dependent on the network elasticity.

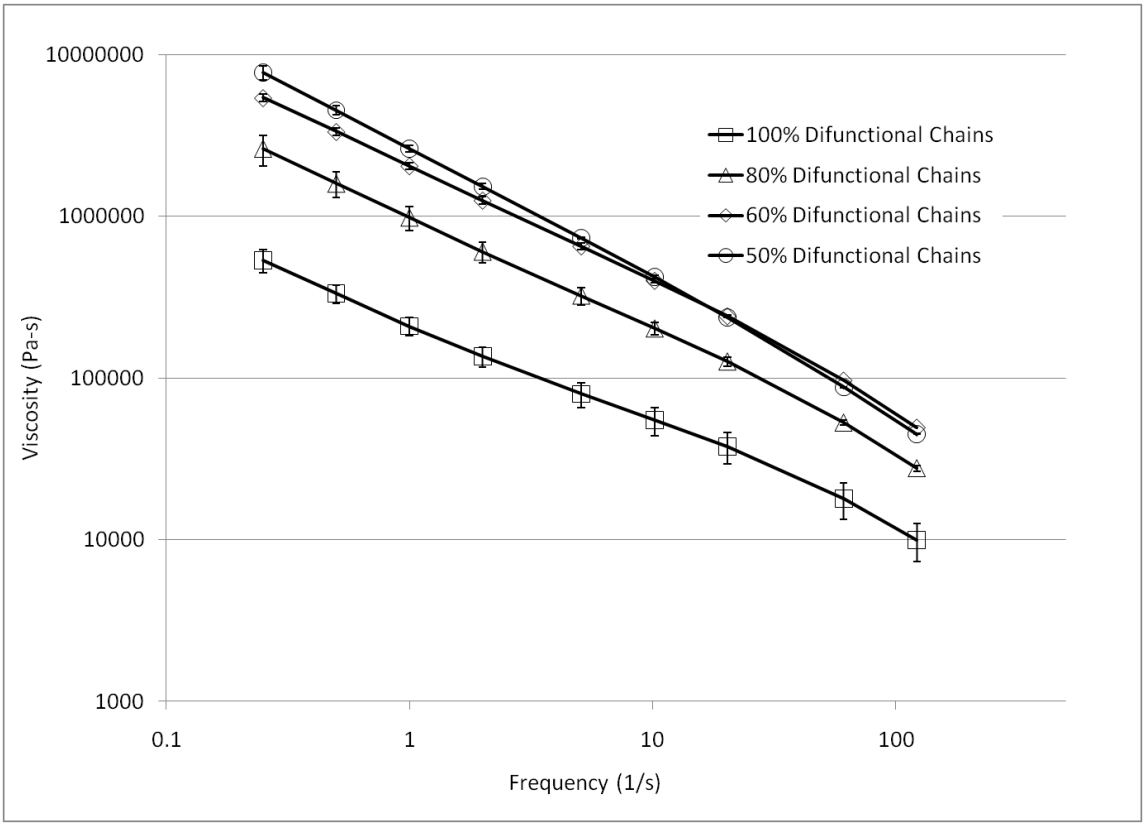

Figure 3.8. Surface viscosity vs. frequency curves for PDMS network systems made of varying amounts of 27000 precursor molar mass difunctional chains and 61000 precursor molar mass monofunctional chains. The load is constant at 4000 nN.

intercept trend holds for most sliding velocities investigated, as seen in Figure 3.9.

For a PE-PDMS interface, γ is expected to have a value of approximately 0.028 nN/nm. If one assumes that the critical load extracted from the residual force measured in shear is equivalent to the pull-off force F_a given in Eq. (7), one can extract a value of γ from the intercepts in Figure 3.2. However, as can be seen in Table 3.2, such values for all systems examined are at least one order of magnitude larger than the expected value. This is partly a result of the intercept providing only an approximate correlation between the critical load and the actual pull-off force. The higher interfacial tension values may also develop from the PDMS networks being constrained and stiffened in predominantly shear situations during friction measurement. The reduced flexibility within the network and at the interface in shear would act to increase the interfacial tension to levels much higher than would be measured in standard vertical JKR testing.

One concern with calculations indicating that contact area decreases as the concentration of pendent chains increases is that this may appear counter to expectations. Studies have shown that increasing the concentration of pendent chains in a network will decrease the elastic modulus, and the AFM measurements in Table 3.1 indicate that the network moduli agree with this prediction.[32,33] The lower elastic moduli imply that the contact area calculated from Eq. (4) should be increasing as the pendent chain concentration decreases. What this result does not consider, however, is the width of the contact area; when the hard PE bead is brought into contact with the PDMS elastomer, the more elastic networks will have much wider areas of deformation, as reflected by Figure 3.7. The contact area is thus actually larger for the more elastic systems, and this is accounted for by the adhesive pull-off forces being largest for the model network. AFM force mode measurements indicate F_a for the model network is almost an order of magnitude larger than all the networks with

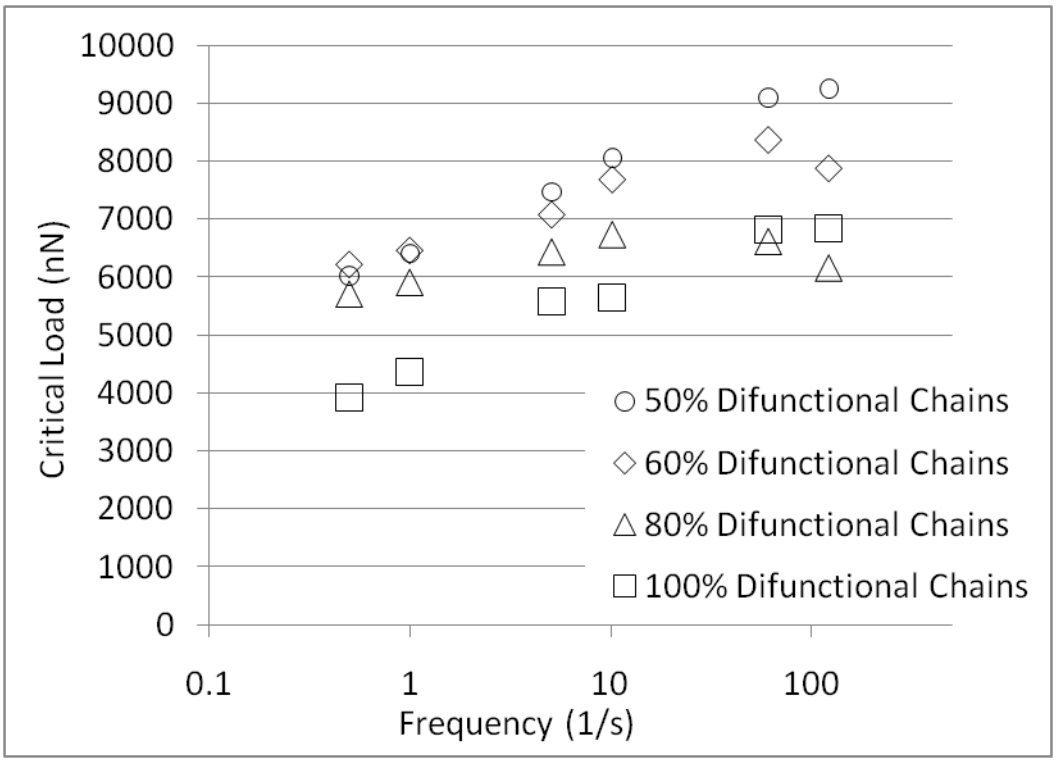

Figure 3.9. Critical load values obtained from the F vs. N curve intercepts over a range of frequencies. All networks are cross-linked from 27000 g/mol precursor molar mass with varying precursor concentrations of difunctional chains.

pendent chains, and F_a decreases as the concentration of monofunctional chains increases from 0 to 20 to 40 percent. The significant decrease may be a reflection of the pendent chains having a precursor molar mass that is larger than that of the difunctional chains by a factor of 2.3; the number of chain ends at the point of contact that can promote adhesion in shear will decrease as the pendent chain concentration increases. Thus, the contact area decreases with an increase in pendent chains.

3.4.3. Bulk Analysis. The atomic force microscope allows for friction measurements conducted at single-asperti conditions, and for characterizing physical properties at the sample surface. Macroscopic measurements of bulk properties of the samples are conducted in order to analyze the relevance of the bulk properties on the surface properties.

It is known that the dynamic viscosity, η', provides information about the viscous character of a material and the energy dissipation that occurs. As increasing the concentration of pendent chains within the network will increase viscoelastic effects, investigating η' as a function of the angular frequency, ω, and comparing to the AFM surface viscosity measurements can provide insight into the degree of viscoelasticity within the network as compared to the surface.[34] The dynamic viscosity shows large power-law regions at intermediate frequencies, providing opportunity to compare the power-law exponents of the different samples for both network $\eta'(\omega)$ measured in a rheometer and surface viscosity η measured as a function of shear rate $\dot{\gamma}$ with an AFM.

Comparisons can be made between the surface shear stress and the bulk loss modulus. The surface viscosity can be calculated from the stress, and the bulk viscosity can be determined from the loss modulus, G″.[35]

$$\eta' = \frac{G''}{\omega} \tag{12}$$

Table 3.2. Interfacial energy γ calculated for lubrication systems from the critical load obtained from the F vs. N curves, tabulated over a range of sliding frequencies. A theoretical value of 0.028 nN/nm is expected for a polyethylene-PDMS interface.

		Calculated network γ (nN/nm) from critical load Nc			
		100% Difunc.	**80% Difunc.**	**60% Difunc.**	**50% Difunc.**
Frequency (1/s)	0.5	0.318	0.484	0.527	0.511
	1	0.286	0.502	0.548	0.544
	5.09	0.223	0.547	0.600	0.634
	10.2	0.221	0.572	0.652	0.684
	61	0.183	0.562	0.710	0.773
	122	0.183	0.523	0.668	0.785

The loss modulus is a measurement of viscous losses in the bulk, and has a similar relationship with the bulk viscosity as the surface shear stress does with the surface viscosity. The loss modulus can be directly determined from the relaxation modulus, G(t), according to the empirical relation:

$$G(t) = \frac{\sigma(t)}{\gamma} = G_E\left(1 + \left(\frac{t}{\tau_E}\right)^{-m}\right) \tag{13}$$

where m is a constant and τ_E is a material parameter.[36] Knowing the elastic modulus, G_E, the loss modulus is calculated from the relationship:

$$G''(\omega) = \omega\int_0^\infty [G(t) - G_E]\cos(\omega t)dt \tag{14}$$

Substituting Eq. (13) into Eq. (14), the loss modulus in a network is thus seen to have a power-law relationship with the frequency:

$$G''(\omega) = G_E B\omega^m \tag{15}$$

where B is a constant. Power-law exponent values should be extractable from both η' vs. ω and G'' vs. ω curves. Comparison can be made between the bulk and surface frequency properties by relating the bulk frequency analysis to a surface frequency analysis conducted with the σ vs. $\dot{\gamma}$ and η vs. $\dot{\gamma}$ curves obtained from the AFM. The values will be different for $\eta'(\omega)$ and $\eta(\dot{\gamma})$, as both have similar power-law relationships but are not directly proportional to each other. Trends in changes to the power-law exponent values may be extractable for different pendent chain network concentrations. A comparison between $\eta'(\omega)$ and $\eta(\dot{\gamma})$ will thus reflect different responses at the surface and within the bulk.

To conduct bulk property measurements, a Physica MCR 300 rheometer was used. PDMS networks were allowed to cross-link as previously described in 100 micron gap spacing between two 15 mm diameter parallel plates. To prevent slipping between the network and the parallel plates after cross-linking had completed, the gap spacing was set immediately after catalyst had been added to the precursor polymer mixture and the mixture had been poured onto the lower plate. Excess PDMS was

scraped and removed from the outside of the upper parallel plate to eliminate edge effects. Measurements were conducted at a constant temperature of 35 ^{o}C within a heating chamber. Frequency sweep measurements were conducted over a range of angular frequencies from 600 to 0.1 1/s at a constant strain of 0.1%. The frequency sweeps were repeated to ensure experiments were conducted after complete curing and the network structure was no longer evolving. Both G'' vs. ω and η' vs. ω curves were obtained from the frequency sweeps and analyzed using a power-law relationship.

Characterization results from both surface microscopy and bulk rheology for the pendent chain systems are seen in Table 3.1. Similar trends exist for both sets of measurements. From the AFM experiments, the stress exponent and the viscosity exponent determined from power-law relationships against the sliding frequency both decrease with increasing pendent chain concentration. This indicates that a wider range of stresses can be achieved with respect to sliding velocity as the pendent chain concentration increases. Similarly, the decrease in the viscosity exponent is indicative of the increased surface viscous dissipation in the more poorly cross-linked networks. The bulk viscosity exponent as measured by the bulk rheology is practically constant. This points to the network modifications having a much more significant effect at the surface than within the bulk for viscous relaxation behavior, which may be understood in the terms of the greater ease of viscous relaxation at the surface.

It is also important to consider the comparison between elastic moduli measured by microscopy and by rheology. While there is strong correlation between the moduli values measured for both the model elastic network and the network synthesized from 50 percent difunctional chains (i.e. the network with the most pendent chains), the network lubricants with 60 and 80 percent difunctional chains have very different moduli values. The rheology-measured moduli value is 3.7 times larger than the microscopy-measured modulus for the 80 percent system and 2.6 times

larger than for the 60 percent system. The difference between measurements is surprising in consideration of the accuracy of AFM nanoindentation. Mareanukroh et al. showed that the AFM can have a high accuracy for network elastic modulus measurements on styrene-butadiene rubbers over a range of cross-link densities, with moduli values deviating by only five or six percent from values measured through other techniques.[37] However, the researchers recognize that the adhesion hysteresis must be minimized in order to achieve accurate values. As an example, they depict a force-distance curve developed from AFM force mode where the hysteresis curve is approximately 80 nm wide; our force-distance curves repeatedly indicate hysteresis curves that are a minimum of 400 nm wide. Thus some inaccuracy is expected in our results because of the high surface adhesion of PDMS. Mareanukroh et al. also recognize that the measurements should be conducted on surfaces with low surface roughness. Measurements of the surface thickness indicate uniform surfaces; this implies that any surface roughness defects should be difficult to distinguish compared to the width of the micron-sized cantilever bead, and should not introduce inaccuracy into the nanoindentation measurements.

The differences between the rheology and microscopy elastic modulus values are likely in part a result of the surface roughness and the increased adhesion hysteresis. However, it is more likely that the differences in the 60 and 80 percent difunctional networks can be attributed to a difference in the network structure at the surface and within the bulk. While the rheology experiments measure the average elastic modulus of the entire network, microscopy uses measurements at the surface with the purpose of estimating the elastic modulus for a much thicker system. If the pendent chains that are present at the surface have formed a thin layer on top of the network, the lower elastic modulus of the dangling chains may dominate the higher elasticity within the network. While the model network should have few defects at the

surface and within the bulk, and the network with the most pendent chains will be hyperbranched throughout the entire structure, the networks with an intermediate concentration of pendent chains may have a structure where defects at the surface do not accurately portray the entire network. Thus the microscopy measurements likely represent the structure at the surface and rheology measurements are more descriptive of the structure within the network.

3.4.4. Surface Mobility. The degree of surface mobility can be determined by applying an Eyring-like model developed by Zhang and Archer, which takes into account the counter-acting effects of molecular chain relaxation, macroscopic sliding speed, and viscous and elastic forces.[38] In this model, it is assumed that the motion within a system is restricted by potential obstacles within the surrounding material. Motion between particles occurs as a result of an applied stress, providing sufficient energy to overcome a potential energy barrier. If motion is to continue at a constant velocity, v, the particles must overcome a regular series of these harmonic potential barriers of height, Q, separated by a constant distance, b. The molecular velocity can be evaluated from the relation:[38]

$$v = 2\upsilon b \exp\left[-\frac{(Q + P\Omega)}{kT}\right] \sinh\left(\frac{\tau\varphi}{kT}\right) \qquad (16)$$

where T is temperature, k is the Boltzmann constant, P is the pressure, τ is the imposed stress, and ν is the effective vibration frequency of the molecule. Here Ω is the stress activation volume while φ is the pressure activation volume; these parameters describe the effective volume barrier to motion under a normal or lateral force, respectively.

Assuming that the macroscopic sliding velocity, v, is proportional to the molecular velocity, V, and that the friction force is a product of the imposed stress and contact area, it is therefore possible to relate the friction force to the sliding velocity in

terms of molecular motion. The imposed stress can be evaluated from typical boundary lubrication measurements where τφ/kT > 1, allowing Eq. (16) to be rewritten as:

$$\tau = \frac{kT}{\varphi}\ln\left(\frac{V}{V_o}\right) + \frac{(Q + P\Omega)}{\varphi} \tag{17}$$

where V_o is proportional to bν as V is proportional to v. The relationship between friction force (F_f) and sliding velocity is thus given as:

$$F_f = \frac{AkT}{\varphi}\ln\left(\frac{V}{V_o}\right) + \frac{A(Q + P\Omega)}{\varphi} = \frac{A}{\varphi}\left[kT\ln\left(\frac{V}{V_o}\right) + Q + P\Omega\right] \tag{18}$$

Assuming that the characteristic relaxation time of the material, τ'_o, is related to the time-dependent pressure by:

$$P(t) = 1 - \exp\left(-\frac{t}{\tau'_o}\right) \tag{19}$$

Eq. (18) can then be simplified to:

$$F_f = B\ln\left[V\left(1 - \exp\left(-\frac{\omega_o}{V}\right)\right)\right] + D \tag{20}$$

where B, D, and ω_o are constants:

$$B = AkT / \varphi \tag{21}$$

$$D = \frac{A(Q + P\Omega)}{\varphi} - \frac{AkT}{\varphi}\ln(V_o) \tag{22}$$

$$\omega_o = \delta_o / \tau'_o \tag{23}$$

Here δ_o is a molecular length scale, describing the length on which molecules will move in response to external stress applied at the interface, and is related to the stress activation volume by

$$\varphi \approx (\delta_o)^{1/3} \tag{24}$$

Even if this model is used to the data from the pendent chain networks, and values of the parameters B, D, and ω_o are obtained, it is very difficult to draw out much information without significantly more physical and molecular data, particularly for D. However, the actual contact area was determined using nanoindentation measurements, thus allowing a value to be determined for φ from Eq. (21) and a value for B. Furthermore, the parameter ω_o can be used to determine the constrained

relaxation time, τ'_o, by Eq. (23), thus providing insight into the relaxation time of the networks at the interface.

The results of such an analysis are presented in Table 3.3. From these results, it is clear that relaxation time increases with the concentration of pendent chains in the network. Because these relaxation times are dramatically shorter than the relaxation times typically measured for bulk PDMS networks, the model is clearly providing relaxation times of the surface chains. This would suggest that the elastic network is constrained, and a surface viscous layer exists for the pendent chain systems. Evidence for an overcoat of pendent chains is also demonstrated by the decrease in the molecular length scale with the increase in pendent chain concentration. As an elastic network will present greater resistance to molecular sliding than a free chain end, the decrease in δ_o indicates a thicker viscous surface layer from pedant chain ends. It should be noted that references to a pendent chain surface layer does not imply that the pendent chains ends will go to the surface, but that the chain ends that are present at the interface will respond to external forces and thus have a physical effect on the friction and bulk properties of the material.

The surface overcoat of pendent chains may explain the decrease in friction for networks with increased viscoelasticity at higher sliding velocities. The elastic networks will be forced to distribute the tension created by the applied stress at the surface. Pendent chains may align in the direction of the sliding velocity, thus preventing tension from distributing throughout the network and decreasing the constraint in the network.

The surface mobility characterization can also be used to provide more insight into the adhesion and F vs. N intercept data. A correlation developed by Chen et al.[39] from adhesion hysteresis models and friction theories indicates that the following relationship between the friction force at zero load, $F_f(0)$, and the contact area exists as

$$F_f(0) = \varepsilon A \Delta\gamma / \delta \quad (25)$$

where $\Delta\gamma$ is the adhesion hysteresis determined from AFM force mode measurements, and ε is the fraction of kinetic energy transferred to the network upon contact. Essentially, ε describes the fraction of the adhesion force that contributes to friction. This is an important factor to consider as the adhesion forces were not trivial for the pendent chain networks.

Chen found that the values for ε for polystyrene and poly(vinyl benzyl) chloride surfaces to range from 0.2 to 1.0.[39] As seen in Table 3.3, however, the elastic PDMS-PE surface exhibits much lower values, as low as 0.016 for a model network. This result is not entirely surprising, as the linearity in the F vs. N curves indicates the adhesion contribution to friction is negligible. The fact that ε is so much lower for the model PDMS network - PE system is likely a result of the low surface energy and low interfacial shear stress exhibited by PDMS. The PDMS-PE ε values are much more comparable as the concentration of pendent chains increases, with values as high as 0.27. The increase in ε with the pendent chain concentration indicates a significantly larger adhesion contribution. Based on the molecular model of adhesion, an increased number of chain ends that exist at the interface should increase the adhesive interactions between the two surfaces that occur during shear. By creating more hyperbranched networks, the fraction of the friction force that comes from the contribution of adhesion should thus increase, as is seen in the much higher calculated values for ε.

3.5. CONCLUSIONS.

Interfacial and bulk properties of PDMS network –SAM multi-tiered lubrication systems have been investigated. Ultrathin (~10 nm) and micro-thick films (~10 μm) have been previously seen to have dramatically low COFs, achieving values

Table 3.3. Pendent chain mobility characterization data based on the Zhang-Archer model and the Chen et al. correlation for intercept data.

	B	**δ_o (nm)**	**ω_o (μm/s)**	**τ'_o (s x 10^{-7})**	**ε**
100% Difunc.	118	1.96	2067	9.48	0.016
80% Difunc.	71	1.22	1426	8.54	0.148
60% Difunc.	70	0.88	932	9.48	0.277
50% Difunc.	59	1.00	589	17.4	0.274

as low as 0.004. In an attempt to determine the source of the low friction results, structural modifications were made to the micro-thick networks to recapture the hyperbranching effect of the ultrathin network structure. Controlled concentrations of pendent chains were introduced into the micro-thick networks to create a hyperbranched structure at the interface. Higher concentrations of pendent chains were seen to dramatically increase surface shear and the viscosity at all sliding velocities. The elastic networks had much lower surface viscosity, implying lower roughness at the interface. Increasing the concentration of pendent chains served to increase the COF at low sliding velocities, but to provide lower COF values than those of elastic networks at high shear rates. The relaxation times indicate that all individual pendent chains and all constrained elastic networks would not be able to relax at any sliding velocity, suggesting the transmission of the tension throughout the networks was much more difficult for the constrained elastic systems at high sliding velocities, thus resulting in the high COFs.

The PDMS networks demonstrated such low friction results because the adhesion contribution to the friction force was negligible. This was not only seen from the decided linearity of the F_f vs. N curves, but also from the fraction of kinetic energy that was transferred to the network upon contact. The low surface energy and shear stress of PDMS made it possible for a decreased adhesion effect; increasing the concentration of pendent chains served to increase the role of adhesion, thus resulting in higher friction and COFs.

Rheological bulk characterization supported interfacial measurements of the network shear stress and viscosity. Greater variation in the power-law exponents calculated from the AFM experiments indicates the presence of pendent chains has a more demonstrative effect at the surface than within the network. The increased mobility of the pendent chains at the surface thus allows for the interfacial friction

transition at high sliding velocities by which lower friction is exhibited by the more viscous-like thick hyperbranched structures than the highly elastic networks. Pendent chains provide a flexible mobile overcoat for the elastic systems at high velocities and prevent tension transmission into the bulk of the network.

REFERENCES

(1) Rymuza, Z. *Microsystem Technologies* **1999**, *5*, 173-180.

(2) Bhushan, B. *Proc. Instn. Mech. Engrs Part J* **2001**, *215*, 77-102.

(3) Cagin, T.; Che, J.; Gardos, M. N.; Fijany, A.; Goddard, W. A., III. *Nanotechnology* **1999**, *10*, 278-284.

(4) Sundararajan, S.; Bhushan, B. *J. Vac. Sci. Technol. A.* **2001**, *19(4)*, 1777-1785.

(5) K. Strawhecker, D.B. Asay, J. McKinney and S.H. Kim. *Tribology Letters* **2005**, *19*, 17-21.

(6) Bhushan, B. *Microelectronic Eng*. **2007**, *84*, 387-412.

(7) Bhushan, B.; Liu, H.; Hsu, S. M. *ASME J. Tribol* **2004**, *126*, 583-590.

(8) Bhushan, B.; Israelachvili, J. N.; Landman, U. *Nature* **1995**, *374*, 607-616.

(9) Xiao, X.; Hu, J.; Charych, D. H.; Salmeron, M. *Langmuir* **1996**, *12*, 235-237.

(10) Tsukruk, V.V.; Bliznyuk, V.N. *Langmuir* **1998**, *14*, 446-455.

(11) Yang, X.; Perry, S. S. *Langmuir* **2003**, *19*, 6135-6139.

(12) Raviv, U.; Glasson, S.; Kampf, N.; Gohy, J. F.; Jerome, R.; Klein, J.. *Nature* **2003**, *425*, 163-165.

(13) Ahn, H-S; Julthongpiput, D.; Kim, D-I; Tsukruk, V.V. *Wear* **2003**, *255*, 801-807.

(14) Julthongpiput, D.; Ahn, H-S; Kim, D-I; and Tsukruk, V.V. *Tribology Letters* **2002**, *13*, 35-40.

(15) Bowden, F.P.; Tabor, D. *Friction and Lubrication.* Methuen & Co. Ltd.: London, 1967.

(16) Wang, W.; Wang, Y.; Bao, H.; Xiong, B.; Bao, M. *Sensors and Actuators* **2002**, *97-98*, 486-491.

(17) Maboudian, R.; Ashurst, W. R.; Carraro, C. *Sensors and Actuators* **2000**, *82*, 219-223.

(18) Zhang, Q.; Archer, L. A. *Langmuir* **2005**, *21*, 5405-5413.

(19) Landherr, L.J.T.; Zhang, Q.; Cohen, C.; Archer, L.A. *J. Poly. Sci. B.*, **2008**, *46*, 1773-1787.

(20) Patel, S.K.; Malone, S.; Cohen, C.; Gillmor, J.R.; Colby, R.H. *Macromolecules* **1992**, *25*, 5241-5251.

(21) Tordjeman, P.; Mutin, P. H.; Tixier, T. *Rheol Acta* **2004**, *43*, 550-558.

(22) Johnson, J.A.; Lewis, D.R.; Diaz, D.D.; Finn, M.G.; Koberstein, J.T.; Turro, N.J. *J. Am. Chem. Soc.* **2006**, *128*, 6564-6565.

(23) Zhang, Q.; Archer, L.A. *Langmuir* **2007**, *23*, 7562-7570.

(24) Liu, Y.; Evans, D. F. *Langmuir* **1996**, *12*, 1235-1244.

(25) Cleveland, J.P.; Manne, S.; Bocek, D.; Hansma, P.K. *Rev. Sci. Instrum.* **1993**, *64*, 403-405.

(26) Johnson, K.L.; Kendall, K.; Roberts, A.D. *Proc.R. Soc. London, Ser. A*, **1971**, *324*, 301-313.

(27) Leger, L.; Raphael, E..; Hevert, H. *Advances in Poly. Sci.* **1999**, *138*, 186-225.

(28) Dimitriadis, E.K.; Horkay, F.; Maresca, J.; Kachar, B.; Chadwick, R.S. *Biophysical Journal* **2002**, *82*, 2798-2810.

(29) Lee, J. *International Journal of Pharmaceutics* **2007**, *340*, 191-197.

(30) Beake, B.D.; Leggett, G.J. *Phys. Chem. Chem. Phys.* **1999**, *1*, 3345-3350.

(31) Tsukruk, V.V.; Bliznyuk, V.N. *Langmuir* **1998**, *14*, 446-455.

(32) Vaenkatesan, V.; Li, Z.; Vellinga, W.-P.; de Jeu, W.H. *Polymer* **2006**, *47*, 8317-8325.

(33) Batra, A.; Cohen, C.; Archer, L. *Macromolecules* **2005**, *38*, 7174-7180.

(34) Bird, R.B.; Armstrong, R.C.; Hassager, O. *Dynamics of Polymeric Liquids: Vol. 1* John Wiley & Sons, New York: **1987**.

(35) Rubinstein, M.; Colby, R. H. *Polymer Physics.* Oxford University Press, New York: **2003.**

(36) Chasset, R.; Thirion, P. In *Proceedings of the Conference on Physics of Non-Crystalline Solids;* Prins, J.A., Ed; North-Holland Publishing Co.: Amsterdam, **1965**.

(37) Mareanukroh, M.; Eby, R.K.; Scavuzzo, R.J.; Hamed, G.R. *Rubber Chemistry and Technology* **2000**, *73*, 912-925.

(38) Zhang, Q.; Archer, L.A. *J. Phys. Chem. B.* **2003**, *107*, 13123-13132.

(39) Chen, N.; Maeda, N.; Tirrell, M.; Israelachvili, J. *Macromolecules* **2005**, *38*, 3491-3503.

CHAPTER 4

THE FRICTION AND WEAR OF THIN PDMS NETWORK LUBRICANTS SWOLLEN WITH FREE CHAINS

4.1. ABSTRACT

This study investigates the lubrication properties of networks swollen with free chains. It also explored the effect that the structural modifications to the network have on the friction, adhesion and wear. Thin network films (~10 μm) were created by cross-linking from a precursor polymer in solution containing a small concentration of non-reactive polydimethylsiloxane (PDMS) chains. The cross-linking reaction also tethered the network film to self-assembled monolayer coated silicon wafers. Network characterization was conducted with an atomic force microscope to determine the surface friction, adhesion, and structural properties of the polymer films. Rheology measurements were performed to evaluate the physical properties of the lubricants in comparison to bulk values extracted from surface microscopy measurements. Most of the swollen networks studied formed a viscous surface layer that significantly increased the surface friction and adhesion compared to model networks not containing free chains. Only networks with an intermediate free chain molar mass displayed improved lubrication properties. Tribology investigations demonstrated that the presence of free chains during the network cross-linking rapidly increase the wear rate of the fully-formed networks.

4.2. BACKGROUND

Advancements made in the field of small devices have driven research into the development of lubricants that can operate on the micro- and nano-lengthscale.[1-3] The reduction in operating size places an emphasis on the surface effects of friction,

adhesion, and wear to create a distinct set of characteristics that a nano- and micro-scale lubricant is expected to meet.[4-8] Specifically, an optimal nanoscale lubricant should exhibit both a small contact area and low interfacial shear stress to minimize friction effects. It must be possible to deposit the lubricant as a thin film to maintain substrate features. The lubricant must also be mechanically durable and strongly tethered to the substrate to minimize wear.

As described in a previous paper,[9] we have proposed a thin film hybrid lubricant based on a PDMS network. The hybrid lubricant consists of two tiers as depicted in Figure 4.1.1; a self-assembled monolayer (SAM) that provides a surface-adhered anchoring layer to which a cross-linked PDMS network is bonded as a softer surface layer. PDMS is an ideal lubricating material because of its low surface energy and high molecular flexibility. These PDMS network – SAM hybrids have previously been reported to exhibit extremely low friction coefficients (COFs), as low as 0.0077 for a model network (approximately 10 μm thick). The low COFs are a result of the low interfacial shear stress and a negligible contribution of adhesion to the friction force.

Several studies have determined that one characteristic of elastomeric lubricants is that the COF of the polymer film decreases as the elastic modulus decreases. The primary theory for this trend focuses on the active process of molecular adhesion. Chernyak and Leonov proposed that a number of polymer chain ends at any time can be considered to form "working chains", meaning they will be in a period of short-lived adherence at the interface with the opposing sliding surface.[10] For networks, these working chain ends can come from either dangling chains bonded at only one end within the networks, or network cross-link sites where several chain ends are bonded together. The energy required to break the attachments increases as the number of working chain ends increases; thus, the COF will increase with the

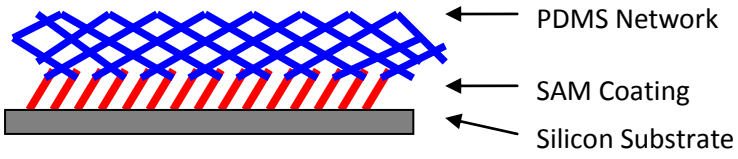

Figure 4.1.1. Illustration of an optimal network lubricant. The PDMS network is fully cross-linked and uniform; the SAM coating is not exposed to surface.

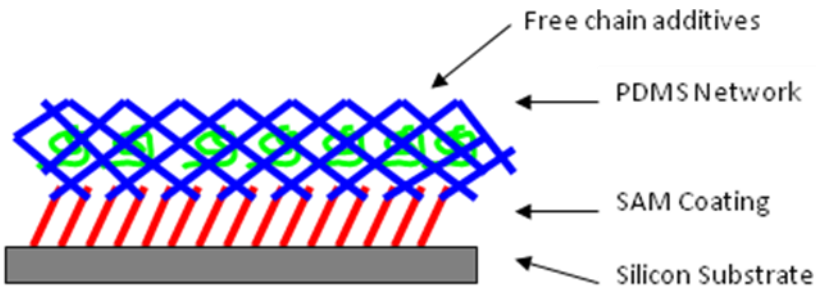

Figure 4.1.2. Illustration of a micro-thick system swollen with free chains. The PDMS network is fully cross-linked.

number of working chains. If a model network is synthesized from end-linking cross-linking process, the number of overall chain ends within a set network volume will increase for polymer chains of a lower precursor molar mass.[11] Thus by increasing the cross-link density, the COF will be larger for networks with shorter precursor molar mass polymer chains. This theory is most effective as an explanation when the contribution of adhesion to the friction force is high.

The other major theory regarding the COF of polymer films focuses on the transfer of stress at the point of contact. Networks with a lower elastic modulus will be more flexible. As the modulus increases, the network will be more constrained, and a greater amount of stress will distribute into the network upon contact between the two surfaces because of the smaller contact area. The increased dissipation of energy into the network will cause the friction and COF of the polymer film to increase.[12] It is necessary to consider the potential of this theory when adhesive forces are low or when there is a negligible contribution of adhesion to the friction force. This result would mean that the effect of adhesion on lateral sliding at the interface is dominated by the load contribution to friction, decreasing the viability of the working chain theory.

In an attempt to further investigate the relationship between elastic modulus and COF, we have modified the structure of our PDMS-SAM hybrid lubricants to create networks swollen with free chains, as depicted in Figure 4.1.2. These free PDMS chains do not participate in the cross-linking reactions that form the network; by including the free chains in the precursor polymer melt, the PDMS network cures in a swollen state. Ideally, the free chains in this modified structure serve to decrease the elastic modulus of the lubrication system while holding the interface constant. We have previously modified the network structure by systematically adding pendent chains; this study revealed that increasing the viscoelasticity at the network surface

will increase the adhesion and friction at the interface and serve as a detriment to the overall quality of the lubricant.[13] If the free chains are present at the interface, the introduction of a viscous layer could potentially diminish any effect of a lower elastic modulus.

Introducing free PDMS chains in polymer films to reduce friction and wear has been previously investigated and shown to have some success. Hill et al. created blends of thermoplastic polyurethane and low concentrations of high molar mass PDMS (~1 to 3 percent) and measured both the wear rate and the COF.[14] They found that the presence of PDMS not only reduced the COF by approximately 75 percent, but that the wear rate also decreased by 15 percent for certain cases. They attributed these results to improved surface lubrication and reduced crystallinity within the system as a result of the presence of PDMS. Galliano et al. investigated the surface shear of PDMS networks before and after the extraction of uncross-linked PDMS chains.[15] They determined the friction resistance was slightly reduced for systems containing free chains as a result of a viscous layer decreasing the elastic contact at the interface and slightly reducing the shear resistance.

4.3. EXPERIMENTAL

4.3.1. Preparation of SAMs. 10-undecenyl trichlorosilane was purchased from Gelest, Inc. Hexadecane ($C_{16}H_{34}$), chloroform ($CHCl_3$), dichloromethane (CH_2Cl_2), and methanol (CH_3Cl) were purchased from Aldrich Chemicals. Three-inch (100) silicon wafers purchased from University Wafer were cut into 1.5 cm by 1.5 cm pieces using a diamond tipped stylus. The wafer pieces were rinsed ultrasonically in chloroform and treated for 30 minutes in a piranha solution of 10 mL 30% hydrogen peroxide (H_2O_2) and 12 mL hydrosulfuric acid (H_2SO_4) above 130 ^oC. The oxidized

surfaces were then rinsed in DI water a minimum of eight times and blown dry with nitrogen gas.

Solutions of hexadecane and chloroform were prepared inside a dry nitrogen atmosphere glovebox at a 4:1 volume ratio. Each solution was mixed in a media bottle and had a total volume of 40 mL. Twenty-four μL of 10-undecenyl trichlorosilane were added to each bottle of solution before approximately five cut wafer pieces were placed and arranged in each flask in order to maximize the amount of exposed wafer surface. The wafers sat in solution in the glovebox overnight to allow for the formation of the SAM layers. The silicon wafers were then rinsed successively in dichloromethane, chloroform, and methanol baths for approximately five minutes each to remove any free monolayers and excess solvent. The monolayer-coated wafers were dried under nitrogen and stored.

4.3.2. Preparation of PDMS Networks. Networks were synthesized according to the process detailed by Patel et al.[16] Vinyl-terminated PDMS precursor molecules with a molar mass of 28,000 g/mol, cross-linking agent tetrakis(dimethylsiloxy)silane and a platinum catalyst were purchased from Gelest. Toluene was purchased from Aldrich. PDMS and the cross-linking agent were mixed in vials based on optimal ratios described previously.[17] Trimethoxy-terminated PDMS chains were added into these solution at set volume concentrations of 10 and 20 percent. In a separate vial, 100 μL of the platinum catalyst was diluted in 10mL of toluene. Immediately after the catalyst solution was added to the PDMS and cross-linker and vigorously mixed, enough polymer solution was poured onto the SAM-coated silicon wafer substrates to just cover the surface of the wafer. The solution and cut wafers were spincoated at 3,000 rpm for 60 seconds using a SCS P6708 spincoater. The silicon pieces were heated in an oven at 35 ^{o}C to ensure complete annealing of the vinyl-PDMS chains. The annealing process continued for four days. To prevent deswelling of the

networks, the final silicon pieces with free chains were not rinsed. Networks that did not contain free chains were rinsed for five minutes twice in dichloromethane to remove any excess unbonded material. Dichloromethane was then removed by reheating the systems for one hour at 75 ^{o}C. The surface coating thicknesses were then remeasured.

4.3.3. Characterizing the Thickness of the PDMS Networks. Film thickness of the PDMS networks was measured with a F20 Film Metrics Spectrophotometer. A constant refractive index of 1.4 was assumed for the PDMS layer.[18] Approximately five measurements were conducted on each film at multiple positions to determine the average thickness and film uniformity.

Analysis of the PDMS network thickness was based on a one-layer film on a silicon substrate. Measuring the SAM layer coating using a Rudolph Research Auto-EL Ellipsometer has shown the SAMs to consistently have an average thickness of 1.2 nm. This thickness is negligible in comparison to the micro-scale PDMS.

4.3.4. AFM Analysis. A DI3000 Atomic Force Microscope (AFM) was used for friction, adhesion, and indentation measurements. Cantilevers were purchased from Novascan for friction and indentation analysis. The cantilevers included polyethylene and silica bead tips with 5 μm radii; the spring constant of the polyethylene bead cantilevers was 4.5 N/m, while silica bead cantilevers were purchased at both 4.5 N/m and 0.58 N/m. The friction analysis reported in this paper was conducted using the polyethylene-bead tips because they provide highly reproducible data and do not contaminate easily. The silica-bead tips were used to corroborate the nanoindentation results.

Surface friction force data were obtained in contact mode by scanning the AFM cantilever probe against the sample in the forward and reverse cantilever directions. By creating a friction loop as a result of disabling other scan lines, the

friction force could be determined from the average difference between values from opposing scan directions. The wafers were held in place by both a vacuum and double-sided tape. Data were collected at fixed scan rates ranging from 0.1 to 122 Hz and scan lengths of 5.0 μm. The sliding speed is determined as the product of the scan rate and the scan distance traveled laterally by the cantilever. The applied load was varied by changing the cantilever operating height of setpoints ranging between 0 to 8 volts. Friction measurements were conducted at five applied loads, and friction values were recorded after a steady-state friction force value was reached for each new load. Final friction-load plots were constructed from an average of the measurements at several different points for each system. The normal and lateral AFM force values (N and F) can be converted from voltage, V, through the relations

$$N = K_n S_n V_n \quad (1)$$

$$F = K_l S_l V_l \quad (2)$$

Normal sensitivity, S_n, was found from force-distance curves for each sample and used to determine lateral sensitivity, S_l, as described by Liu and Evans.[19] Cantilever dimensions were used to determine the lateral force constant K_l. The added-force method described by Cleveland et al. was used to determine the normal force constant K_n.[20] This method was used to check reported force constant values for all cantilevers. Glass particles ranging in diameter from 10 to 50 μm were attached to the cantilever tip by pressing down on the tip after aligning the cantilever vertically on the glass particles. The resonant frequency of the cantilever with the added weight was then recorded. The masses of the glass particles used were calculated from the diameter of the particle and the bulk density of glass. The normal force constant was calculated to be 4.47N/m for the reported 4.5 N/m polyethylene bead cantilever, 4.48 N/m for the reported 4.5 N/m silica bead cantilever, and 0.60 N/m for the 0.58 N/m silica bead cantilever.

The relative humidity can have a significant effect on the COF when measuring the friction of different surfaces with an AFM. Increased humidity can cause higher degrees of contamination in the form of a viscous layer on the sample surfaces and result in higher friction forces.[21] An improved comparison between the COFs of two different lubrication systems can thus be determined by evaluating the percent reduction in COF from that of the substrate. While traditional F vs. N curves were developed and analyzed from all AFM measurements, comparisons of the COFs for different networks are much more accessible, utilizing calculations of the difference in COF for each system and the substrate measured during the same series of experiments.

4.4. RESULTS

4.4.1. Interfacial Friction. The friction force (F_f) vs. load (N) results for the 10 volume percent free chain samples are reported in Figure 4.2. Several trends can be seen from these data. First, all the lubricant systems exhibit reduced COF (μ), relative to that of bare silicon by at least 60 percent. Second, only the networks with 2000 g/mol and 5900 g/mol molar mass free chains had slightly lower COFs than the model network films developed without free chains. Finally, the systems with the shortest and longest free chains exhibit relatively high friction while minimum friction exists for an intermediate molecular weight of 5900 g/mol. Similar friction force vs. load results for systems made with 20 percent free chains are reported in Figure 4.3. For these data, only the networks containing 5900 g/mol molar mass free chains exhibited slightly lower friction than the model network system. Large error bars also exist for many of the F_f vs. N curves, indicating that the surfaces are likely not uniform and potentially have a free chain surface layer of significant thickness. Humidity effects are also present as evidenced by the increased COF for a bare silicon substrate.

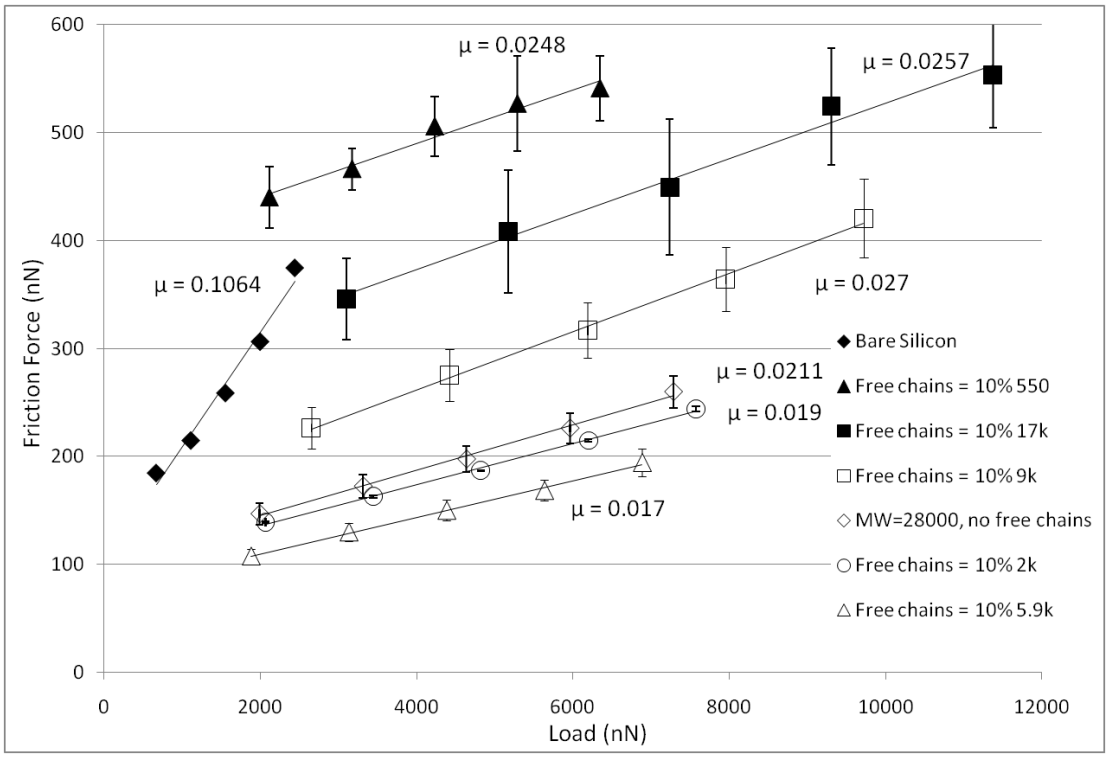

Figure 4.2. Friction force vs. load curves for micro-thick networks with free chains (10 volume percent in the precursor mixture).

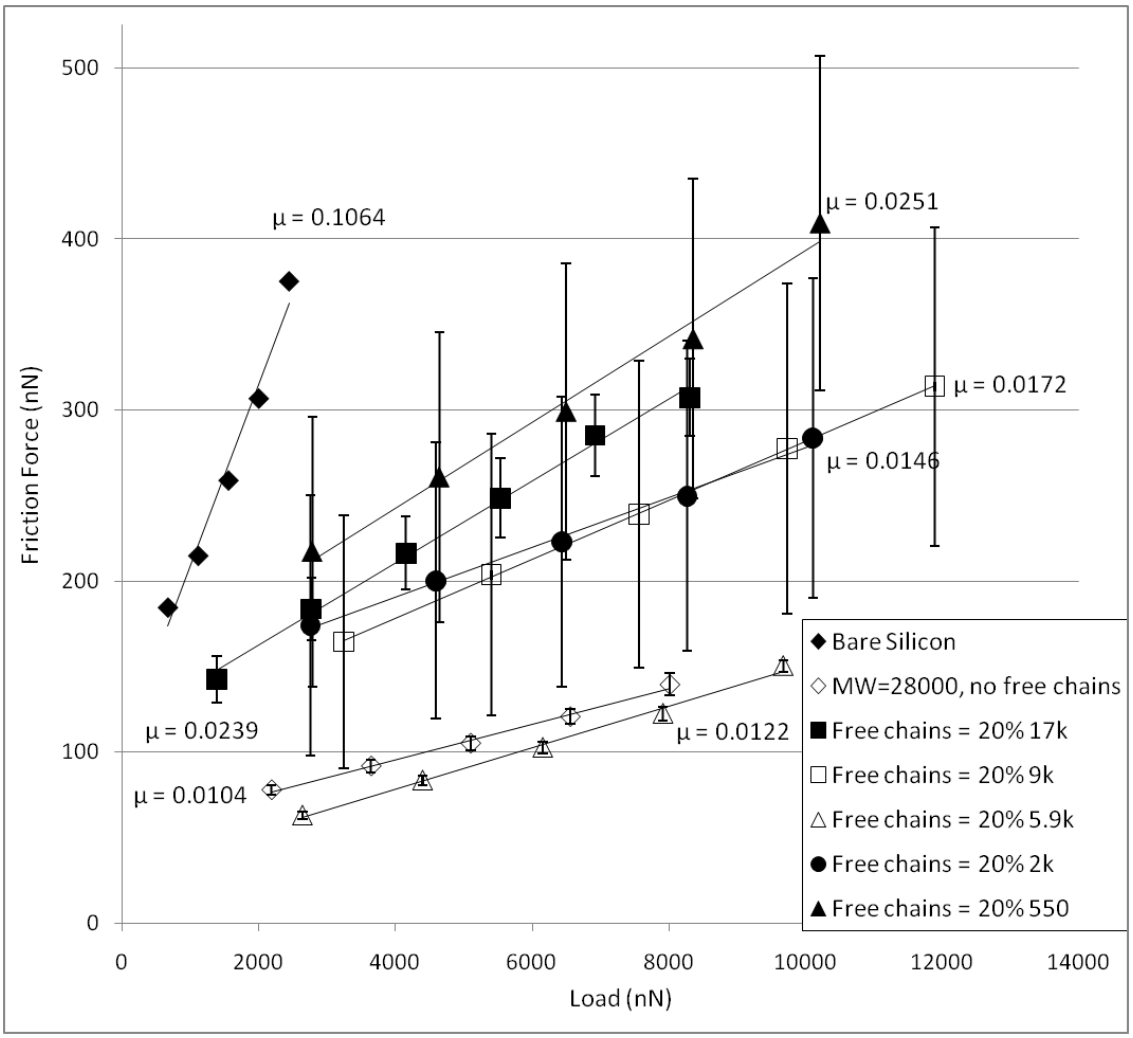

Figure 4.3. Friction force vs. load curves for micro-thick networks with free chains (20 volume percent in the precursor mixture). The large error bars indicate that the surfaces are likely not uniform and potentially have a free chain surface layer of significant thickness.

It is important to consider the decided linearity in all friction force vs. load curves. A modified form of Admonton's friction law recognizes that there are two contributions to friction: a load component, and an adhesion component consisting of the critical shear stress (τ_o), which is a value indicative of the surface chemistry, and the actual contact area (A) between two interfaces.

$$F_f = \tau_o * A + \mu * (N + N_c) \quad (3)$$

Here N_c is the critical load, a finite force required to separate the surfaces vertically.[18] While F_f is directly proportional to N, the relationship between the contact area and load is much more complicated. Johnson, Kendall, and Roberts (commonly referred to as JKR) proposed the relationship between the contact area and the load to be non-linear.[22] For the friction curves to be linear, as is clearly demonstrated in Figures 4.2 and 4.3, the adhesion contribution to the friction force must be negligible.

From both sets of results it is clear that a minimum COF exists for a network with 5900 g/mol molar mass free chains. This is particularly apparent in Figure 4.4, the comparison of the reduction in COF for the lubricant samples from the COF of bare silicon, calculated to normalize any effect of humidity. Lubricant systems with shorter or longer free chains show a considerable decrease in the friction. The COFs indicate that the presence of free chains primarily increase the friction of the polymer network. The peak in the COF reduction at an intermediate free chain molecular weight suggests the interface is not constant for all systems. As previously discussed, the friction coefficient will increase with increased viscous effects at the surface. This can potentially occur for the free chain networks; the formation of a free chain viscous layer across the network surface would limit the presence of the elastic network at the interface. Further characterization measurements of the surface and network structure were completed to draw more complete conclusions from these results.

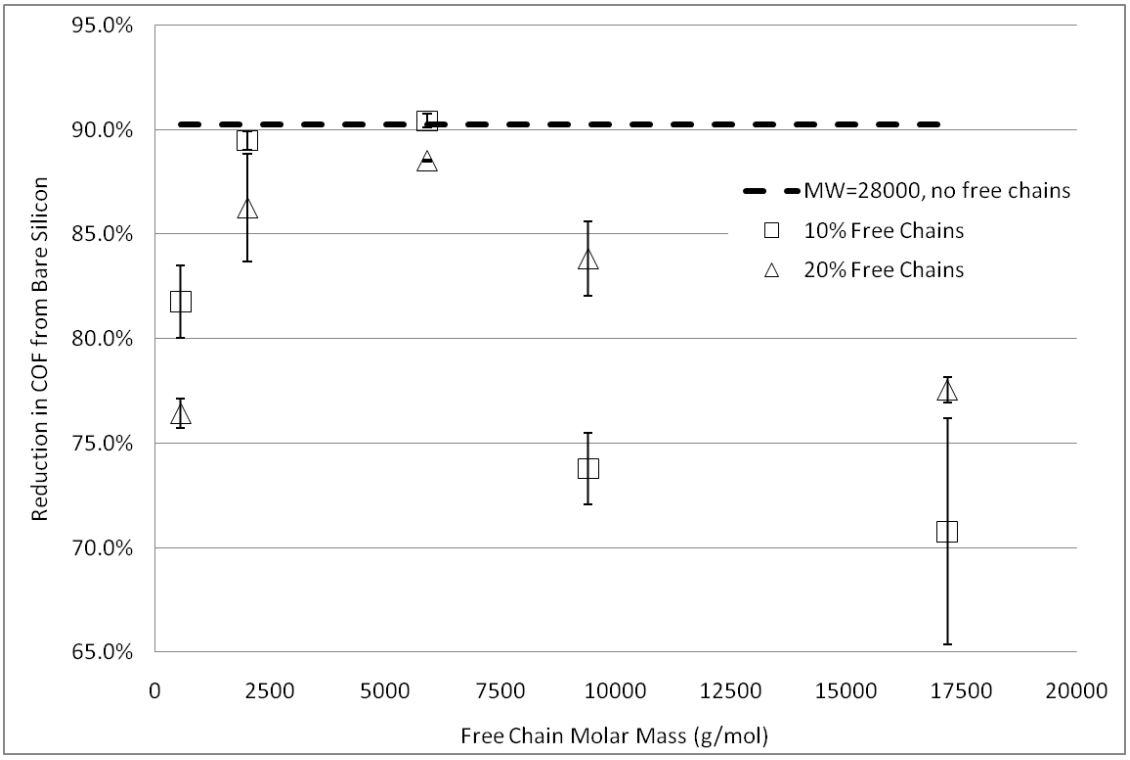

Figure 4.4. Comparison of reduction in friction coefficient from bare silicon for PDMS networks with different concentrations of free chains with different molar mass. The dotted line represents a 28000 g/mol molar mass network with no free chains present. The COF reduction values are determined from the calculation $(COF_{silicon} - COF_{sample}) / COF_{silicon}$.

4.4.2. Surface Characterization. AFM force mode analysis was used to determine the samples' elastic modulus, *E*. In force mode, the cantilever piezo moves vertically with respect to the sample and cantilever deflection resulting from surface attraction and adhesion is recorded. As the piezo retracts from the surface, the cantilever will adhere to the surface beyond the piezo height where the cantilever was first pulled into contact with the sample surface while extending downwards. The pull-off adhesive force, F_a, which is the force necessary to overcome adhesion and separate the opposing surfaces, can be determined from an evaluation of the depth of the force curve less the zero-force cantilever deflection height. The cantilever indentation into the PDMS surface is calculated from the difference of the piezo location and cantilever deflection, normalized in relation to the zero force point of the cantilever prior to the effect of adhesion introduce attractive forces.

The actual contact area between cantilever tip and sample surface is determined using the JKR theory[22] of surface contact:

$$A = \pi (R/K)^{2/3} \{N + 3\pi R\gamma + [6\pi R\gamma N + (3\pi R\gamma)^2]^{1/2}\}^{2/3} \quad (4)$$

where R is tip radius, γ is the reduced surface tension:

$$\gamma = \gamma_1 + \gamma_2 - \gamma_{12} \quad (5)$$

based on the surface tension of both materials at the interface (γ_1, γ_2) and the interaction between them (γ_{12}). *K* is the reduced elastic modulus:

$$K = \frac{4}{3}[(1-\nu_1^2)/E_1 + (1-\nu_2^2)/E_2]^{-1} \quad (6)$$

Here ν_1 and ν_2 are the Poisson ratios of the two materials at the interface, and E_1 and E_2 are the corresponding elastic moduli. The reduced surface tension and the pull-off force are directly related by:

$$F_a = -3\pi R\gamma / 2 \quad (7)$$

Combining Eq. (4) and (7), the only remaining unknown constants are the elastic modulus of the sample and the interfacial contact area. A modified Hertzian analysis[23]

can be used to estimate the elastic modulus that accounts for the film thickness, h, of the sample by:

$$F = \frac{16E}{9} R^{1/2} \delta^{3/2} [1 + 1.133\chi + 1.283\chi^2 + 0.769\chi^3 + 0.0975\chi^4] \quad (8)$$

where χ represents:

$$\chi = \sqrt{R\delta} / h \quad (9)$$

and δ is the indentation at the interface. A plot of E vs. δ using results from Eq. (8) depicts a plateau region for E that represents the average elastic modulus value for the system. The accuracy of this calculation can be determined from a comparison to bulk modulus measurements. The modulus can then be substituted into Eq. (4) to determine the contact area.

The Hertzian calculation works best for measuring systems with high elastic moduli at low adhesion forces, or for systems with high adhesion forces at low elastic moduli. High elastic moduli in the presence of high adhesion forces leads to smaller and less well-defined plateaus on the E vs. δ curve. The difficulty in measuring these systems can be minimized by conducting the experiments with a more flexible cantilever, which increases the range of the force on the cantilever between initial attraction to the surface and the maximum indentation.

The friction force can then be normalized by using the contact area determined from the indentation measurements to calculate the surface shear stress, σ:

$$\sigma = F_f / A \quad (10)$$

Systems of different elasticity can be better compared in terms of sliding velocity by converting friction to shear stress. As this scan rate can be treated as a shear rate, $\dot{\gamma}$, thus the surface viscosity, η, can be calculated by:

$$\eta = \sigma / \dot{\gamma} \quad (11)$$

These relationships allow for surface rheological characterization to be extracted from lateral force microscopy measurements, and provide an expanded analysis of the surface material characteristics.

Further investigation into the surface stress and viscosity of the networks with embedded free chains indicates trends similar to the friction results, as reported in Figures 4.5 and 4.6 for the 10 volume percent free chain networks. The only network with stresses and viscosities consistently lower than the 28000 g/mol precursor molar mass network with no free chains is the 5900 g/mol molar mass free chain system. Increasing or decreasing the molar mass of the free chains from 5900 g/mol leads to higher stresses and surface viscosities.

The surface viscosity results are particularly interesting, as they are indicative of surfaces with increased amounts of viscous material as opposed to a pure elastic surface. This would suggest that a viscous polymer layer exists on the elastic network surface in most cases for the free chain networks. The surface viscosity, η, is expected to have a power-law relationship with the frequency.[24] These power-law exponents are expected to become less negative as the surface becomes more elastic with less surface mobility, and thus the effective surface viscosity of the network decreases. The power-law exponents extracted from low frequency data, summarized in Table 4.1, provide some insight into the possible viscous layer. All lubricant systems have larger exponents than a model network except for the 5900 g/mol free chain system; this system has an exponent approximately 20 percent lower than the model network. The exponents are largest for the longest and shortest free chains, indicating the highest degree of a viscous-like behavior at the surface for these systems. The minimum that occurs for the 5900 g/mol free chains indicates any viscous layer that may be developing is small, and that the majority of free chains remain within the network and are not driven towards the surface during the friction measurement.

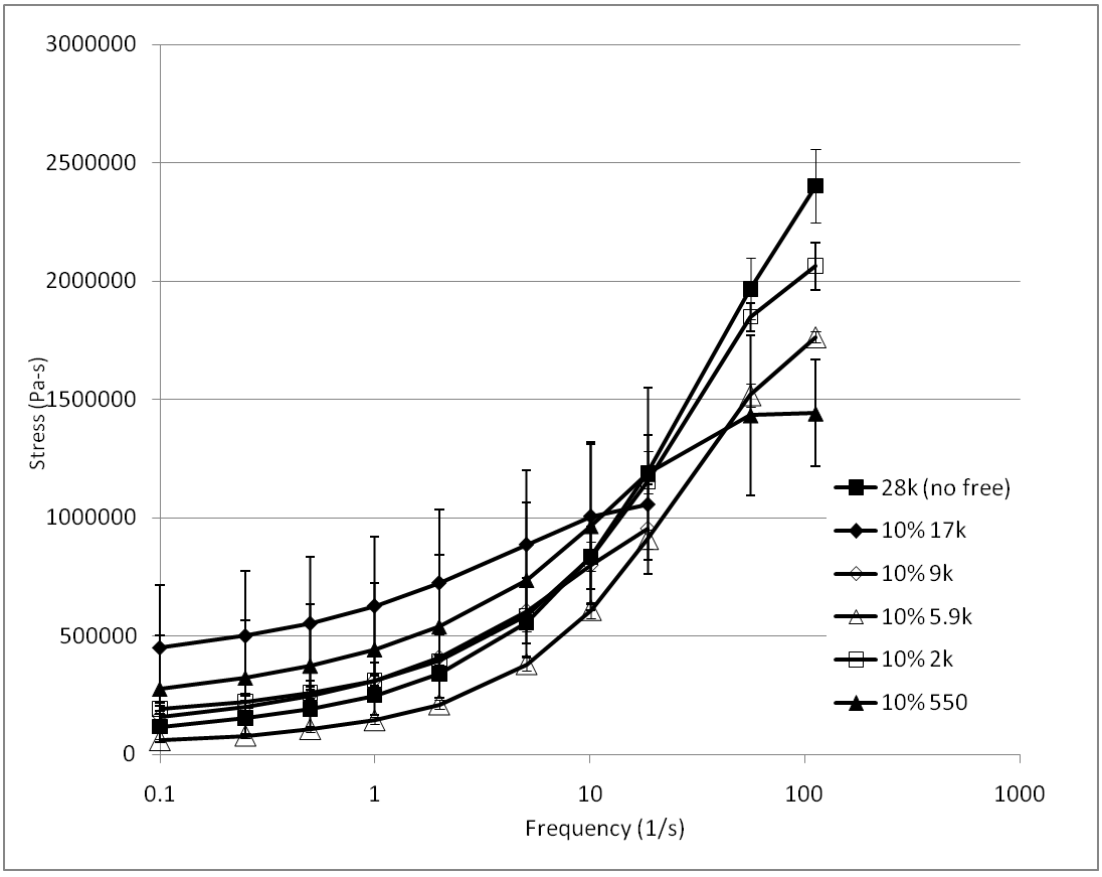

Figure 4.5. Shear stress vs. frequency curves conducted with AFM for 28000 MW PDMS network systems with 10 volume percent PDMS free chains of varying molar masses.

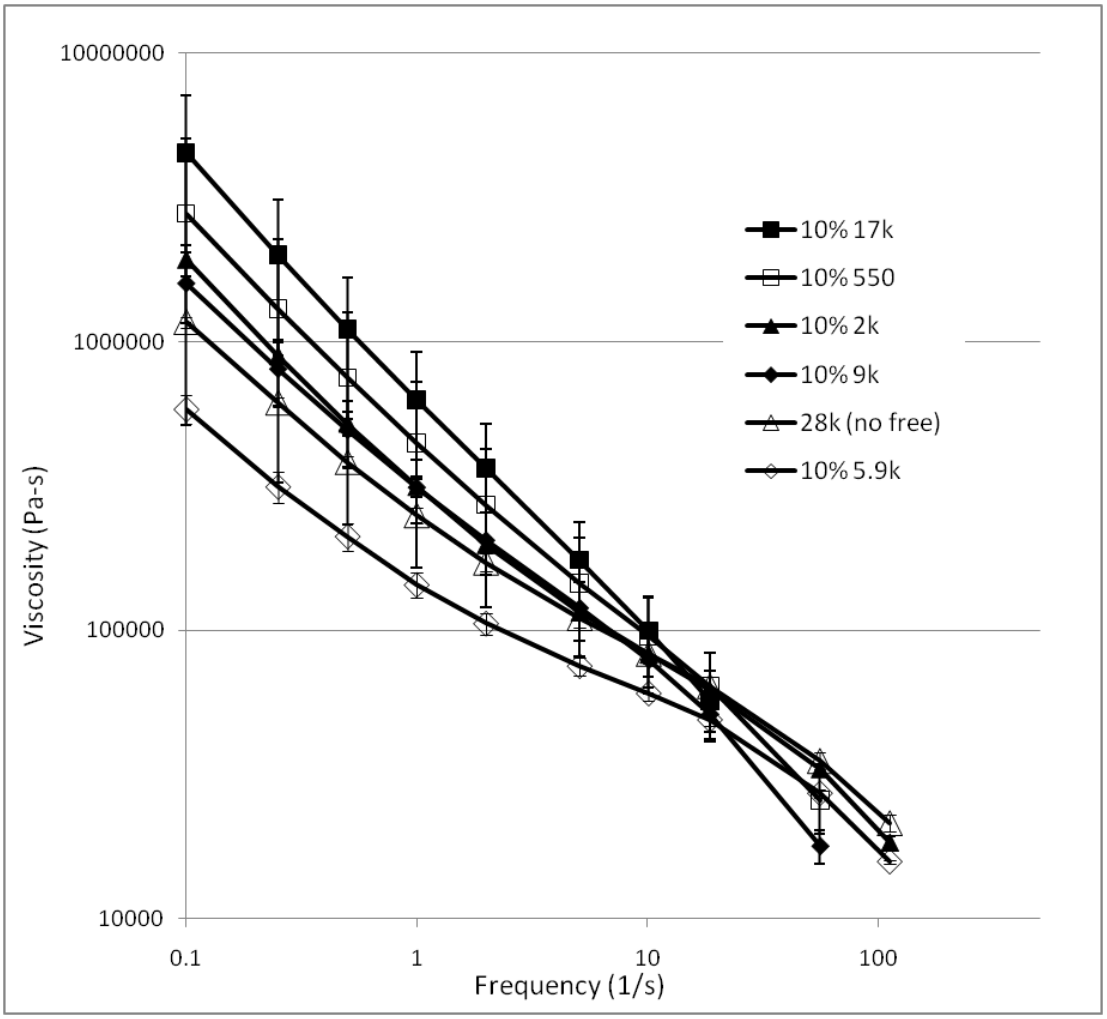

Figure 4.6. Surface viscosity vs. frequency curves conducted with AFM for 28000 MW PDMS network systems with 10 volume percent PDMS free chains of varying molar masses.

Table 4.1. Comparison of AFM surface microscopy and bulk rheology experiments for 10 percent volume free chain systems.

	AFM		Rheometer
	E (MPa)	**η exponent**	**E (MPa)**
28k	0.495	-0.620	0.522
10% 17k	0.133	-0.824	0.495
10% 9k	0.151	-0.674	0.522
10% 5.9k	0.279	-0.472	0.429
10% 2k	0.300	-0.630	0.438
10% 550	0.221	-0.721	0.486

The potential development of a viscous surface layer is an important factor to consider for the free chain systems. While standard oil used in macroscopic lubrication also creates a viscous layer, the oil in those systems acts primarily to eliminate or diminish the contact between two rigid surfaces. If the free chains were to develop a viscous layer, however, the effects of increased viscous behavior could dominate in comparison the benefits provided by the presence of an elastic network lubricant at the interface. The higher pull-off adhesion forces indicate the increased viscous material at the interface, as a viscous surface layer will increase the force needed to separate the surfaces as measured by the AFM force mode measurements at low extension and retraction speeds.[15] When evaluating the pull-off force values for the free chain swollen networks (reported in Table 4.2), it is apparent that the adhesive forces for all the networks are larger than the model 28000 g/mol network, and that almost all the adhesion forces are larger for systems with free chains longer or shorter than 5900 g/mol.

Further analysis can be conducted by evaluating the elastic moduli at both the microscopic and bulk scale. While the stress and viscosity provide some insight into the nature of the interface, the value of the elastic moduli for the free chain systems in comparison to a model network offers the best evaluation whether the free chains are remaining in the network or driven towards the surface. The AFM can be primarily used to conduct friction measurements at single-asperti conditions, and for extracting bulk physical properties from the surface. The moduli can then be compared to bulk measurements to determine whether the elastic moduli measurements at the surface are more indicative of a viscous layer or swollen network.

A Physica MCR 300 rheometer was used to conduct the bulk measurements. PDMS networks were synthesized as previously described in 100 micron gap spacing between two 15 mm diameter parallel plates. The gap spacing was set immediately

Table 4.2. Adhesive pull-off forces for the free chain swollen networks at both 10 and 20 volume percent concentrations, as well as a model network with no embedded free chains.

	10 vol. %	**20 vol. %**
Free Chains (g/mol)	**Fa (nN)**	**Fa (nN)**
550	345.3	332.5
2000	249.0	316.4
5900	269.2	300.6
9400	387.4	330.9
17200	468.1	445.6
Model network 28000 g/mol	208.4	

after catalyst had been added to the precursor polymer mixture and the mixture had been poured onto the lower plate to prevent slipping between the polymer network and the parallel plates. Excess precursor PDMS material was scraped and removed from the outside of the parallel plates to eliminate edge effects. A constant temperature of 35 ^{o}C was maintained during synthesis by a heating chamber. Frequency sweep measurements were conducted over a range of angular frequencies from 600 to 0.1 1/s at a constant strain of 0.1% and repeated over time to ensure the networks had finished curing.

The characterization measurements conducted by AFM surface microscopy and the bulk rheology for the free chain systems are summarized in Table 4.1. From the microscopy experiments, it is clear that the elastic modulus of the lubricant at the surface is significantly decreased for the free chain systems; the moduli are at least 40 percent lower than that of a model network. Bulk rheology measurements indicate the presence of free chains at a low volume concentration have almost no effect on the modulus. Structural network modifications therefore have a greater effect at the surface than within the bulk. A given concentration of free chains should result in the same elastic modulus for any free chain with a molar mass lower than the network cross-linking molecular weight.[25] At the surface, however, both the 2000 g/mol and 5900 g/mol free chain networks have elastic moduli close to the 28000 g/mol precursor molar mass network without free chains. It is likely the moduli values are more representative of the viscoelasticity of the surface and any viscous layer that may develop than the actual network elasticity. The larger moduli for the 2000 g/mol and 5900 g/mol free chains systems compared to the other networks suggests the surface viscous layers are much smaller for these systems; this result would seem to support the viscoelasticity conclusions drawn from the surface friction measurements.

The minimum in frictional and adhesive forces that exists for the 5900 molar mass free chain systems raises the question of why thicker viscous surface films would develop for shorter and longer free chains, but not for intermediate lengths. The diffusion coefficients for the free non-reactive PDMS chains through a precursor 28000 g/mol network can be determined using an extrapolation from the calculations done by Gent and Tobias.[26] As would be expected, the diffusion coefficients (listed in Table 4.3) sequentially increase with the precursor molar mass of the free chains. Because all of the chains are below the PDMS entanglement molecular weight, of approximately 24500 g/mol,[27] the potential remains for all the free chains to diffuse to the surface under an external driving force. From the diffusion coefficients, it is clear that the 550 g/mol free chains are the most mobile, with mobility increasing sequentially with the free chain molar mass. When an external normal force is applied to the network, the shorter chains would then be driven out of the network to create a film on the surface. Thus, the surface friction would increase for the networks containing the shortest free chains. Because of longer diffusion times, this is not as likely for the longer chains, implying a different source for the increased friction and adhesion properties of these films.

It is also important to consider the equilibrium free chain concentrations of the swollen networks. The equilibrium volume swelling ratio, Q_{3D}, provides a theoretical prediction for the amount of free chains as a swelling agent that a three-dimensional network can contain:[26]

$$Q_{3D}^{\ 2}\ln(1-Q_{3D}^{\ -1})+Q_{3D}+\chi_o+(M_s/M_c)(Q_{3D}^{\ 5/3}-2Q_{3D}/f)=0 \quad (12)$$

Here M_s is the molar mass of the free chain swelling agent, M_c is the network chain molar mass, f is the network cross-linking functionality, and χ_o is the parameter describing interaction between the free chains and the network. The equilibrium swelling ratio can also be calculated for swollen networks in a one-dimensional state,

Table 4.3. Estimates of free chain diffusion coefficients through a 28000 g/mol network based on studies by Gent and Tobias.[26]

Free Chain MW (g/mol)	D (m^2/s)
550	1.39E-11
2000	6.83E-12
5900	3.76E-12
9400	2.91E-12
17200	2.09E-12

which is based on the assumption that a swelling agent will only be able to enter or exit a thin network film from one interface. For this condition, the ratio, Q_{1D}, is determined by:[18]

$$Q_{1D}^{4} - Q_{1D}^{2} - \frac{r}{2}(1 - 2\chi_o M_s)Q_{1D} - \frac{r}{3} = 0 \qquad (13)$$

where r is the ratio of M_c/M_s. For both equations, Mc can be calculated from measured values of E by the relation:

$$E = 3\rho RT / M_c \qquad (14)$$

Here ρ is the density, T is the temperature, and R is the universal gas constant. Because experimental values for Q can be calculated from the sample precursor volume concentration (e.g. Q = 1.10 for the 10 percent free chain films), comparisons can be made to the theoretical state of the swollen network films.

The theoretical equilibrium and experimental swelling ratios for the 10 percent free chain swollen network films are reported in Table 4.4, and visually represented in a plot of Q vs. the ratio of M_s/M_c in Figure 4.7. M_c was determined for these networks from the measured value of E for a 28000 g/mol model network without free chains. From the data, it is clear that the experimental Q values are all below the equilibrium swelling ratios for the three-dimensional state, with experimental and equilibrium ratios being closest for network films swollen with free chains with the highest molar masses. A comparison of Q and Q_{1D} reveals that synthesizing swollen networks with 10 volume percent of 17200 g/mol free chains creates a swollen film slightly above equilibrium. Network films with 10 percent 9400 g/mol free chains are also almost at equilibrium in the one-dimensional case. In order to maintain equilibrium in the network films, the longer free chains are more likely to be expelled and driven out than the shorter free chains.

Combining both the effects of diffusion and expulsion may explain the lowest friction and adhesion characteristics occurring for the network films swollen with the

Table 4.4. Swelling ratios for the 10 percent free chain networks in terms of experimental design and theoretical 1-dimensional and 3-dimensional values. For the calculated values, the the assumption was made that $\chi_o = 0$.

	Experimental	**Theoretical**	
Molar Mass (g/mol)	**Q**	**Q_{1D}**	**Q_{3D}**
500	1.10	2.31	6.00
2000	1.10	1.52	3.08
5900	1.10	1.20	1.98
9400	1.10	1.12	1.68
17200	1.10	1.07	1.40

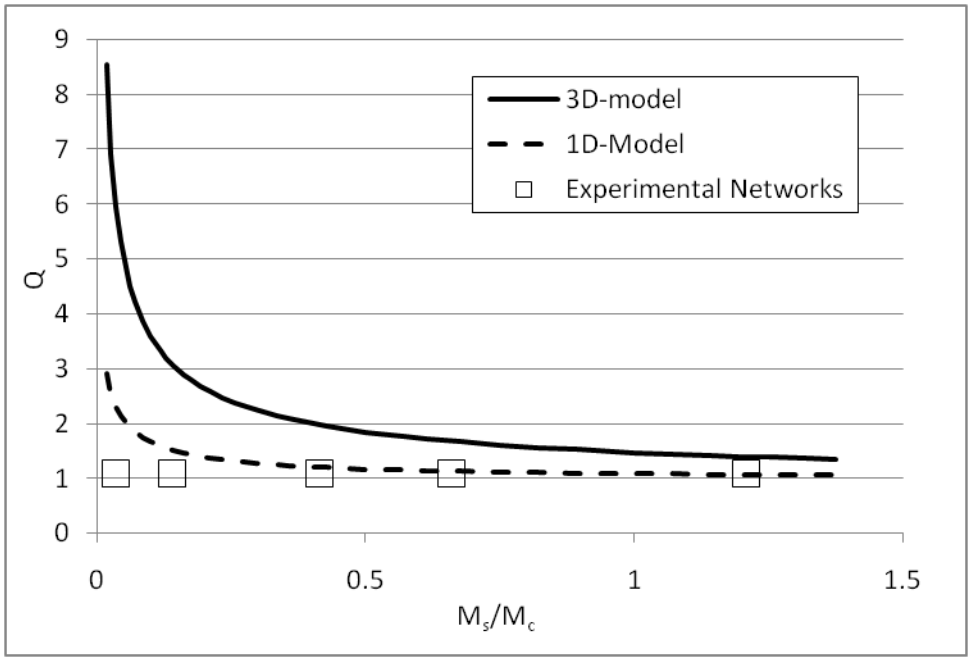

Figure 4.7. Swelling ratios vs. the swelling agent molar mass divided by the molar mass between effective cross-links. The curves represent theoretical predictions based on one-dimensional and three-dimensional swelling states with the assumption $\chi_o = 0$.

intermediate molar mass 5900 g/mol free chains. While shorter chains will have a higher mobility and be more likely to diffuse toward the surface, longer chains are more likely to be expelled from the network to maintain an equilibrated swollen state. These driving forces will be smaller for free chains with an intermediate molar mass, as there will be some level of a balance between the two cases. Thus, the 5900 g/mol free chains will be less likely to create a viscous surface layer, and the network films swollen with these intermediate length free chains will maintain a more elastic interface.

4.4.3. Wear and Tribology. An Anton-Paar Physica 501 MCR tribology device was used to evaluate the macroscopic wear and lubrication properties of each sample. This device brings a rotational rod with a solid steel sphere tip into contact with three wafers of equal height at a constant load. The torque and rotational velocity of the rod can be varied and measured to change the friction force and determine the COF of the modified wafer surfaces. The main results extracted from this apparatus are the variations of the COF with the rotational velocity of the solid sphere while in contact with the surface, more commonly referred to as a Stribeck curve. While the velocity is steadily increased under a constant load, the friction response indicates the lubricant is in one of the three frictional regimes – boundary lubrication, where molecular adhesion is the dominant source for friction; a transition regime where the COF decreases; and an elastohydrodynamic regime, where the friction is operating at the continuum level.[28-30] Stribeck curves typically compare the COF of a lubricant to the product of the sliding velocity, lubricant viscosity, and pressure exerted on the lubricant, where the pressure is the load applied to the surface over the contact area. An illustration of an example Stribeck curve is depicted in Figure 4.8. In these present experiments, the load was held constant at 10 N, while velocity was increased from

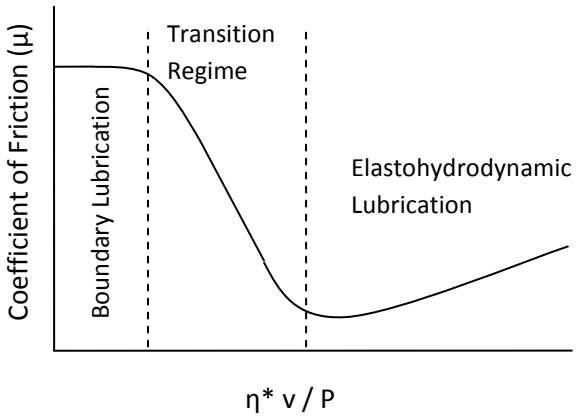

Figure 4.8. Example of a typical Stribeck curve, denoting three distinct lubrication regimes. The curve is not necessarily to scale, as the transition regime can be much shorter with a larger slope. On the x-axis, η is the lubricant viscosity, v is the sliding velocity, and P is the pressure existing as a result of friction and/or torque.

approximately 50 μm/s to 20 cm/s, or until the bearing was audibly scoring the silica surface (and thus having completely worn through the network). Samples were developed on silica wafers purchased from Esco Products, and a SAM layer and a PDMS network were applied as previously described for the silicon wafers.

A plot of the friction coefficient vs. sliding velocity, while the velocity is steadily increasing and in the act of wearing the surface, is reported in Figure 4.9 for several lubricant systems. The form of all the Stribeck curves clearly shows all systems exist in the elastohydrodynamic regime; this conclusion is based on the COF trending to increase after a plateau with increasing velocity, instead of the COF decreasing as would be expected in the boundary lubrication/transition regime. This regime is expected as the approximately 15 μm thick samples are three orders of magnitude thicker than the monolayer films typical of boundary lubrication. The thickness of the samples are also several times larger than surface roughness, which is also indicative of elastohydrodynamic lubrication.[31] The sharp increases in COF at different critical velocities signify distinct wear at the lubricant surfaces. The Stribeck curves also show delineation in the wear resistance of the different lubricants. The model network with no free chains maintains a low COF over the widest range of sliding velocities before rapidly wearing at 30 mm/s. The 5900 g/mol free chain system is the only lubricant exhibiting a similar wear resistance up to 2 mm/s. Both the 17200 g/mol and 9400 g/mol systems sharply increase immediately before achieving a plateau, while the 2000 g/mol free chain lubricant has the worst wear resistance over the entire range of sliding velocities.

The presence of plateaus for all lubricants indicates structural stability over some velocity range. Static friction measurements using the tribology device signified that the lubricant systems have a tendency to wear away in small layers as the torque slowly increases on the networks at the surface. Thus each plateau on the Stribeck

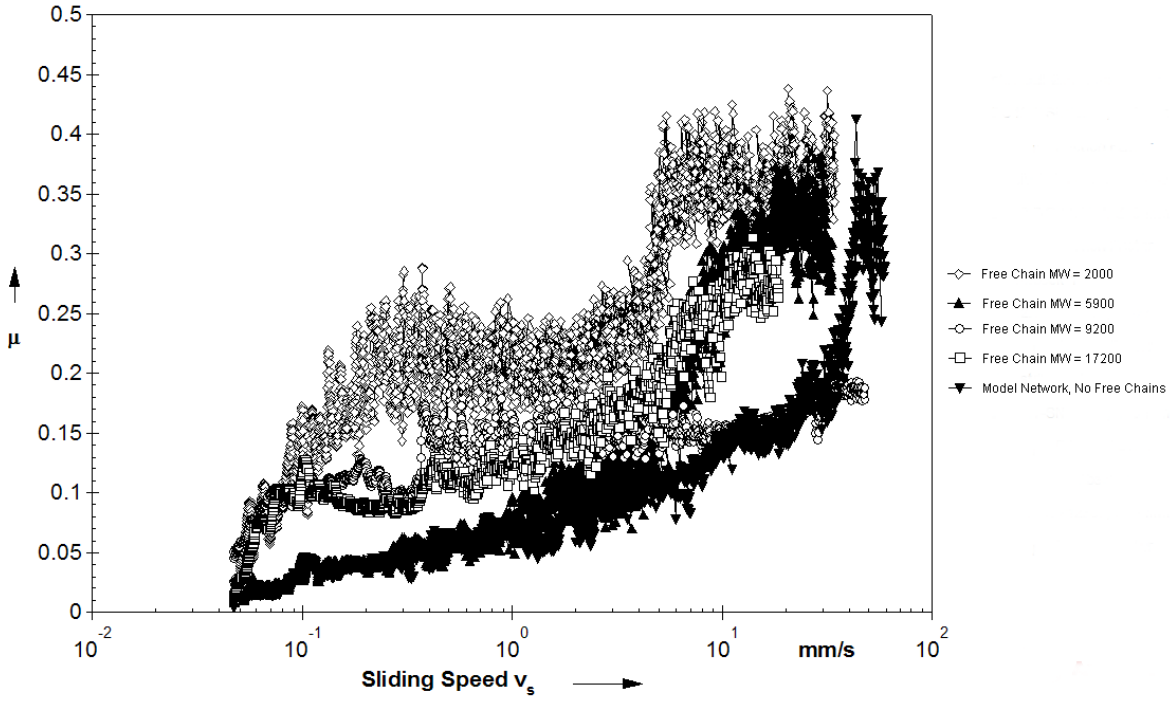

Figure 4.9. Stribeck curves for free chain lubricant systems and 28000 g/mol model network.

curve signifies the lubricant's resistance to wear while every increase in COF represents removal of the lubricant. Decreases in COF are likely indicative of either spreading of the free chains at the surface, or orientation of dangling ends of broken polymer strands or free chains still partially penetrated into the network surface.

From these results, it appears that any swelling modifications to the lubricants will only decrease the overall wear resistance of the network film. While some free chain systems may be comparable to the model network over a range of sliding velocities, they all still exhibit either immediate or eventual wear at a velocity approximately one order of magnitude earlier than the model network. This implies that by swelling the networks, the overall lubricant is weakened structurally, decreasing the wear resistance of the film.

4.5. CONCLUSIONS

Modifications were made to a microscale polymer lubrication system consisting of a cross-linked PDMS network tethered to a self-assembled monolayer, enabling an investigation into the effect of the interfacial elastic modulus and surface viscosity on the lubrication properties. Networks were synthesized from a precursor polymer solution of difunctional and non-reactive PDMS chains, allowing the networks to cure in a swollen state. These systems were developed using different molar masses of free chains and at different volume concentrations in the precursor melt. The friction, adhesion, and wear properties of these films were analyzed to further determine the effect of physical structure.

Friction results showed that nearly all swollen networks exhibited higher COFs than a model network synthesized with no free chains. Bulk property values for stress and viscosity extracted from interfacial measurements indicated that the formation of a viscous layer at the interface was responsible for the increase in friction. Systems with

lower friction results than a model network also had lower surface stress and viscosity, meaning viscous material at the surface was minimal. Decreasing the elastic modulus did not appear to have a significant effect unless the surface viscous layer was small. All the swollen films exhibited higher adhesive pull-off forces than a non-swollen network as well.

Wear measurements conducted over a range of sliding velocities indicated that all the free chain systems demonstrated lower wear resistance than a non-swollen network. Incrementally increasing the sliding velocity caused several of the swollen networks to wear, rapidly increasing the COF. All of the swollen networks showed some degree of wearing and increase in friction before the model network began to fail.

From these results, it is clear that the introduction of free chains as a swelling agent will not improve the lubrication properties of a microscale network. While the presence of the free chains within the network may decrease the elastic modulus, the development of a surface viscous layer appears to minimize any effect this may have on the friction properties. The swollen networks also all manifest higher adhesive forces and lower wear resistance, making them impractical for use as a microscale lubricant coating. These friction and characterization measurements indicate that surface viscous-like characteristics need to be minimized in order to optimize the lubrication properties.

REFERENCES

(1) Rymuza, Z. *Microsystem Technologies* **1999**, *5*, 173-180.

(2) Bhushan, B. *Proc. Instn. Mech. Engrs Part J* **2001**, *215*, 77-102.

(3) Cagin, T.; Che, J.; Gardos, M. N.; Fijany, A.; Goddard, W. A., III. *Nanotechnology* **1999**, *10*, 278-284.

(4) Bowden, F.P.; Tabor, D. *Friction and Lubrication.* Methuen & Co. Ltd.: London, 1967.

(5) Wang, W.; Wang, Y.; Bao, H.; Xiong, B.; Bao, M. *Sensors and Actuators* **2002**, *97-98*, 486-491.

(6) Maboudian, R.; Ashurst, W. R.; Carraro, C. *Sensors and Actuators* **2000**, *82*, 219-223.

(7) Sundararajan, S.; Bhushan, B. *J. Vac. Sci. Technol. A.* **2001**, *19(4)*, 1777-1785.

(8) Briscoe, B.J.; Sinha, S.K. *Proc. Instn. Mech. Engrs.* **2002,** *216*, 401-413.

(9) Landherr, L.J.T.; Zhang, Q.; Cohen, C.; Archer, L.A. *J. Poly. Sci. B.*, **2008**, *46*, 1773-1787.

(10) Chernyak, Y.B.; Leonov, A.I. *Wear* **1986**, *108*, 105.

(11) Chen, N.; Maeda, N.; Tirrell, M. Israelachvili, J. *Macromolecules* **2005,** *38*, 3491-3503.

(12) Galliano, A.; Bistac, S.; Schultz, J. *J Colloid Interface Sci* **2003**, *265*, 372–379.

(13) Landherr, L.J.T.; Cohen, C.; Archer, L.A. *In preparation*.

(14) Hill, D.J.T.; Killeen, M.I.; O'Donnell, J.H.; Pomery, P.J.; St. John, D.; Whittaker, A.K. *J. Appl. Poly. Sci.* **1996**, *61*, 1757-1766.

(15) Galliano, A.; Bistac, S.; Schultz, J. *J. Adhesion* **2003**, *79*, 973-991.

(16) Patel, S.K.; Malone, S.; Cohen, C.; Gillmor, J.R.; Colby, R.H. *Macromolecules* **1992**, *25*, 5241-5251.

(17) Tordjeman, P.; Mutin, P. H.; Tixier, T. *Rheol Acta* **2004**, *43*, 550-558.

(18) Zhang, Q.; Archer, L.A. *Langmuir* **2007**, *23*, 7562-7570.

(19) Liu, Y.; Evans, D. F. *Langmuir* **1996**, *12*, 1235-1244.

(20) Cleveland, J.P.; Manne, S.; Bocek, D.; Hansma, P.K. *Rev. Sci. Instrum.* **1993**, *64*, 403-405.

(21) Mate, C. M. *Tribology on the Small Scale: A Bottom Up Approach to Friction, Lubrication and Wear*. Oxford University Press, New York: **2008**.

(22) Johnson, K.L.; Kendall, K.; Roberts, A.D. *Proc.R. Soc. London, Ser. A*, **1971**, *324*, 301-313.

(23) Dimitriadis, E.K.; Horkay, F.; Maresca, J.; Kachar, B.; Chadwick, R.S. *Biophysical Journal* **2002**, *82*, 2798-2810.

(24) Bird, R.B.; Armstrong, R.C.; Hassager, O. *Dynamics of Polymeric Liquids: Vol. 1* John Wiley & Sons, New York: **1987**.

(25) Flory, P.J.; Rehner, J. Jr. *J. Chem. Phys.* **1943**, *11*, 521-526.

(26) Gent, A.N.; Tobias, R.H. *J. Poly. Sci.: Poly. Phys. Ed.* **1982**, *20*, 2317-2327.

(27) Yilgor, I.; Eynur, T.; Yilgor, E.; Wilkes, G.L. *Polymer* **2009**, *50* 4432-4437.

(28) Maru, M. M.; Tanaka, D.K. *J. of the Braz. Soc. of Mech. Sci. & Eng.* **2007,** *29*, 55-62.

(29) Lu, X.; Khonsari, M.M.; Gelinck, E.R.M. *J. of Tribology* **2006**, *128*, 789-794.

(30) Persson, B.N.J. *Sliding Friction: Physical Principles and Applications*. Springer, Berlin: **1998**.

(31) Kurokawa, T.; Tominaga, T.; Katsuyama, Y.; Kuwabara, R.; Furukawa, H.; Osada,Y.; Gong, J.P. *Langmuir* **2005,** *21*, 8643-8648.

CHAPTER 5

PHYSICAL AND CHEMICAL CHARACTERIZATION OF THE INTERFACIAL FRICTION AND ADHESION OF ULTRATHIN POLYMER BRUSH FILMS

5.1. ABSTRACT.

The friction and adhesion properties of polymer brushes are studied in order to relate the physical structure and chemical characteristics to the lubricant properties. Brushes were synthesized at several chain lengths and surface coverages from polymer chains of polydimethylsiloxane (PDMS), polystyrene (PS), and a polypropylene glycol – polyethylene glycol block copolymer (PPG/PEG). Surface characterization studies conducted by atomic force microscopy and ellipsometry indicated several important trends. For ultrathin PDMS brushes at a high surface coverage, the friction coefficients (COFs) are among the lowest ever reported for a dry lubricant ($\mu \approx .0024$), and an order of magnitude lower than a bare silicon surface with no lubricant. Brushes synthesized from higher molar mass chains exhibit higher friction forces as a result of chain extension and distribution of applied shear stress. Increased surface coverage significantly reduces the COF by creating a uniform surface of stretched chains with a decreased surface viscosity. Brushes with the lower surface tension and interfacial shear stresses display the lowest COF. In particular, PDMS chains exhibit COFs lower than PS by a factor of 3.7 and lower than PPG/PEG by a factor of 4.7. However, this effect is smaller than for bulk materials as the contribution of adhesion to friction is negligible for all ultrathin brush systems. A scaling analysis conducted on the surface coverage (σ) in relation to the fraction (ε) of the friction force developing from adhesion predicts a relation $\varepsilon \sim \sigma^{4/3}$, which is supported by our experimental data.

5.2. BACKGROUND.

Advancements made in the field of small devices, such as microelectromechanical systems (MEMS) and self-administered syringes, have been a driving force for research on advanced lubricants that will function on the lengthscale of these micro- and nano-scale devices.[1-3] In order to meet the needs of these technological developments, a wide range of lubrication systems have been studied, including freely mobile oils,[4-6] self-assembled monolayers (SAMs),[7-11] thin polymer films,[12] and tethered polymer gels.[13,14] From these studies, it is known that the ideal lubricant must meet several criteria; a thin film must be formed during deposition in order to maintain the substrate structure, strong tethering to the substrate is required to increase the wear resistance, and a low interfacial shear stress and minimal contact area are necessary to reduce friction.[4,15-17]

One of the concerns with conducting research on lubricants with highly specified structures is that it can be difficult to distinguish between the influences of the physical interfacial structure and the surface chemistry. As an example, we have previously developed a series of two-tiered hybrid lubricants based on a soft polydimethylsiloxane (PDMS) network surface tethered to a densely packed SAM anchoring layer. These PDMS-SAM hybrids have consistently exhibited dramatically low friction coefficients despite a number of structural modifications to the network layer, ranging from model, low-defect end-linked networks to ultrathin hyperbranched structures caused by the introduction of pendent chains.[18,19] The complexity of these lubricants makes it difficult to determine the fundamental origins of the low friction forces measured. To overcome this difficulty, we investigate a deconstructed lubricant system to determine the origin of low friction forces and other defining characteristics.

In consideration of this argument, we choose to focus on polymer brushes and their lubrication properties in this study.

Polymer brushes have been the subject of many experimental and theoretical investigations, with research focusing on complex interfaces and both dry and solvent-based media. Many studies have specifically attempted to determine how chain flexibility, mobility, and interaction with an opposing/contacting surface affect interfacial stress and friction. Raviv et al. measured the friction coefficient (COF) of two opposing mica surfaces coated with tethered sulfonated polyelectrolyte brushes in the presence of water.[20] From their measurements with a surface forces apparatus (SFA), the brushes were reported to produce some of the lowest COFs ever recorded ($\mu = 0.0006$). The researchers attributed the low friction results to a high resistance to brush interpenetration as a result of repulsion of the opposing surface. Brown characterized the shear stress of a PDMS network sliding over tethered PDMS brushes of different chain lengths.[21] He determined that the chain mobility, the chain ability to adjust laterally to interfacial contact was a significant determinant of friction; short polymer brushes increase the interfacial friction by penetrating into the network, but longer brushes with higher chain end mobility display liquid-like flexibility and greatly reduce the interfacial shear stress.

More recently, Casoli et al. investigated the friction force on PDMS brushes in contact with a PDMS network in a dry state.[22] They found that a transition in the brushes from a liquid-like to a solid-like state occurs by changing the sliding speed. This transition is evidenced by lower sliding velocities and higher molar mass chains. Casoli et al. attributed the molar mass effect to the increased relaxation times for longer brushes, which result in chains existing in a stretched state more frequently. They also concluded that friction properties of polymer brushes are primarily an effect of the surface coverage and overlap between brushes.

In this paper, we investigate the interfacial behavior of tethered polymer brush films in a dry state against a simple rigid opposing surface at the interface to permit a direct evaluation of the lubricant features. Specifically, PDMS brushes are synthesized with different precursor molar masses to characterize the effect of chain length, coverage and chemistry. Brushes are also developed with different surface coverages to investigate the effect of chain stretching and surface viscosity. In order to evaluate the effect of the surface chemistry, brushes were synthesized from polystyrene (PS) and a polypropylene glycol – polyethylene glycol block copolymer.

5.3. EXPERIMENTATION.

5.3.1. Preparation of Vinyl-Terminated SAMs. Three-inch (100) silicon wafers were cut with a diamond tipped stylus into 1 cm by 1 cm pieces. The wafer pieces were cleaned with Kimwipes, rinsed ultrasonically in chloroform, and treated for a minimum of 30 minutes above 130 ^{o}C in a piranha solution of 10 mL 30% hydrogen peroxide and 12 mL hydrosulfuric acid. The cleaned wafer pieces were rinsed in DI water at least eight times and blown dry with nitrogen gas.

Media bottles were placed in a dry nitrogen atmosphere glovebox along with the prepared wafers. Solutions of hexadecane and chloroform with a 4:1 volume ratio were prepared in each media bottle for a total volume of 40 mL. Approximately five cleaned wafer pieces were placed in each flask and arranged to maximize exposed surface. 24 µL of 10-undecenyl trichlorosilane (TCS) was then added to each bottle. The wafers sat in solution in the glovebox overnight to allow the SAM layers to form. Outside the glovebox, the silicon pieces were successively rinsed in dichloromethane, chloroform, and methanol baths for approximately five minutes each to remove excess solvent and un-tethered TCS. The monolayer-coated wafers were dried under a nitrogen stream and stored.

5.3.2. Preparation of Monofunctional Vinyl-terminated PDMS. Purified hexamethylcyclotrisiloxane was dried with calcium hydride in at 20 weight percent in a benzene solution. The monomer solution was filtered to remove the calcium hydride and placed in a glovebox filled with nitrogen. Sec-butyl lithium was added at previously determined ratios to the monomer solution, which was then placed in an oil bath and heated to 30 ^{o}C. After 2 hours, THF was added to the flask to reduce the monomer concentration to 10 weight percent. After completion of the polymerization, vinyldimethylchlorosilane was added in excess to the flask. The monofunctional PDMS solution was washed in a separatory funnel ten times in DI water and then decanted in methanol. The PDMS chain molar mass and polydispersity were determined using a Waters 510 GPC.

5.3.3. Preparation of PDMS brushes. Monofunctional PDMS was diluted in toluene down to certain volume ratios in small scintillation vials and mixed with a difunctional cross-linker 1,1,3,3,5,5-hexamethyl trisiloxane. A vinyl-terminated SAM treated wafer was placed into each vial, after which calculated amounts of a diluted platinum catalyst solution was added. The wafers remained in solution for 24 hours before being removed and placed in a Petrie dish. The wafers were then heated at 35 ^{o}C for 24 hours before being rinsed in a dichloromethane bath for five minutes.

5.3.4. Preparation of Sulfonic SAMs. Silicon wafer pieces were cut and cleaned as previously described. Media bottles were filled with 40 mL of DI water and placed in an oil bath at 70 ^{o}C. Approximately five wafer pieces were added to each bottle as for the vinyl-terminated SAMs, after which 72 µL of 3-(trihydroxysilyl)-1-propanesulfonic acid was added to each bottle. The wafers sat in solution for 24 hours in the oil bath before being thoroughly rinsed in DI water and blown dry by nitrogen gas.

5.3.5. Preparation of PS and PPG/PEG Polymer Brushes. Amine-terminated monofunctional polystyrene was prepared by Praveen Agarwal of Cornell University according to a synthesis developed by Quirk et al.[23] An amine-terminated copolymer (poly(propylene glycol)–*block*–poly(ethylene glycol)-*block*–poly(propylene glycol) bis(2-aminopropyl ether)) and tetrahydrofuran (THF) were purchased from Aldrich Chemicals. Each polymer was diluted in THF to certain volume ratios and mixed in small scintillation vials. A wafer was placed into each vial after complete mixing had occurred and allowed to sit for 24 hours. Each vial was then uncapped and placed in an oven where the tetrahydofuran and excess solution was evaporated for 24 hours. The wafers were then removed and rinsed in THF before being dried under a nitrogen stream.

5.3.6. Brush Thickness Measurement. The film thickness of each brush system was measured with a Rudolph Research Auto-EL Ellipsometer. Approximately five measurements were conducted on each brush at multiple locations on the film to determine the average thickness. Analysis of each system was based on a one-layer film, calculating the thickness of the brushes and the SAM layer together. The known SAM layer thickness was then subtracted from the total thickness for a final value of the brush height. Measurements of the vinyl-terminated SAMs have shown the SAMs to consistently have an average thickness of 1.2 nm, and the sulfonic SAMs have an average thickness of 2 nm.

5.4. ANALYSIS.

5.4.1. Surface Coverage and Bulk Properties. The surface coverage, σ, can be determined from the measured height of the brushes, *h*, using the formula:[24]

$$\sigma = \frac{h\rho_o}{N} \qquad (1)$$

where N is the degree of polymerization and ρ_o is the monomer density:

$$\rho_o = \frac{1}{b^3} = V^{-1} \quad (2)$$

Here b is the monomer length and V is the monomer volume.[25] Depending on the polymer bulk density and molar mass, other methods for calculating σ provide a close approximation. However, these are heavily dependent on assumptions that the bulk density accurately characterizes the polymers on a molecular scale and more commonly used for brushes in aqueous media.[26] As our measurements are conducted in a dry atmosphere, to reduce error in our calculations, we will use Eq. (1) to determine σ in this paper.

The surface coverage can be used to determine the structure of the polymer film. High surface coverage will result in densely packed, stretched brushes, while at low surface coverage the polymer chains will exhibit random-walk statistics, causin the brush to exist in flatter configuration. The brush structure specifically breaks down into three regimes: a "mushroom" regime where the chains interact weakly, flatten and attempt to spread over the poorly-covered surrounding surface area (as depicted in Figure 5.1.1); a "crossover" region where chains may be partially aligned; and a brush regime in which chains stretch away from the substrate (as depicted in Figure 5.1.2). The structure the chains adopt in any given regime can be determined from the reduced surface coverage, Σ, which is given by:

$$\Sigma = \sigma \pi {R_g}^2 \quad (3)$$

where the radius of gyration, R_g, of the polymer chains is determined by:

$$R_g = N b^2/\sqrt{6} \quad (4)$$

The precise values of Σ depend on the medium that the tethered polymer chains are in. Typically, the transition regime is thought to exist at $\Sigma \approx 1$, with the mushroom regime at $\Sigma < 1$ and the brush regime at $\Sigma > 1$.[27] These values assume ideally grafted chains and do not take into account polydispersity or irregular distances between active tethering sites on the surface. A review conducted by Brittain and Minko of published

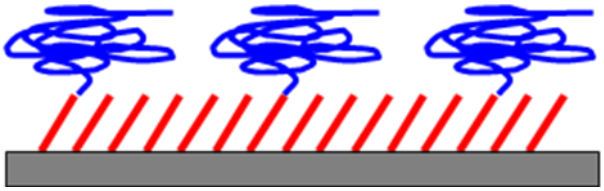

Figure 5.1.1. Cartoon depiction of polymer brushes in a mushroom state anchored to a SAM-coated substrate. Surface coverage is low, and the distance between tethered ends of the polymer chains is high.

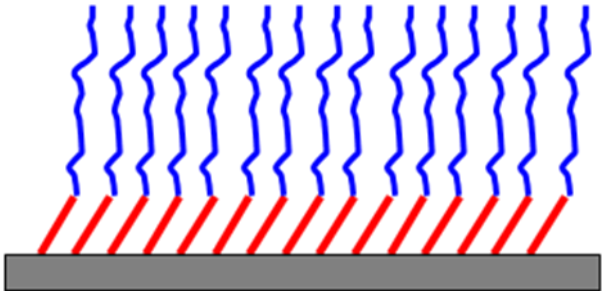

Figure 5.1.2. Cartoon depiction of polymer brushes in a stretched brush state anchored to a SAM-coated substrate. Surface coverage is high, and the distance between tethered ends of the polymer chains is low.

studies found the transition regime can actually occur over a range of reduced surface coverage values.[27] Work by Wu et al. on polyacrylamide brushes for example found the transition regime to occur as high as $\Sigma \approx 6$.[28] Brittain and Minko suggested the transition regime be considered over the range $1 < \Sigma < 5$ based on an average of reported values for high molar mass brushes. This larger transition regime is a result of the irregular surface coverage produced by grafted chains; even with ordered monolayer linking sites spaced evenly, chains will not be able to graft uniformly across the surface because steric constraints will block access to some linking sites, particularly for high molar mass polymer chains.

5.4.2. Friction Measurements. A DI3000 Atomic Force Microscope (AFM) was used in both contact and force modes to conduct friction and adhesion measurements. Cantilevers with polyethylene bead tips of 5 μm radius with a cantilever spring constant of 4.5 N/m were purchased from Novascan. Polyethylene-bead tips were used for the friction analysis as they provide highly reproducible data and do not contaminate easily.

Surface friction force data were measured by using the AFM in contact mode. In this setting, the AFM cantilever probe scans in the forward and reverse directions against the sample. Disabling the other scan lines serves to create a friction loop. The friction force can then be calculated from the average difference between the force values of opposing scan directions.

Wafers were held in place by both a vacuum and double-sided tape. Data were collected at a fixed scan rate of 1 Hz and scan length of 5.0 μm. The applied load was varied from 0 to 8 volts by changing the cantilever operating height setpoint. Friction values were recorded after a steady-state friction force was reached for each load. Final friction-load plots were constructed from averages of measurements conducted

at several surface locations on each lubricant system. Normal and lateral AFM force values (N and F_f) were converted from voltage, V_n and V_l, through the relations

$$N = K_n S_n V_n \quad (5)$$

$$F_f = K_l S_l V_l \quad (6)$$

Normal sensitivity, S_n, was determined from force-distance curves measured by the AFM in force mode. This was used to determine lateral sensitivity, S_l, as described by Liu and Evans.[29] The lateral force constant K_l was determined from the dimensions of the cantilever. The normal force constant K_n was determined using the added-force method developed by Cleveland et al.[30] The normal force constant was calculated to be 4.47N/m for the reported 4.5 N/m polyethylene bead cantilever.

The relative humidity can have a significant effect on the COF when measuring the friction force of different surfaces with an AFM. Increased humidity can induce surface contamination in the form of a viscous layer on the sample surfaces which would lead to higher friction and stiction forces.[31] The AFM experiments were conducted in a room where the humidity was not controlled, introducing some error between sets of data. The relative humidity was approximately 35 percent when investigating brushes with different chain lengths, and approximately 40 percent for all other measurements. To account for the effect of humidity, friction coefficients measured on any system are normalized by the value obtained for bare silicon under the same measurement conditions.

5.4.3. Adhesion Measurements. The AFM was used in force mode to determine the adhesion characteristics of each sample surface. In this mode, the cantilever moves vertically with respect to the surface, and its deflection with respect to its non-deflected state provides a means of characterizing the adhesion force. Measurements

are made in terms of voltage readings and converted to a force using the cantilever spring constant.

An example of a force-distance curve produced from these experiments is depicted in Figure 5.2. The cantilever is first extended toward the surface by slowly lowering the piezo, which holds the base of the cantilever. At some piezo height, the attractive forces between the cantilever tip and the surface will be large enough to cause the cantilever to deflect down to the surface (point A on the schematic). As the cantilever remains in contact with the surface and the piezo continues to move downwards, the deflection on the cantilever will decrease until it is no longer deflecting (point B). The piezo will continue to lower, bending the center of the cantilever upwards, until the force is equivalent to a caution setpoint set by the user/manufacturer to prevent damage to the tip. The piezo then begins to retract from the surface. The adhesive forces will maintain contact between the surface and the tip beyond the piezo height which would be equivalent (point C) to the original cantilever deflection that developed from the extension direction. The surface will attempt to extend upwards to maintain adhesive contact (point D), creating a reverse indentation at the interface. Eventually the force on the retracting cantilever is large enough to overcome the adhesive forces, and the cantilever tip is released from the surface (point E). The area between the extension and retraction curves is a quantification of the work done by adhesion; the maximum value between the zero-deflection baseline and the base of each curve is an evaluation of the pull-off force, F_a, which is the force necessary to overcome adhesion. This pull-off force is directly related to the surface tension of the sample:

$$F_a = -3\pi R\gamma / 2 \tag{7}$$

where R is the cantilever tip radius, γ is the reduced surface tension:

$$\gamma = \gamma_1 + \gamma_2 - \gamma_{12} \tag{8}$$

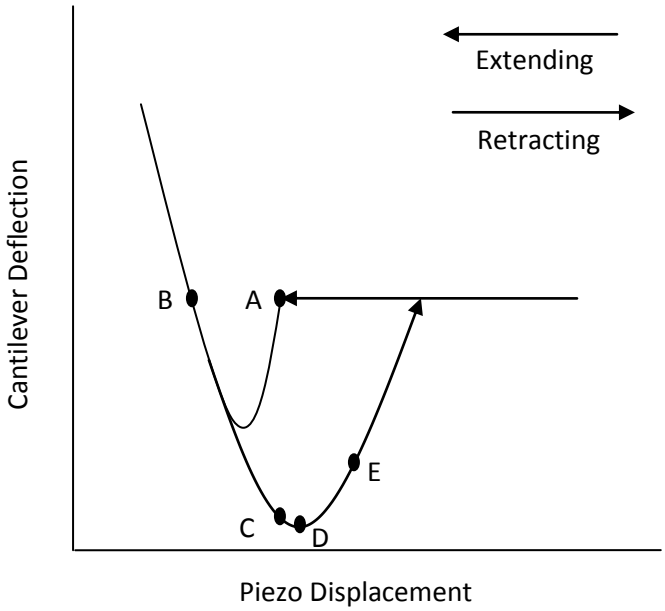

Figure 5.2. Schematic of a force-distance curve produced by an AFM in force mode.

based on the surface tension of the two materials at the interface (γ_1, γ_2) and the interaction between them (γ_{12}).

5.4.4. Friction and Adhesion Characterization. Friction force vs. load plots (F_f vs. N) can be developed for all materials from the AFM measurements. According to a modified form of Admonton's Law, the curve should be a representation of two contributions to the friction force: a load component which reflects a basic proportional relationship between F_f and N in which the proportionality constant is the COF, μ; and an adhesion component, consisting of the product between the interfacial shear stress, τ_o, a value describing the surface chemistry, and the interfacial contact area between surfaces, A:

$$F_f = \mu(N + N_c) + \tau_o A \tag{9}$$

Here N_c is the critical load, a finite value representing the force needed to pull the two opposing surfaces apart. It is important to note that A is non-linear with respect to N, as derived by Johnson, Kendall, and Roberts (henceforth referred to as JKR)[32]:

$$A = \pi\left(\frac{R}{K}\right)^{2/3}\left\{N + 3\pi R\gamma + \left[6\pi R\gamma N + (3\pi R\gamma)^2\right]^{1/2}\right\}^{2/3} \tag{10}$$

K is the reduced elastic modulus:

$$K = \frac{4}{3}\left[\left(1-\nu_1{}^2\right)/E_1 + \left(1-\nu_2{}^2\right)/E_2\right]^{-1} \tag{11}$$

where ν_1 and ν_2 are the Poisson ratios of the materials at the interface, and E_1 and E_2 are the respective elastic moduli.

From Eq. (9) and (10), it is clear that if a linear relationship exists between F_f and N, the contribution of adhesion to the friction force is negligible. This is most likely to occur when the interfacial shear stress is low. Under these conditions, the slope of the linear F_f vs. N plot would be μ and the intercept would be (μ N_c).

The intercept of F_f vs. N is often referred to as the residual force, F_o, and believed to correlate to the work done by adhesion and the pull-off force, F_a. Thus the

slope of a linear F_f vs. N plot provides a characterization of the surface friction, and the intercept describes the surface adhesion. While some researchers have reported that F_o is proportional to F_a, a broader review of the literature indicates that no simple relationship ever been developed that allows for one value to predict the other.[33] However, the work done by friction can be compared to the work done by adhesion, providing a means of quantifying the contribution of adhesion to friction. This comparison can be descriptive when the two contributions to the friction force seen in Eq. (9) are not necessarily equal. If the adhesion contribution is dominated by the load contribution, quantifying the fraction of the friction force that comes from adhesive work may help to understand the balance between the chemical and physical lubrication effects at the interface.

A correlation developed by Chen et al. effectively relates the work done by friction and adhesion.[34] First, the work done by friction at zero-load is recognized as the product of the friction force required to laterally move some distance, δ, and that distance δ, which is a molecular lengthscale often equated with the distance that surface molecules will move in response to external applied stress. The work of friction is thus (δF_o). The work done by adhesion can be evaluated as the effect of the pull-off force applied over the contact area. A value for F_a can be obtained from both the extension and retraction curves of the AFM force-distance curve; using Eq. (7), these values can then be converted to surface tension values. The difference between surface tension values,

$$\Delta\gamma = \gamma_R - \gamma_E \tag{12}$$

where γ_R and γ_E are the values calculated from retraction and extension, respectively, is the adhesion hysteresis for the sample. Essentially, the difference between the loading and unloading of the opposing surface at the interface is an evaluation of the energy dissipated during adhesive contact. As this occurs over the interfacial contact

area, the work done by adhesion is ($\Delta\gamma\, A$). The relation between friction and adhesion at zero-load is thus:

$$F_f(0) = \varepsilon\, A\, \Delta\gamma / \delta \qquad (13)$$

Here ε is the fraction of kinetic energy transferred into the interface upon contact, and can be considered as the fraction of the overall friction force that comes from the contribution of adhesion. For polymer surfaces developed from high molecular weight PS (MW ~ 200 kg/mol), Chen et al. found ε to range from 0.2 to 1.0.[34] For thick PDMS networks (~10 μm), we have found ε to be much lower, ranging from approximately 0.05 to 0.1.[19] The significant reduction in ε is in part a result of the lower surface energy for PDMS than PS. It should also be noted that ε is dependent on the two materials in contact; while we found lower values for ε using polyethylene beads as the opposing surface, Chen et al. conducted their measurements with two opposing surfaces of PS. Thus the decrease in ε is also representative of the differences in surface energy between PS and polyethylene.

It is interesting to note that theoretical polymer brush characterization equations can be used to predict the value of ε. The shear modulus of the polymer brushes provides insight into the potential mobility of the chains as they are stretched in response to lateral movement. The shear modulus, μ_p, can be derived from a force balance on the brush and is a function of σ:

$$\mu_p = \frac{3kT}{b^2} V\sigma^2 \qquad (14)$$

where k is the Boltzmann's constant and T is temperature. Young's elastic modulus, E, is related to μ_p by:[35]

$$E = 3\,\mu_p \qquad (15)$$

Combining Eq. (2) and (6) yields:

$$E = 9\, k\, T\, b\, \sigma^2 \qquad (16)$$

From Eq. (16), it is clear that $E \sim \sigma^2$. This relation can be extended through the JKR adhesion derivations. When the elastic modulus of the brush material is significantly smaller than the elastic modulus of the cantilever tip material, the reduced elastic modulus K should be related to the elastic modulus by $K \sim E$ of the sample. Further, if we ignore the second and third terms in Eq. (10), then as $A \sim K^{2/3}$ according to Eq. (10), $A \sim \sigma^{-4/3}$. And by Eq. (13):

$$\varepsilon \sim \sigma^{4/3} \tag{17}$$

If this relationship holds for brushes made from different materials, then it is clear that the effect of surface tension and interfacial shear stress is small, as ε will scale with the degree of coverage of the surface and not with the surface chemistry. Because the effect of surface tension is primarily exerted through the contribution of adhesion, and ε reflects the fraction of the friction force that comes from adhesion, it can be expected that ε will be small for all brushes as well.

5.4.5. Surface Viscosity Characterization.

Values measured for E can be similar to those of polymer networks with very short distances between cross-links, and can be compared by associating a certain length of each brush chain with this distance between cross-links.[35,36] The stretched chains can be considered as a sequence of Gaussian blobs of g monomers each. The shear modulus equation can be used to take into account the description of the brushes as blobs by:

$$\mu_p = \frac{3kT}{gb^3} \tag{18}$$

This equation recognizes that brushes behave like incompressible elastic films because the chains are anchored at one end and incompressibility is assumed. Equating Eq. (14) and Eq. (18) with $V = b^3$, it follows that:

$$g = b^{-4}\sigma^{-2} \tag{19}$$

It has been noted that g is also equal to the number of monomers between cross-links for an elastomer with a shear modulus equal to μ_p despite the polymer brushes not being attached at the surface.[36] The similarities between these values thus indicate that the polymer brushes can be treated as elastic films.

Dynamic properties of the brushes can then be calculated using the usual approaches for polymers in bulk. The relaxation time τ_b can be found by:[37]

$$\tau_b = \frac{\zeta b^2}{3\pi^2 kT} g^2 \qquad (20)$$

Here ζ is the monomeric friction coefficient. Because the stretched brushes often have values for g that are consistent with that of cross-linked networks, and entanglement does not typically occur among stretched brushes, it is consistent to calculate the dynamic properties of the brushes in a method similar to a polymer network. Thus this relaxation time can be used to determine the bulk viscosity at low frequencies:

$$\eta_o = \tau_b \mu_p \qquad (21)$$

We have previously seen that increasing the surface viscosity of PDMS network lubricants serves to increase the friction force and COF.[19]

5.5. RESULTS.

5.5.1. Effect of chain length. Brushes were synthesized from monofunctional PDMS chains of three different precursor molar masses: 10900 g/mol (PDI = 1.1), 25000 g/mol (PDI = 1.3), and 52000 g/mol (PDI = 1.3). The polymer was dissolved in toluene to approximately 10 percent polymer by volume before synthesis on the SAM-coated silicon wafers began.

Surface characterization of the brushes is reported in Table 5.1 and F_f vs. N curves are presented in Figure 5.3. A dramatic reduction of more than an order of magnitude in the COF exists for nearly all the PDMS brush lubricants compared to the

Table 5.1. Surface characterization for PDMS brushes synthesized from different molar masses.

MW	μ (COF)	h (nm)	σ (chains/nm^2)	Σ	E (Pa)	η_o (cP)
52000	0.0090	53.8	0.646	56	7.58E+06	13.0
25000	0.0057	20.8	0.519	22	4.90E+06	20.0
10000	0.0024	14.8	0.924	15	1.55E+07	6.34

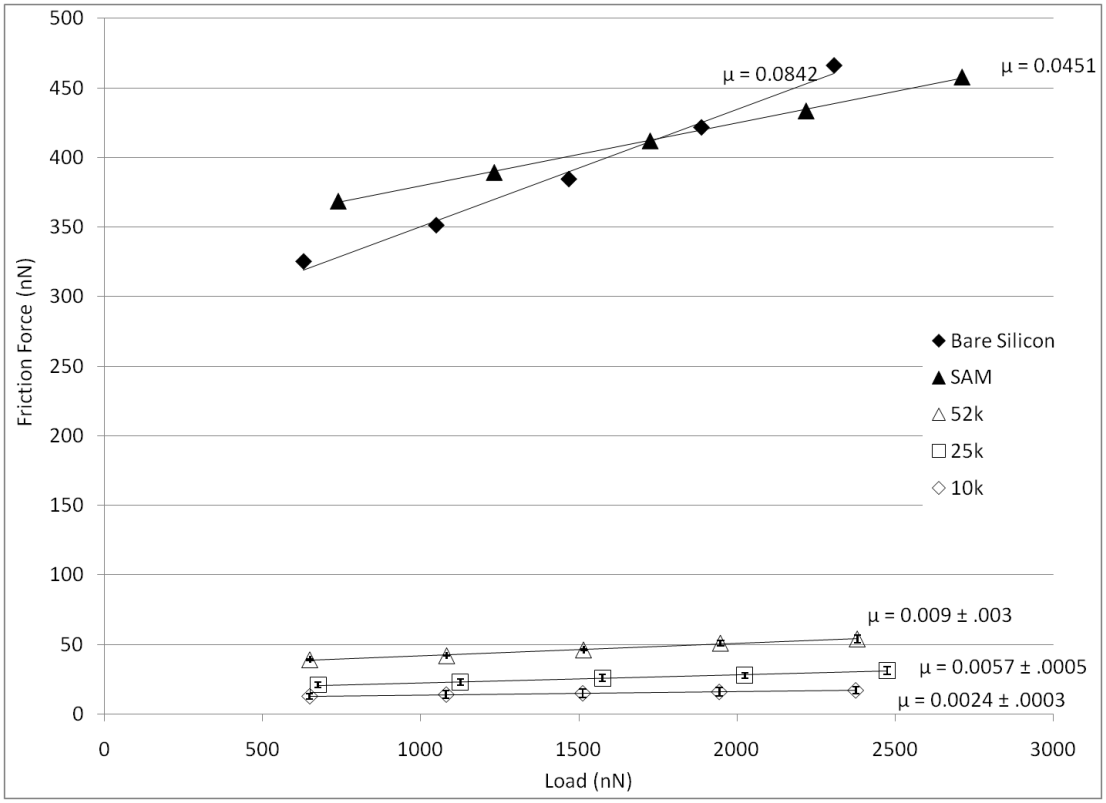

Figure 5.3. Friction force vs. load plot for PDMS polymer brushes of different chain lengths. The precursor molar masses used were 52000, 25000, and 10900 g/mol.

COF for bare silicon. While there may be significant differences between each brush system, it is important to recognize that introducing any of the brush lubricants induces a substantial improvement in the surface friction properties.

Another considerable feature related to the order of magnitude decrease in the COF is the specific COF values for the lubricant brushes. The lowest COF for any of the brushes is 0.0024 for the 10900 g/mol chains. This is lower than the friction coefficients we reported previously for ultrathin hyperbranched PDMS network films,[18] and is the lowest COF we have found in the literature for dry lubricant systems. Here a dry system is defined as a lubricant with no solvent or mobile liquid-like material present. The low friction characteristics primarily develop from the low surface energy of PDMS and the low interfacial shear stress that the polymer exhibits. This can be seen from the decided linearity that exists for all F_f vs. N curves, implying that the contribution of adhesion to the friction force is negligible for each system as previously discussed. This supports the premise that the low interfacial shear stress of PDMS allows for its low COF.

A comparison of the friction of the three brush lubricants indicates that increasing the molar mass and/or decreasing surface coverage of the brushes leads to an increase in the COF. The reduced surface coverage of each sample also greatly increases with the brush chain length. Greater chain extension is necessary for the longer chains to achieve similar graft densities on the substrate as the shorter chains. The chain extension is important when considering the mobility of the chains as the brushes adjust laterally to interfacial contact. When an external stress is applied, the brushes will elongate in the direction of the lateral movement, as the cartoon in Figure 5.4 depicts. In order for higher mobility to be achieved, the extension of the chains away from the substrate will need to be greater; more flattened conformations will exhibit decreased surface mobility. The extension of the longer chains will mean a

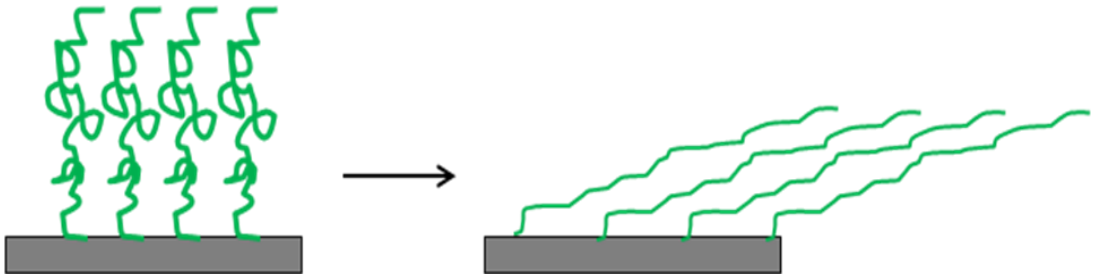

Figure 5.4. A cartoon depiction of elongated brushes flexing and stretching in response to an external stress applied in a lateral direction.

higher degree of stress will be distributed down the length of the brush to allow for lateral mobility. While the shorter chains may also be highly extended from the surface, their shorter length means less stress is necessary to achieve a similar degree of mobility.

This finding confirms the results reported by Casoli et al., who had concluded that longer chains will have a higher relaxation time and thus higher external stresses will be necessary to achieve lateral movement.[22] We note that this result depends critically on the material used on the opposite side of the interface. Here the microscopy analyses were conducted with a solid polyethylene bead as the opposing surface. Brown[21] conducted studies with a polymer network as the opposing surface and observed brush penetration into the network for the shorter chains whereas the longer chains created a liquid-like surface coating and reduced the friction. Because the potential increased friction forces needed for shorter brushes to be pulled out of the network has been eliminated in our experiments, we are able to observe an opposite relation between brush length and the friction properties.

5.5.2. Effect of surface coverage. PDMS brushes were synthesized from diluted monofunctional polymer solutions at different volume concentrations. The concentrations of the precursor solutions ranged from 2.5 to 30 volume percent and served to control the number of polymer chains that could bond with the SAM layer; dilute solutions would lead to large distances between tethered chains across the substrate, while added material in high concentrations would permit a more dense surface coverage to develop.

Surface characterization data are summarized in Table 5.2 and F_f vs. N curves are presented in Figure 5.5. It is clear that the friction properties (μ and F_o) decrease from SAM layer values as the polymer brush surface coverage increases.

Table 5.2. Surface characterization for PDMS brushes (all MW = 10900 g/mol) synthesized with different surface coverages.

	μ (COF)	**h (nm)**	**σ (chains/nm^2)**	**Σ**	**E (Pa)**	**η_o (cP)**
2.5%	0.0405	0.8	0.046	1	3.82E+04	2576
5.0%	0.0389	1.8	0.103	2	1.93E+05	509
7.5%	0.0127	3.8	0.218	4	8.61E+05	114
10%	0.0076	4.8	0.275	5	1.37E+06	72
20%	0.0072	6.3	0.361	7	2.37E+06	42
30%	0.0063	13.8	0.790	14	1.14E+07	9

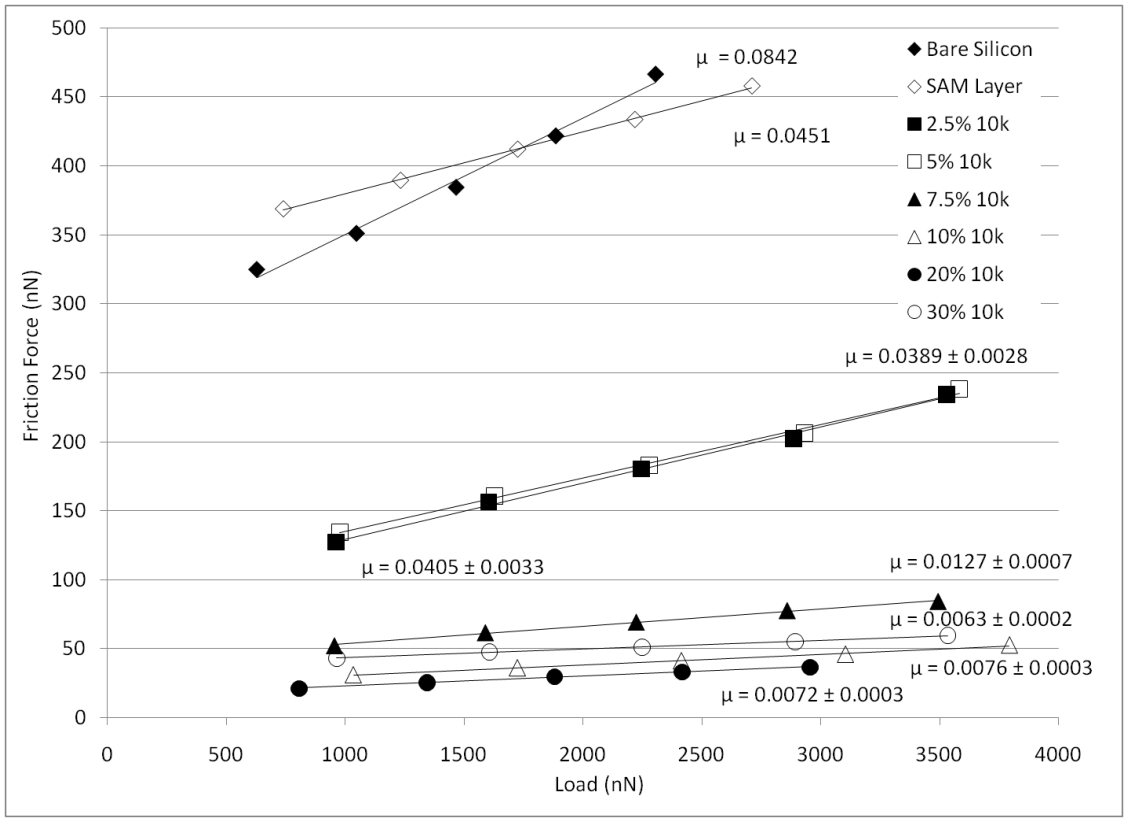

Figure 5.5. Friction force vs. load curves for PDMS brushes developed at different surface coverages. Brushes are listed by the precursor polymer solution concentration used to graft the chains. All brushes have a 10900 g/mol precursor molar mass.

Unsurprisingly, lubricant systems with poor surface coverage exhibit COFs approaching the COF of the SAM layer, and the two brushes with the lowest surface coverage display residual forces closest to the SAM system. The similarity in the friction properties between the brushes with low surface coverage and the SAM coatings suggests that patchy coverage develops at low surface coverages. Friction force measurements are taken as an average over the sample surface, allowing for PDMS chains and SAM material to both contribute to the friction properties when the brushes do not fully cover the surface. For brushes tethered at higher surface coverages, the COF significantly decreases from the SAM value, implying the SAM layer is more uniformly coated by the brushes across the substrate.

For higher surface coverages, the COF and F_o steadily decrease. As previously mentioned, lower surface viscosities have been seen to correlate with decreased COF.[19] Increasing the surface viscosity of tethered lubricants increases the viscous dissipation at the surface and thus creates greater surface friction. An evaluation of the viscosity shows a steady decrease as the surface coverage increases and the COF decreases. The viscosity calculation is based on the assumption that the brushes densely cover the surface; this assumption is not met for the lower surface coverages based on the Σ transition value. For higher surface coverages, however, the densely packed brush condition is true, and so the surface viscosity effect appears to hold for polymer brushes as well as bulk network lubricants.

The relationship between the COF for the brushes and the surface coverage is clearly established in Figure 5.6. Between reduced surface coverages of approximately 2 and 4, the COF decreases dramatically. This transition in COF appears to coincide with a transition from the mushroom to brush regime within the Σ range deduced by Brittain and Minko.[27] While the COF decreases over the entire range of reduced surface coverages, the COF seems to plateau in both the mushroom

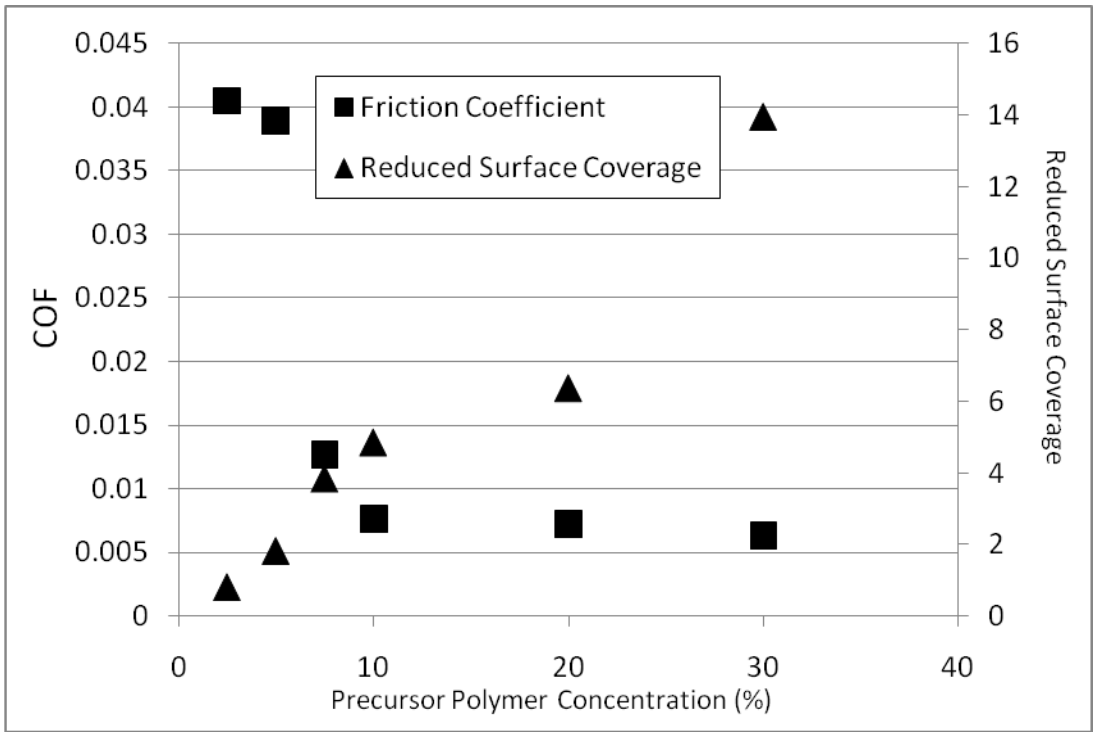

Figure 5.6. Comparison between the COF and reduced surface coverage in terms of precursor polymer concentration for 10900 g/mol PDMS brushes.

and brush regimes. We have already discussed the likelihood of patchy coverage for the mushroom regime, resulting in the friction properties approaching SAM layer characteristics. In the brush regime, however, the COF plateau suggests that continuing to increase the grafting density after the brushes are already stretched and extended from the substrate will not have a further substantial effect on the friction force. It is likely that a minimum COF would be achieved for the maximum grafting density, where the densely packed brushes would have a regular arrangement at the surface. This minimum COF only exists in theory because tethered polymer chains will always block other linking sites on the substrate, meaning a 'grafting-to' tethering approach is unlikely to achieve maximum coverage at the molar masses of these chains. The tethered brushes become more stretched at higher surface coverages; chain elongation in response to a lateral applied stress is thus decreased, resulting in lower friction forces.

All brushes show decided linearity in the F_f vs. N curves. Thus the contribution of adhesion to the friction force is low for these systems. We can conclude that this condition is true regardless of the structural regime that the brush exists in. It is likely that because the lubricant films are ultrathin, the effect of adhesion does not manifest at significant enough levels to affect the friction force. It is possible that adhesion would affect much longer polymer brushes at high grafting densities.

5.5.3. Effect of surface chemistry. To this point, we have primarily focused on PDMS brushes because of their low surface energy and low interfacial shear stress, and our desire to produce a lubricant with a negligible contribution of adhesion. In order to evaluate how effective PDMS (MW = 10900 g/mol) is in comparison to other polymers, brushes were also synthesized from monofunctional PS (MW = 8000 g/mol)

and a monofunctional PPG-PEG-PPG block copolymer (MW = 2000 g/mol) hereafter referred to as PPG/PEG. F_f vs. N curves are reported for the PS and PPG/PEG brushes developed from different precursor polymer concentrations in Figures 5.7.1 and 5.7.2, respectively. The friction coefficients for these systems versus the reduced surface coverage are presented in Figure 5.8 with a comparison to the PDMS results, and the surface characterization data is collected in Table 5.3.

Several conclusions can be drawn from the friction results. First, the mushroom-to-brush transition is observed in each set of data. While it is possible that a relationship exists between higher surface energies and the transitions occurring at higher reduced surface coverages, the difference in Σ transition values is more likely an effect of the different molar mass of each set of brushes. The transition occurs between Σ values of 2 and 4 for PDMS, between 3 and 6 for PS, and between 10 and 14 for PPG/PEG. Ignoring the effect of chemistry would imply that the mushroom-to-brush transition occurs at higher surface coverages for lower molecular weight chains. Chains in the mushroom state spread across the surface because of weak interaction between chains and fewer active adjacent tethering sites. For shorter chains, interaction will still be low even if the surface coverage is increased, as the distance between tethering sites required for chain interaction to occur decreases for shorter chains. Thus much higher surface coverages are needed for lower molar mass brushes to transition between regimes and induce a substantial decrease in the COF.

The PDMS brushes exhibit the lowest friction coefficients compared to both the PS and PPG/PEG brushes. Polymer brushes with high surface tension have increased COFs when data is compared within each regime subset. The reduced surface tension (accounting for the polyethylene (PE) bead) for PE-PDMS is 0.0280 nN/nm, 0.0382 nN/nm for PE-PS, and 0.0386 for PE-PPG/PEG. Assuming the COF for the highest surface coverage examined for each polymer brush is

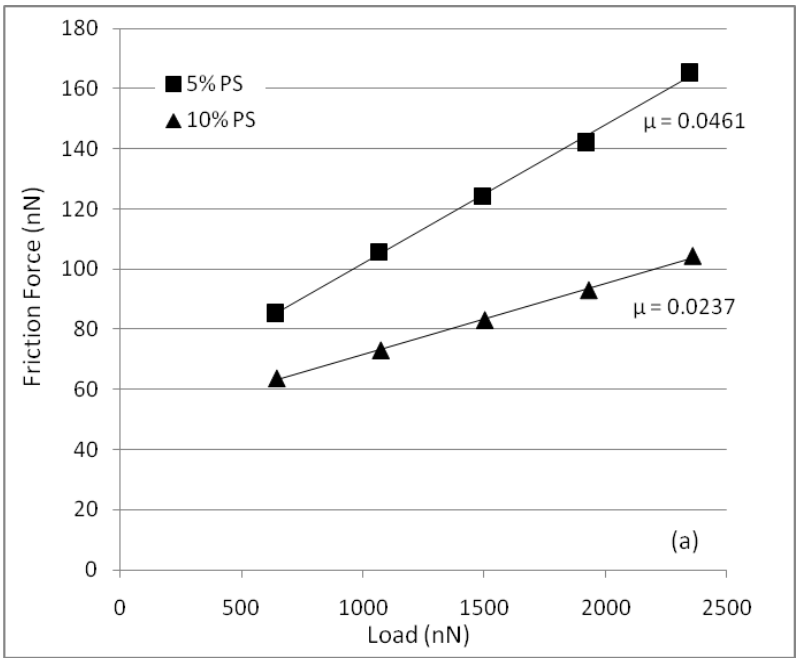

Figure 5.7.1. Friction force vs. load curves for 8000 g/mol PS brushes. Brush systems are listed by their precursor polymer solution concentration.

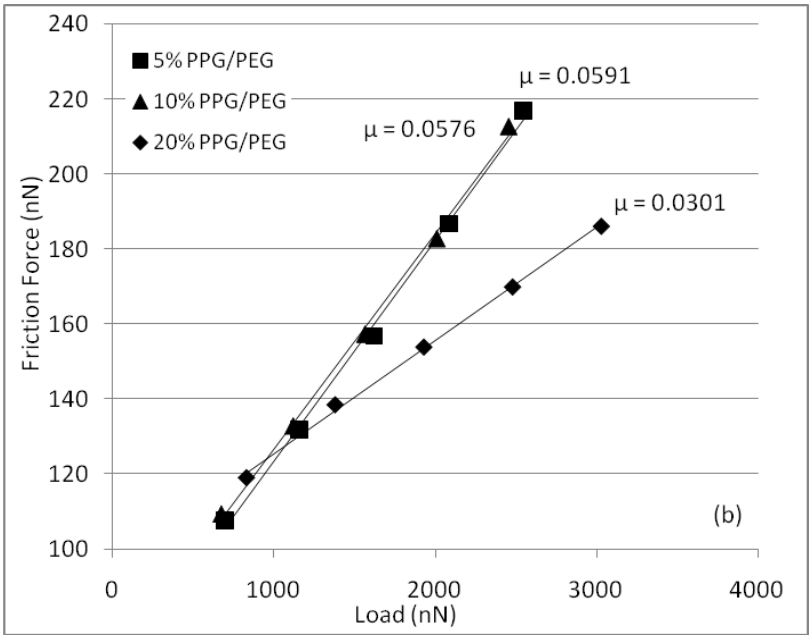

Figure 5.7.2. Friction force vs. load curves for 2000 g/mol PPG/PEG brushes. Brush systems are listed by their precursor polymer solution concentration.

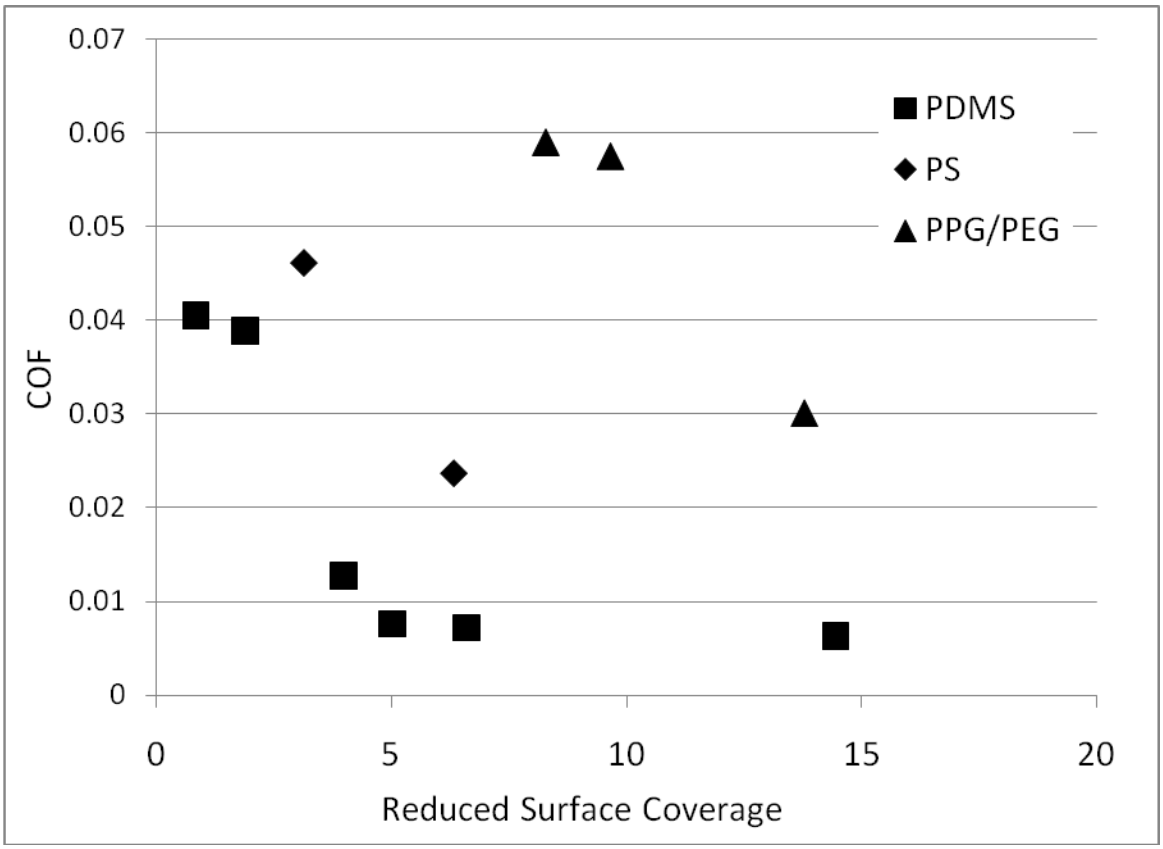

Figure 5.8. COF vs. Σ for polymer brushes developed from different polymer materials. All measurements were conducted at approximately 25 ^{o}C.

Table 5.3. Surface characterization data for PPG/PEG copolymer brushes (all MW = 2000 g/mol) and PS brushes (all MW = 8000 g/mol) synthesized with different surface coverages.

	μ (COF)	**h (nm)**	**σ (chains/nm^2)**	**Σ**
PPG/PEG	0.0591	6.0	2.41	8
	0.0576	7.0	2.81	10
	0.0301	10.0	4.01	14
PS	0.0461	6.0	0.071	3
	0.0237	12.1	0.143	6

representative of the brush regime for that polymer, it would indicate that PDMS has a lower COF than that of PS by a factor of 3.7 and lower than that of PPG/PEG by a factor of 4.7. If the mushroom-to-brush transition is not complete, however, the difference between these systems may be much smaller. Further data are necessary to compare the brush regime plateaus. Extending the data comparison to higher surface coverages may indicate a substantial difference exists for densely grafted, stretched chains. Thus while PDMS brushes demonstrate the lowest friction coefficients as predicted by having the lowest interfacial surface tension, other factors will need to be considered to complete the comparison between polymer systems.

It is also important to recognize that surface tension and by extension the interfacial shear stress may not be the dominant factor in friction properties. Assuming that surface tension has a dominating effect would imply that the PS and PPG/PEG brushes exhibit approximately the same friction coefficient values. However, the PS brushes have lower COFs than PPG/PEG; this goes counter to the chain length conclusions. Thus, it is likely that dynamic factors are contributing to the friction. The experiments were conducted at room temperature (~ 25 ^{o}C), significantly below the glass transition temperature (T_g) of 95 ^{o}C for PS. On the other hand, PDMS and PPG/PEG are both well above their T_g of -120 ^{o}C and -90 ^{o}C, respectively, at room temperature. The PS brushes may be much more solid-like, creating highly different structural states than typical polymer brushes. To further evaluate the differences between polymers, friction measurements would need to be conducted at different temperatures corresponding to the same ΔT_g.

5.5.4. Comparison between adhesion and friction. The correlation factor ε relating friction and adhesion was calculated for the PDMS, PS, and PPG/PEG brushes. As a scaling analysis suggests the fraction of the friction force developing from the

contribution of adhesion should scale with the surface coverage with a power-law exponent of 4/3. The experimental data is plotted in Figure 5.9 and show very close agreement to this prediction with an exponent of 1.32. It is important to note that this scaling relation holds regardless of the polymer material, and is an important factor in evaluating the extent of the surface chemistry effect on the COF and friction force for ultrathin polymer brush films.

Any effect the surface tension or interfacial shear stress has on the friction force should be represented through the adhesion contribution to friction. The surface tension is proportional to the interfacial shear stress, and after determining the proportionality constants for the polymer material of concern, γ could be substituted into the Admonton's law equation in place of τ_o. It should be expected, then, that surface tension would play a significant role when the adhesion contribution is high. However, F_f vs. N curves for each set of polymer brushes display decided linearity, meaning the adhesion contribution is negligible. Thus ε should be small for all the brush films examined here and other brushes of similar chain lengths. Calculations support this conclusion, revealing the adhesion contribution accounts for less than five percent of the friction force for all the samples investigated. With a limited adhesion contribution for all ultrathin brushes, the effect of surface tension will be limited, implying that the difference between the PDMS brushes and PS or PPG/PEG films may be much larger for bulk lubricant structures where the contribution of adhesion to the friction force may be larger for these materials. While the PDMS brushes exhibit lower COFs than the other polymers by significant factors, the difference may be even more substantial in the bulk with an increased influence of surface tension.

Based on the scaling analysis, it is highly unlikely the adhesion contribution to friction would be substantial for polymer brushes of any material. In order to achieve a value for ε that represents a significant adhesion contribution, the surface coverage

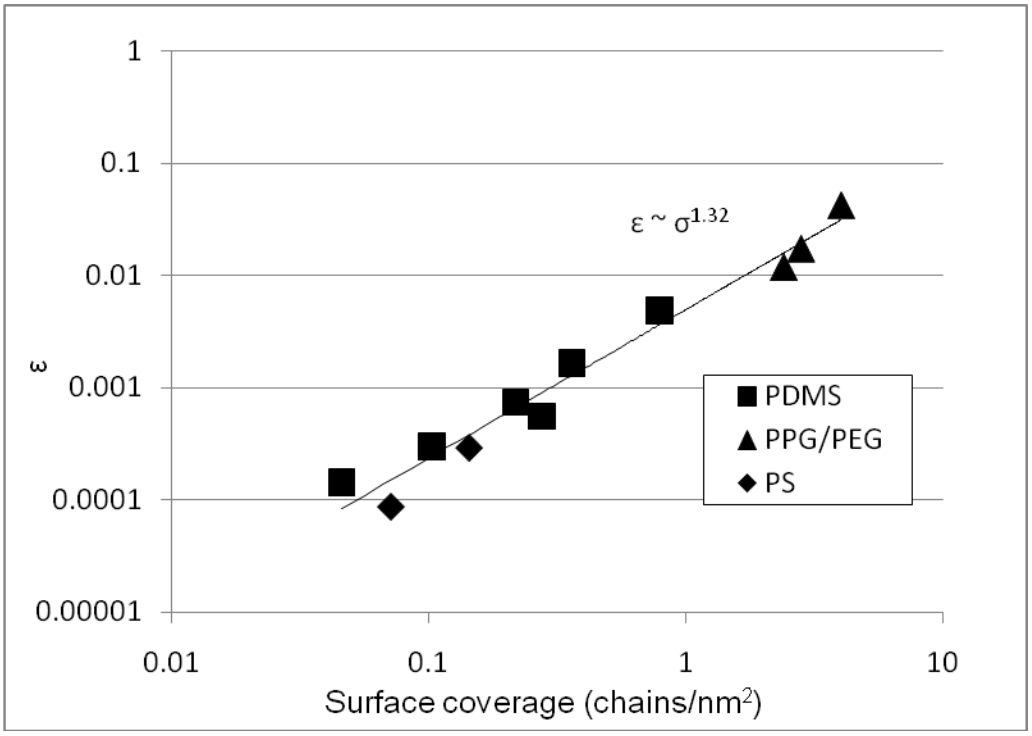

Figure 5.9. Scaling analysis comparison for all brush systems between ε and σ. Theory predicts a relation of $\varepsilon \sim \sigma^{4/3}$.

would need to be extremely dense, meaning very short distances between tethering sites for the grafted polymer chains. As has been found with traditional polymer 'grafting-to' approaches, steric hindrance and excluded volume concerns can prevent dense coverages from developing during synthesis. Decreasing the distance between tethering sites would make it even less likely for higher surface coverages to form. Thus polymer brushes should always demonstrate low adhesion contributions to the friction force and low values for ε.

5.6. CONCLUSIONS.

Polymer brushes were synthesized under a range of different conditions in order to characterize the chemical and physical influences on surface friction and adhesion. From surface microscopy measurements, PDMS brushes were seen to manifest extremely low friction coefficients ($\mu \sim 0.0024$) that are close to the lowest COFs ever recorded for dry polymer systems. These COFs are the result of a low interfacial shear stress and a low surface tension for PDMS.

Friction measurements conducted on PDMS brushes of different chain lengths revealed that longer brushes will exhibit higher friction coefficients as a result of the stretched chains. The polymer brushes will elongate and stretch in response to lateral shear stress. Because greater stresses will be necessary to induce full stretching of the longer brushes, friction will be higher. These results are contrary to previously published data, because the opposing surface is impenetrable to short chains that increase the surface friction in case of an opposing surface of a penetrable elastomer.

PDMS brushes grafted at different surface coverages indicated the COF is highly dependent on the structural regime of the brushes. At low surface coverages, when the brushes will spread in a mushroom conformation, friction is much larger as a result of patchy coverage. As the grafted chains transition to a stretched brush regime,

the COF sharply decreases in correlation with the transition. In the stretched brush regime with a more uniform surface, the COF plateaus to lower values.

Synthesizing brushes from other polymers allows for a comparison of different surface chemistries. PDMS films in the stretched brush regime have COFs lower than PS brushes by a factor of 3.7, and lower than PPG/PEG by a factor of 4.7. The decreased friction coefficients coincide with a decreased surface tension, although a negligible contribution of adhesion to the friction force may minimize the impact of surface tension on the COFs. More data is necessary to determine the complete COF plateaus for the PS and PPG/PEG films in the brush regime. These systems also indicated the mushroom-to-brush transition will occur at higher surface coverages for shorter chain lengths.

All brushes exhibited a linear F_f vs. N dependence, meaning the contribution of adhesion to the friction force was negligible. A scaling analysis was conducted based on theoretical polymer brush characterization equations and on a correlation factor relating the work done by friction to the work done by adhesion. This analysis led to the relationship $\varepsilon \sim \sigma^{4/3}$ between the fraction ε of the friction force developing from adhesion and the surface coverage σ. Experimental data found the power-law exponent to be 1.32, supporting the proposed scaling analysis for polymer brushes.

REFERENCES

(1) Rymuza, Z. *Microsystem Technologies* **1999**, *5*, 173-180.

(2) Bhushan, B. *Proc. Instn. Mech. Engrs Part J* **2001**, *215*, 77-102.

(3) Cagin, T.; Che, J.; Gardos, M. N.; Fijany, A.; Goddard, W. A., III. *Nanotechnology* **1999**, *10*, 278-284.

(4) Sundararajan, S.; Bhushan, B. *J. Vac. Sci. Technol. A.* **2001**, *19(4)*, 1777-1785.

(5) K. Strawhecker, D.B. Asay, J. McKinney and S.H. Kim. *Tribology Letters* **2005**, *19*, 17-21.

(6) Bhushan, B. *Microelectronic Eng*. **2007**, *84*, 387-412.

(7) Bhushan, B.; Liu, H.; Hsu, S. M. *ASME J. Tribol* **2004**, *126*, 583-590.

(8) Bhushan, B.; Israelachvili, J. N.; Landman, U. *Nature* **1995**, *374*, 607-616.

(9) Xiao, X.; Hu, J.; Charych, D. H.; Salmeron, M. *Langmuir* **1996**, *12*, 235-237.

(10) Tsukruk, V.V.; Bliznyuk, V.N. *Langmuir* **1998**, *14*, 446-455.

(11) Yang, X.; Perry, S. S. *Langmuir* **2003**, *19*, 6135-6139.

(12) Raviv, U.; Glasson, S.; Kampf, N.; Gohy, J. F.; Jerome, R.; Klein, J.. *Nature* **2003**, *425*, 163-165.

(13) Ahn, H-S; Julthongpiput, D.; Kim, D-I; Tsukruk, V.V. *Wear* **2003**, *255*, 801-807.

(14) Julthongpiput, D.; Ahn, H-S; Kim, D-I; and Tsukruk, V.V. *Tribology Letters* **2002**, *13*, 35-40.

(15) Bowden, F.P.; Tabor, D. *Friction and Lubrication.* Methuen & Co. Ltd.: London, 1967.

(16) Wang, W.; Wang, Y.; Bao, H.; Xiong, B.; Bao, M. *Sensors and Actuators* **2002**, *97-98*, 486-491.

(17) Maboudian, R.; Ashurst, W. R.; Carraro, C. *Sensors and Actuators* **2000**, *82*, 219-223.

(18) Landherr, L.J.T.; Zhang, Q.; Cohen, C.; Archer, L.A. *J. Poly. Sci. B.*, **2008**, *46*, 1773-1787.

(19) Landherr, L.J.T.; Cohen, C.; Archer, L.A. (in preparation)

(20) Raviv, U.; Glasson, S.; Kampf, N.; Gohy, J. F.; Jerome, R.; Klein, J. *Nature* **2003**, *425*, 163–165.

(21) Brown, H.R. *Science* **1994**, *263*, 1411-1413.

(22) Casoli, A.; Brendle, M.; Schultz, J.; Auroy, P.; Reiter, G. *Langmuir* **2001**, *17*, 388-398.

(23) Quirk, R.P.; Cheong, T.-H.; Yoo, T. *Macromol. Chem. Phys.* **2002**, *203*, 1178-1187.

(24) Milner, S.T.; Witten, T. A.; Cates, M. E. *Macromolecules* **1988,** *21*, 2610-2619.

(25) Léger, L.; Raphael, E.; Hervet, H. *Advances in Polymer Science* **1999**, *138*, 185-225.

(26) Jones, D.M.; Brown, A.A.; Huck, W.T.S. *Langmuir* **2002,** *18*, 1265-1269.

(27) Brittain, W.J.; Minko, S. *J. Poly. Sci. Part A: Polymer Chem.* **2007**, *45*, 3505-3512.

(28) Wu, T.; Efimenko, K.; Genzer, J. *J Am Chem Soc.* **2002**, *124*, 9394.

(29) Liu, Y.; Evans, D. F. *Langmuir* **1996**, *12*, 1235-1244.

(30) Cleveland, J.P.; Manne, S.; Bocek, D.; Hansma, P.K. *Rev. Sci. Instrum.* **1993**, *64*, 403-405.

(31) Mate, C. M. *Tribology on the Small Scale: A Bottom Up Approach to Friction, Lubrication and Wear*. Oxford University Press, New York: **2008**.

(32) Johnson, K.L.; Kendall, K.; Roberts, A.D. *Proc.R. Soc. London, Ser. A*, **1971**, *324*, 301-313.

(33) Tsukruk, V.V.; Bliznyuk, V.N. *Langmuir* **1998**, *14*, 446-455.

(34) Chen, N.; Maeda, N.; Tirrell, M.; Israelachvili, J. *Macromolecules* **2005**, *38,* 3491-3503.

(35) Williams, D.R.M. *Macromolecules* **1993,** *26***,** 5096-5098.

(36) Long, D.; Ajdari, A.; Leibler, L. *Langmuir* **1996**, *12*, 1675-1680.

(37) Doi, M.; Edwards, S.F. *The Theory of Polymer Dynamics*. Clarendon Press: Oxford, **1986**.

CHAPTER 6

THE DEVELOPMENT OF HIGH SCHOOL CURRICULUM TO FURTHER STUDENTS' UNDERSTANDING OF FRICTION AND LUBRICATION IN REAL-WORLD APPLICATIONS.

6.1 ABSTRACT.

A curriculum project was developed and enacted for 10-12th grade high school physics classes to help reinforce students' understanding of the basic concept of friction and to strengthen their ability to draw connections between their classroom studies and the practical applications of their physics knowledge in their daily lives. A series of in-class discussions, demonstrations, structured laboratory experiments, and inquiry-based learning was conducted over a three-day period. Basic sliding friction experiments conducted by the students, in conjunction with discussions of common friction examples and concerns, were used to help the students bridge to the elevated concept of lubrication. Lubrication inquiry experiments in which students measured the coefficient of friction for materials of their choosing enabled them to draw conclusions about optimal characteristics for good lubricant systems. An evaluation of the curriculum based on survey questions conducted both before and after the project indicated that students felt their ability to recognize practical applications of science had been improved by the project.

6.2. BACKGROUND.

Friction is a basic physics concept that exists in a wide range of real-world examples – car tires, ice skates, miniature gears, boating, swimming, plane flight, and many more. However, while all high school students are introduced to friction in physics classes, many do not associate the classroom information with the applications

in their common lives.[1,2] If they are unable to observe the connections between their study of friction and the concepts in practice, their understanding of slightly elevated ideas like lubrication will also be weaker.

Many students view physics as a series of equations and symbols with little connection to reality despite the many practical examples that exist and should dissuade them of this line of thought.[3] The gap between students' learning and recognition makes it difficult to grasp elevated concepts. These problems can develop at any level of their physics education; if students can distinguish connections between their classroom study and reality earlier with simple concepts, it may help them to make connections as they progress onward to new information.

In response to these concerns in high school physics education, we have attempted to develop a curriculum project to further high school students' understanding of the concept of friction and help them make intellectual leaps from friction to the concept and practical use of lubrication. A series of in-class discussions, demonstrations, and laboratory experiments involving some inquiry-based learning were conducted with two different physics classes at Waterloo High School in Waterloo, NY, of approximately 30 total 10-12th grade high school students. This work was conducted in accordance with National Science Foundation GK-12 curriculum development to further scientific understanding. Herein we discuss how the project was successful in helping students make connections between their studies and surroundings.

6.3. PROJECT STRUCTURE.

The curriculum project was conducted over three days (with the daily class period lasting 74 minutes) immediately following the classroom studies and homework introducing the students to the concept of friction. The first two days were

centered around both open-class discussions and structured laboratory experiments. The goal of these discussions was to reinforce the students' background understanding of friction and lubrication. Sliding friction laboratory experiments conducted on the first two days were used to reinforce students' knowledge of the relationship between friction, load, and contact area. The third day provided an opportunity for inquiry-based learning involving lubrication and friction laboratory studies. Dividing each class period between some experimentation and some class discussion helped to reinforce the students' experiences and knowledge and better refine the students' comprehension of the central concepts.

6.3.1. First Day

6.3.1.1. *Class Discussion*

The first day started with an open-class discussion about friction and its role in real-world applications. Students were asked to provide examples of friction at work in solid, liquid and gaseous systems to make sure they understood friction existed beyond the simplistic examples previously seen in their homework and class examples. Most students were familiar with friction between two solid objects – either between two blocks or between tires and a road – but had not considered friction in other forms.

The students were shown and allowed to handle examples of other types of solid-solid friction, including small mechanical gears and medical syringe casings. Providing visual examples immediately helped facilitate further discussion of other examples of friction. When asked to describe friction in liquids, several pointed out a boat moving through water and drag on the hull of the boat, while others described the swimsuits worn by Olympians to reduce drag on the swimmers' bodies. When

discussing friction in gases, students recognized air resistance on planes and other flying crafts as an obvious example.

Students were then asked to think about what the sources of friction are and how they are represented in the examples we had discussed. This led to students easily recognizing the pressure exerted between two solid surfaces, which was followed by a more in-depth discussion of eddies developing in fluid flow both as a cause and effect of friction. We then explained how friction represented itself as forms of energy, such as the transition from kinetic to heat in solids, or from kinetic into tension in rubbery materials.

To reinforce the examples discussed in class, a demonstration of drag reduction in fluid flow was then conducted. In this demonstration, water was poured into a beaker and allowed to flow down a vertical pipe and out a horizontal pipe, as depicted in Figure 6.1. The distance that the water spouted out of the horizontal pipe was measured and marked. Water with a very low concentration of polyethylene glycol was then poured into the beaker. As the water at the outlet changed from pure water to a dilute polymer solution, the flow rate visibly grew, increasing the distance of the water spout by several inches. The class was informed that the dilute polymer solution was a demonstration of a phenomenon known as ‘drag reducing polymers’, where a dilute polymer concentration can reduce the friction in the fluid by up to 80 percent. Students were then asked to suggest practical applications of this type of lubrication. Having already discussed various friction examples, the students were much faster at coming up with more applications, including naval vessel travel and firefighting equipment, both of which have been studied in regard to this phenomenon.

The demo provided a starting point for a brief discussion of lubrication. It was explained that lubrication could encompass all means of reducing friction in solid, liquid, or gaseous systems. The class discussed how friction could be beneficial, such

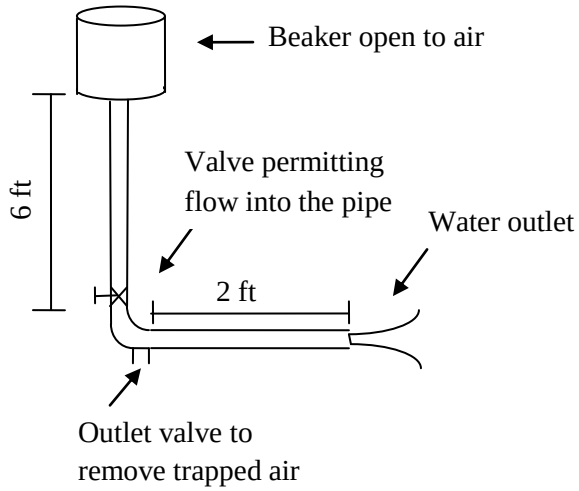

Figure 6.1. Set-up for in-class demonstration of drag reduction in fluid flow as developed by Rodriguez.[4]

as reducing contact area or the material needed for applications like tires, and how friction can be detrimental, such as kinetic energy converted and lost. Having seen in fluid flow how friction could be reduced, students were then asked to think of at least two methods to reduce friction. Most were able to list changing the materials being used or adding a layer of lubrication.

6.3.1.2. *Laboratory*

Having summarized friction and practical applications of the concept, students then began working on the first part of a sliding friction laboratory experiment as depicted in Figure 6.2. The focus of the experiment was to investigate friction on a non-inclined surface without a lubricant. Wood blocks with a hook on one end were attached to a string, which ran over a pulley and was tied to a weight stand. Students could add small weights that would increase the horizontal driving force on the block when the stand was pulled vertically by gravity. The block would then be steadily pulled on a nearly frictionless surface after enough weight had been added to overcome the static coefficient of friction (COF). This nearly frictionless surface was a smooth hard plastic sheet with minimal surface roughness.

Students were asked to measure the weight required to move the block, three times each for a series of laboratory designs:

- The wooden block with a piece of sandpaper on one side

- The block covered by a sheet of plain paper (reducing roughness from the wood surface)

- The block, covered by plain paper, turned on to its thinner side

- The block, covered by plain paper, with a weight placed on top of the block

These experiments demonstrated to the students the effects of changing the surface of the sliding object, of changing the contact area, and of changing the applied normal

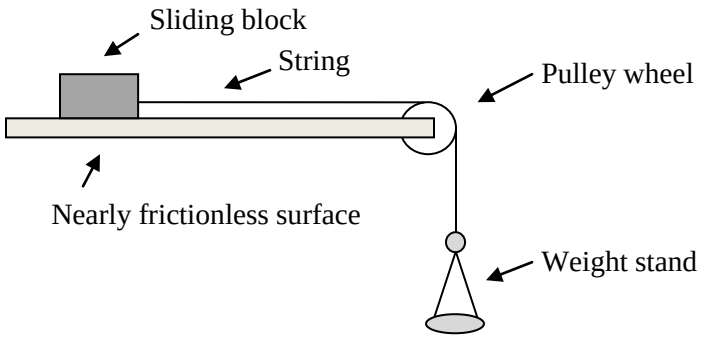

Figure 6.2. Equipment design for the sliding friction laboratory experiment.

force. From their weight stand measurements, students were then asked to calculate the average COF for each set of measurements and compare between data sets.

6.3.2. Second Day

6.3.2.1. *Laboratory*

The second day of the project began by having students conduct friction lab experiments similar to the lab they had conducted on the previous day. The main difference involved adding a slope to the platform. This served to not only reinforce the students' ability to calculate normal load for a surface at an angle, but also to help the students determine if a relationship exists between COF and angle of the platform.

Students added an angle to their platform by placing textbooks underneath the side of the frictionless surface closest to the pulley, thus creating an upward slope. Students continued working in their same groups of three as the previous day, and were asked to make three weight measurements and COF calculations for each of three angles.

6.3.2.2. *In-Class Discussion*

After students had finished the laboratory and calculations, the class was brought together and asked to analyze which changes to their equipment design had an effect. After the groups summarized what they had measured, they were asked how the COF of the experiment could be either increased or reduced. This began to shift the focus of the experimentation and class discussions to an elevated level conceptually, hoping to push the students to begin to make intellectual leaps from a reinforced base understanding. In response to the questions, most students were able to list both changing the surface of the sliding block and adding a lubricant.

A demonstration involving equipment borrowed from Cornell University was then conducted to reinforce these methods of changing the COF. Five different strips

of material (glossy paper, plain paper, polyester, teflon, and nylon) were taped lengthwise to a clipboard. When a motor was turned on, one end of the clipboard would slowly lift to create a gradually-increasing slope. Small discs placed on each strip would then slide down the slope after the slope was steep enough to allow the disc to overcome the static COF. Students were shown the process using both rubber stoppers and metal discs.

This demonstration served to simplify the basic methods of lubrication. Having observed five different substrate materials and two different sliding objects, the experiment indicated how the static COF changed not only between different surface materials but also for different sliding materials. It was explained that the introduction of a lubricant was similar to changing the substrate, and the friction properties would change when different materials were used. The different sliding materials represented the interaction between the opposing surfaces, and that lubricants could be ineffective depending on how they interacted with the sliding surface.

Building on the lubrication discussion, students were told they would be able to investigate several friction-changing lubricants in an inquiry-based atmosphere the next day. Each group was informed they would investigate three different lubricants and were asked to bring in household materials they chose to study. Examples we suggested included liquid-like materials such as ketchup and toothpaste, and more solid chemicals such as deodorant and baking powder. Finishing the in-class discussion, each group planned the experimental design for their inquiry study, and predicted the results they would observe for each lubricant.

6.3.3. Third Day

6.3.3.1. *Laboratory*

Almost the entire third day of class involved the students completing the inquiry-based portion of the laboratory. Most groups volunteered to bring in their own materials instead of using some basic substances provided. The lubricants brought in by students included bathroom soaps, cocoa powder, pudding, BB gun pellets, fruit candy, and eggs.

Three different types of sliding discs had been manufactured in a Cornell University machine shop to provide discs that would be easy to wash and not interact with the lubricant. There discs were approximately three inches in diameter and 1.5 inches thick. Most plastic discs used in the laboratory were delrin. To allow for groups to measure the effect of interaction between the lubricant and the sliding object, one teflon disc and polycarbonate disc were also manufactured and provided.

Students were first asked to measure the COF of the disc with no lubricant provided to provide a control for their experimentation. After that, they were expected to test the sliding friction of three different lubricant systems and take a minimum of three measurements to determine each COF. The students were offered some guidance at times, but otherwise were left to conduct the experiments on their own.

The lubricants that the groups chose not only provided an incredibly wide range of COFs, but also introduced students to other types of friction beyond the standard static friction they were familiar with. One group wrapped their disc in fruit roll-up candy and let it slide on a pudding coated-track; the pudding dissolved the candy to generate an extremely low COF, demonstrating the potential of reaction-aided lubrication. A group investigating BB pellets observed rolling friction with their experiment. Several groups attempting to measure powdered lubricants witnessed low

initial COFs before the discs stopped as a result of a build-up of the powder. This repeated development introduced the concept of plowing friction.

6.3.3.2. *In-Class Discussion*

An in-class discussion followed the laboratory to summarize the friction experimentation and help the students draw conclusions from their lubrication studies. After discussing the COFs measured and evaluating their successes, students recognized that adding a material would not necessarily decrease the friction but could potentially increase the COF. From the wide range of lubricants used, the students came to agree one important criterion to control was the lubricant viscosity. A high solid-like viscosity could increase friction and prevent sliding from occurring, while a liquid-like mobile fluid could cause spread too easily. They thus determined that a balance needed to be achieved between a lubricant that would remain in place on the substrate and a material that would allow for a non-sticky, more liquid-like surface. The discussion concluded by asking the students which systems would be most viable in real-life applications.

6.4. EVALUATION OF THE CURRICULUM.

In order to evaluate the success of the curriculum, the students were asked to fill out a series of survey questions pre- and post-curriculum. Five short answer questions were asked both before and after the project:

1) How would you define friction?

2) What causes friction?

3) What can you do to reduce friction?

4) What are some of the disadvantages of having a system with high friction?

5) What are some of the advantages of having a system with high friction?

Because the curriculum was conducted after the concept of friction had been introduced in terms of its basic physical nature and related equations, the initial answers for these questions reflected the students' experience having previously studied the subject matter. Few students changed their answers for any of the questions between surveys. The only question that demonstrated any change in the students' knowledge was question 3; approximately one-fifth of the students surveyed changed their pre-project answer from "smoother surfaces" or "reduce rough surfaces" to an answer reflecting the benefit of changing both the surface and adding a lubricant layer.

Two rating statements were presented in both the pre- and post- project surveys, asking students to choose the answer that described them best. Ratings ranged from 1 to 4, with 1 meaning strong disagreement, 2 meaning disagreement, 3 meaning agreement, and 4 meaning strong agreement. These questions are reported in Table 6.1.

A t-test was conducted on each set of answers. While the answers from all the students reflected a positive understanding of friction as well as personal enjoyment in science classes, overall no statistically significant change between the pre- and post-survey questions existed.

Six rating statements were presented in the post-project surveys, also based on the 1 to 4 scale. With an average value of 2.5 reflecting no opinion, the standard deviation of these results was used to evaluate the significance of any of the students' responses. The questions and results are reported in Table 6.2.

Several conclusions can be drawn from these answers. As was seen from the questions in Table 6.1, students' opinions about science classes did not change because of the project. However, students felt that the project was successful in its primary goal of helping them develop the ability to draw connections between their

Table 6.1. Survey questions based on a 1-4 agreement scale, asked both pre- and post-curriculum.

Question	Pre-Mean	Post-Mean	P-value
I understand the general process and concept of friction.	3.17	3.26	0.624
I enjoy science.	2.87	2.74	0.641

Table 6.2. Post-curriculum survey questions based on a 1-4 agreement scale.

Question	Average	St Dev	Meaning	Significant?
After conducting this research experiment, I feel I understand how science can be applied to real-world applications.	**3.28**	**0.69**	**YES**	**YES**
I am more exicted about science than before	**1.89**	**0.88**	**NO**	**NO**
I enjoyed this research experiment more than most labs.	**2.91**	**0.73**	**YES**	**NO**
After conducting this research experiment, I feel I understand how scientists design their own experiments.	**2.74**	**0.86**	**YES**	**NO**
Doing this experiment, I was more bored than in most classes.	**1.57**	**0.66**	**NO**	**YES**
This experiment was more difficult than most labs.	**1.65**	**0.71**	**NO**	**YES**

studies and the applications of those studies in their daily lives. Students' strong agreement with feeling more knowledgeable about practical science after having completed the project indicates the curriculum helped to strengthen their students' understanding of friction.

A common difficulty with inquiry-based laboratories is that concrete answers do not exist, thus denying students a definite goal that they can work toward.[5] Students conducting these type of experiments will often be frustrated, as it represents a dramatic change from highly structured study to more open-ended questioning. This typical frustration was indeed characteristic of these students, as reflected by the lack of significant positive answers from the third and fourth questions. One solution for this issue would be to introduce other inquiry-based laboratories for other physics experiments to help students feel more comfortable with this advanced scientific technique. A positive can be taken in that students did not find inquiry experiments to be difficult, as evidenced by the final question.

Four short-answer questions were also asked as part of the post-project survey. The number of students with a certain answer was grouped together as listed in Table 6.3. The short answers indicate the students viewed the curriculum as an entire three-day project and did not differentiate between the in-class discussions and the laboratory experiments. While many students did not feel the project could be improved, nearly as many students felt the project should be expanded to allow them study with more lubricant materials. This is a reflection of the students' enjoyment of the inquiry-based experimentation, even though they were uncomfortable with the open-ended nature of the study. Significant enthusiasm was shown for the lubrication inquiry experiments, not only for the hands-on nature of the experimentation, but also the freedom each group had in being able to choose their own lubricants. It is also important to note several students listed enjoying being able to conduct their own

Table 6.3. Post-project short answer responses, with the number of responses of similar answers.

1) What did you especially like about the in-class portion of the project?	
Working with and suggesting their own materials	7
Hands-on nature of the experiment	4
Freedom in experiment design	4
Having a laboratory	2
Being able to investigate material already studied	2
Other	2
2) What did you especially like about this experiment?	
Working with different lubricants	9
Having freedom and control over the experiment	5
Witness friction and lubrication effects	4
It was fun	2
Hands on nature of experiment	1
Other	1
3) What would you suggest for improving the in-class portion of the project?	
Nothing	7
More time	3
Expand the inquiry-based experiment	1
Expand the in-class discussion	1
(Suggestions for equipment changes)	2
Other	4
4) What would you suggest for improving the lab?	
Nothing	6
Fewer calculations	5
More time to work with more materials	4
Less independence between groups	2
Other	3

investigation of real-world friction and lubrication examples after discussing many applications in the beginning of the project.

6.5. CONCLUSIONS.

We have developed a curriculum to help students draw connections between their studies in physics classes and the many real-world applications that exist in their daily lives. Focusing on the basic physics concept of friction and then slightly elevated, related concept of lubrication, students were provided with a series of structured friction experiments and demonstrations to help summarize their knowledge of the subject matter. Students then progressed into an inquiry-based study of the lubrication properties of common household materials.

Survey questions showed that while the students did not feel their knowledge of friction improved, they strongly believed their ability to connect their studies to common examples and uses was strengthened. The students did not necessarily feel comfortable being able to design their own experiments, but greatly enjoyed having freedom in their ability to experiment with a hands-on activity.

A number of changes could be made to the structure of laboratories or in-class discussions to accommodate other teachers, their classrooms and their students. The demonstrations could be modified or eliminated based on the materials available or the extent of the in-class discussions. Introducing other inquiry-based laboratories into the overall curriculum would also help students adjust to designing their own experiments and feel more comfortable with studies where the final goal is open-ended. The nature of the project serves to reinforce much of the classroom information already taught to the students. It is possible that by presenting the material earlier in the range of class friction studies, the students' understanding of the subject matter would be accelerated.

REFERENCES

(1) Halloun, I. *J. Research in Science Teaching* **1996**, *33*, 1019-1041.

(2) Duch, B.J. *AIP Conf. Proc.* **1997**, *399*, 557-566.

(3) Elby, A. *American J. Physics* **2001**, *69,* S54-S64.

(4) Rodriguez, F. *Engineering Education* **1974**, *65*, 245-246.

(5) Colburn, A. *Science Scope* **2000**, *March*, 42-44.

CHAPTER 7

CONCLUSIONS

The research investigations discussed in this thesis have focused on the lubrication properties of polydimethylsiloxane (PDMS) network – self-assembled monolayer (SAM) hybrid systems. My specific goals were to investigate the effects that structural and chemical modifications can have on the friction, adhesion, and wear. The primary structure consisted of a model cross-linked network tethered to a SAM coated silicon substrate; the two tiers create a series of internal tethering that allow the lubrication properties to essentially be an effect of the surface layer with low interfacial shear stress and low surface energy. Modifications including the introduction of pendant or free chains during cross-linking added a degree of viscoelasticity into the network and at the surface. Deconstructing the networks to a basic polymer brush film permitted a comparison between PDMS lubricants and systems based on other polymers.

The PDMS films demonstrated dramatically low friction coefficients almost independent of the physical lubricant structure. The friction coefficients measured for these systems (as low as $\mu = 0.0024$) were an order of magnitude lower than the COFs measured for bare silicon substrates. These results are to my knowledge the lowest friction coefficients ever recorded for dry polymer films. These low friction results were primarily a result of a negligible contribution of adhesion to the friction force, which developed from the low interfacial shear stress and low surface energy of PDMS.

Several factors have been observed to influence the COF. Decreased or minimal viscous-like mobility at the surface is an important characteristic for all lubricant films. This was demonstrated by the introduction of pendant chains or free

chains into micron-thick network structures, which would create a viscous liquid-like layer on the surface. Similar viscous surface effects were seen for polymer brushes that spread across the surface in a mushroom conformation as opposed to a stretched conformation with increased tension present in all chains. Wear studies also indicated that increased viscoelasticity was detrimental to the lubrication properties; tribology measurements conducted on networks swollen with free chains demonstrated that model networks would be resistant to wear to much higher sliding velocities than the swollen networks with viscous surface layers.

Lower elastic moduli in the surface layer also serve to decrease the friction. This characteristic has the greatest effect in model network systems where the viscoelasticity is negligible, or for ultrathin hyperbranched films with a limited contact area between surfaces. The increased flexibility at the surface serves to decrease the fraction of the friction force that develops from the contribution of adhesion; the adhesion hysteresis will be higher for films with higher elastic moduli, thus causing more flexible films that deform more easily under an external load to have lower friction forces. A more viscous surface for these network films will diminish the effect of decreasing the elastic moduli, and can create much higher COFs than model networks if the viscous layer is of significant thickness.

Adhesive forces were significant for all PDMS films, but a limited contribution of adhesion to the friction force allowed for low friction properties to be displayed by all structures. Decided linearity in all friction force vs. external load plots indicated this negligible adhesion contribution. Quantification of the adhesion contribution could be conducted by measuring the intercept of the friction force vs. load plots developed from lateral sliding analysis in relation to the adhesion hysteresis measured from a normal sliding analysis. The adjustment factor, ε, had been found in previous

studies to range from 0.2 to 0.6 for polystyrene; for the PDMS films, it was found to range from 0.0001 to 0.2, indicating the effect of the decreased surface shear.

PDMS was used in all of the network structures because its chemical structure allowed for a low surface energy. In order to determine if the low friction properties were a result of the chemical characteristics of PDMS, polymer brushes were developed from other polymer materials and analyzed. PDMS brushes were found to have COFs lower than polystyrene brushes by a factor of 3.7, and lower than polypropylene glycol / polyethylene glycol brushes by a factor of 4.7. These significantly decreased friction results occurred despite having a surface tension that was less than half of the other polymer systems. The full effect of the differences in surface chemistries may have been limited because of differences in the brush crystallinity between materials, and because adhesive effects were minimized for all systems as a results of the ultrathin brush height.

From these studies, it can be concluded that an optimal lubricant film should be developed using a hybrid structure to allow for a tethered lubricant with internal anchoring for a flexible surface layer with low energy. Measurements conducted on each of the hybrid materials alone indicated that the combined overall structure had much lower friction properties. If the lubricant was being used in conjunction with an application that did not require significant wear resistance (as a result of limited use or some other concern), a PDMS brush layer with high surface coverage would provide the lowest surface friction and adhesion contribution to the friction force. If wear resistance is a concern, a network hybrid lubricant produced from high precursor molar mass PDMS chains would perform best. The COF would be slightly elevated in comparison to the polymer brush, but the wear resistance would be significantly improved. Low viscoelasticity within this network would be crucial to limit wear and reduce friction and adhesion. PDMS should be used as the polymer surface material

because its low surface tension and interfacial shear stress will produce lower COFs than other polymers.